

12-2022

Redox sensing by yeast Hsp70 facilitates modulation of protein quality control and the cytoprotective response

Alec Santiago

Follow this and additional works at: https://digitalcommons.library.tmc.edu/utgsbs_dissertations



Part of the [Molecular Genetics Commons](#)

Recommended Citation


Santiago, Alec, "Redox sensing by yeast Hsp70 facilitates modulation of protein quality control and the cytoprotective response" (2022). *The University of Texas MD Anderson Cancer Center UTHealth Graduate School of Biomedical Sciences Dissertations and Theses (Open Access)*. 1224.
https://digitalcommons.library.tmc.edu/utgsbs_dissertations/1224

This Thesis (MS) is brought to you for free and open access by the The University of Texas MD Anderson Cancer Center UTHealth Graduate School of Biomedical Sciences at DigitalCommons@TMC. It has been accepted for inclusion in The University of Texas MD Anderson Cancer Center UTHealth Graduate School of Biomedical Sciences Dissertations and Theses (Open Access) by an authorized administrator of DigitalCommons@TMC. For more information, please contact digitalcommons@library.tmc.edu.


Redox sensing by yeast Hsp70 facilitates modulation of protein quality control and
the cytoprotective response

Alec Santiago, B.S.

APPROVED:



Kevin A. Morano, PhD
Advisory Professor



Nayun Kim, PhD



Anna Konovalova, PhD



Ambro van Hoof, PhD



Sheng Zhang, PhD

APPROVED:



Dean, The University of Texas
MD Anderson Cancer Center UTHealth Graduate School of Biomedical Sciences

Redox sensing by yeast Hsp70 facilitates modulation of protein quality control and
the cytoprotective response

A

Dissertation

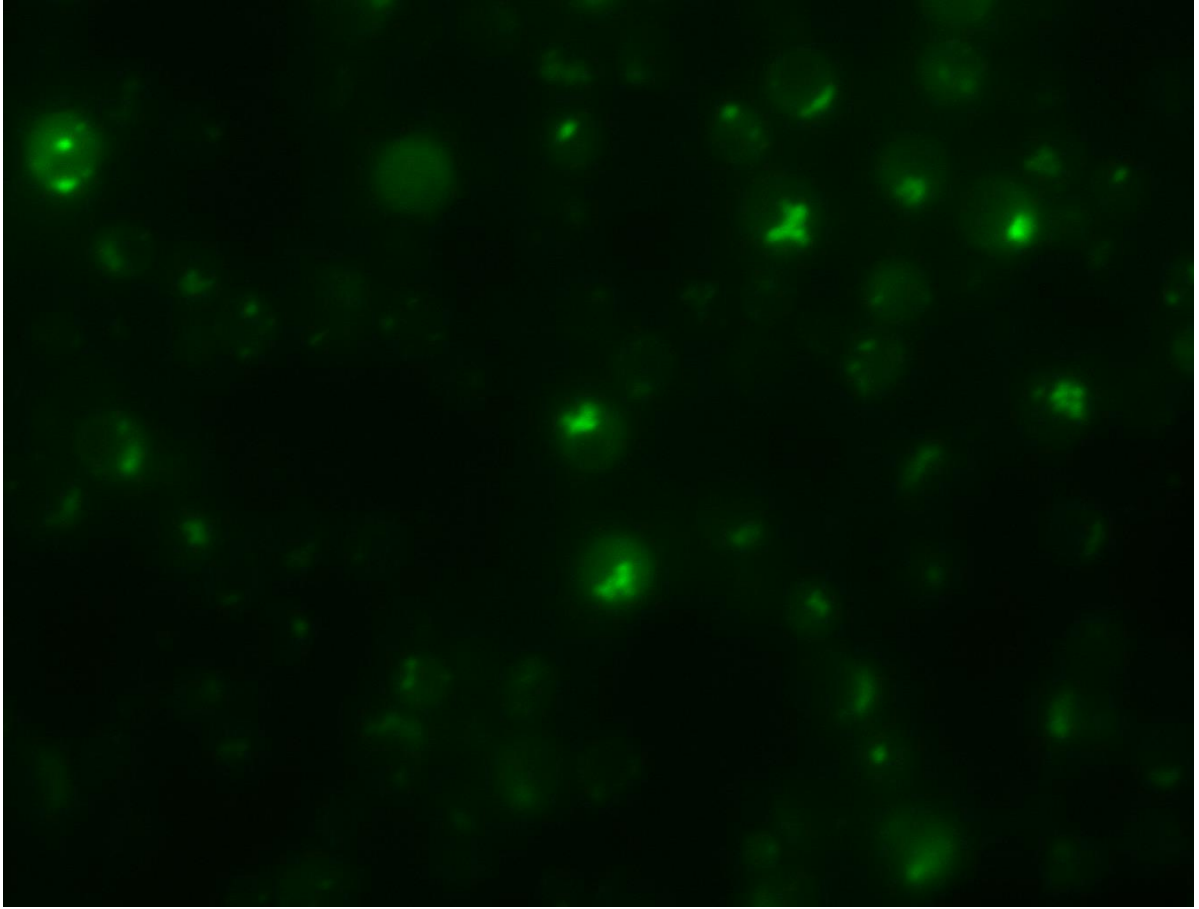
Presented to the Faculty of
The M.D. Anderson Cancer Center/ UTHealth
Graduate School of Biomedical Sciences
In Partial Fulfillment
of the Requirements
for the Degree of
DOCTOR OF PHILOSOPHY

By

Alec Morgan Santiago, B.S.

Houston, Texas, USA

December 2022



I primarily acknowledge and dedicate this work to my entire family. The endless unconditional love you have given to me throughout my life has fundamentally impacted my entire person, and all that I am is thanks to your oversized hearts and rich, vibrant souls.

I love you all.

ACKNOWLEDGEMENTS

I would like to primarily thank my advisor, Dr. Kevin A. Morano, for giving me a chance when I really needed it. Your mentorship provided a sturdy support for me to grow into my potential, and a higher standard of which to set expectations for my own work. Your kindness, understanding, and unshakeable resoluteness in all of our success really let myself and everyone else in the lab leave as much stronger humans and scientists than we began as. I truly appreciate that I had a mentor who was so heavily invested in the underlying concept of Mentorship, and that I was never able to relate to any of the struggles that my peers expressed from their own experiences. Your lab molded me in ways that I will forever benefit from.

Next, I want to thank my Advisory Committee: Drs. Nayun Kim, Anna Konovalova, Ambro van Hoof, and Sheng Zhang. You all have been exceedingly kind in every meeting, and actively tried to support my growth and the impact of my work. You all came together to make each committee meeting a fun and engaging exploration of my work, as opposed to a rigorous test of knowledge. Every one of you has been able to offer me key suggestions and protocol insights that were stepping stones from failure to success for my assays. The open-door policy that each of you keeps is so helpful to have had in my back pocket as a safety net throughout my PhD. Thank you all as well for the endless patience with recommendation letters, Doodle schedulings, and incorrect word choices on my part. It has been very much appreciated.

To all of the labmates throughout my career: Sara Peffer, Unekwu Yakubu, Davi Goncalves, and Amy Ford. You guys made our windowless little lab a warm space to work. You all are extremely kind and patient, which was a heartening experience for a very green scientist such as myself. Thank you for explaining everything to me in ways that I was able to understand, and for keeping a distant eye on my work to prevent me from making obvious mistakes. Unekwu, thank you especially for being my PIC through so many things, including SMDP, the ABRCAMS conference, the BIO conference, Rodeo Gatekeepers, a couple crazy nights on the town, and a path to walk forward through as I stepped into your established footprints along the way. Davi, thank you for being my sounding board for all things biotech and entrepreneurship, and for having so many wonderful conversations with me about values, purpose, and meaning throughout the scientist's journey. Sara, thank you for being my first bench mentor, for being the biggest impact in my introduction to grad school, and for being a role model for kindness in the bench space. Amy, thank you for being a fun and enthusiastic person in lab, and a joy to be around.

I want to also thank all of the organizations that helped me to pursue my graduate education. Thank you to GSEC and the GSBS for the travel awards, so that I could attend conferences across the country. Thank you to the Federation of Women's Club for selecting me as an Endowed Scholar. Thank you to the GSBS for providing so many wonderful resources and just all-around excellent people. Especially to Raquel and Spitz, you were both so kind and wonderful to me and made me feel like the GSBS fully supported me as an individual.

I want to thank the MMG department for supporting me, especially Dr. Carolyn Agurcia-Parker for being a constant source of positivity, fun conversation, and crucial information that saved my behind on many occasions, to AlySha and Justin for the considerable amount of assistance, and Dr. Nick De Lay for the above and beyond assistance on my Candidacy exam. Thank you to all of the students who were helpful in ways that are both scientific and humanistic, helping me as friends and as colleagues. Robert Williams, Sara Siegel, Sarah Lach, Jenn Hurtig, LeeAnn Notice, Allie Berroyer, Melissa Martinez, and so many others. Thank you also to the friends in my cohort that struggled and succeeded with me along the way: Celso Catumbela, Medina Colic, Dan Zamler, and the whole rest of the incoming 2017 class.

I want to thank Drs. Qinglian Liu (Virginia Commonwealth University), Randy Hampton (UC San Diego), Nadinath Nillegoda (Monash University), Elizabeth Craig (University of Wisconsin), Andrew Truman (University of North Carolina, Charlotte) and Francis Tsai (Baylor College of Medicine) for advice and reagents. I want to additionally thank Dr. Santosh Kumar (McGovern Medical School) for protein purification assistance.

Thank you also to everyone in Enventure and beyond that helped foster my passion for entrepreneurship and the business of life science.

Thank you also to Morgan Unruh, as your endless support and resonating goodness was a pillar of positivity in my life and I am very thankful that in the unfathomable scope of the endless universe, the ever-widening expanse of time, and the broad swaths of geographical possibility, that I got to exist at the same time as you. You're the best.

Redox sensing by yeast Hsp70 facilitates modulation of protein quality control and the cytoprotective response

Alec Morgan Santiago

Advisor: Kevin A. Morano, PhD

Neurodegenerative disease affects millions of Americans every year, through diagnoses such as Alzheimer's, Parkinson's, and Huntington's diseases. One factor linked to formation of these aggregates is damage sustained to proteins by oxidative stress. Cellular protein homeostasis (proteostasis) relies on the ubiquitous Hsp70 chaperone family. Hsp70 activity has been previously shown to be modulated by modification of two key cysteines in the ATPase domain by oxidizing or thiol-modifying compounds. To investigate the biological consequences of cysteine modification on the Hsp70 Ssa1 in budding yeast, I generated cysteine null (cysteine to serine) and oxidomimetic (cysteine to aspartic acid) mutant variants of both C264 and C303 and demonstrate reduced ATP binding, hydrolysis and protein folding properties in both the oxidomimetic as well as hydrogen peroxide-treated Ssa1. In contrast, cysteine nullification rendered Ssa1 insensitive to oxidative inhibition. The oxidomimetic *ssa1-2CD* (C264D, C303D) allele was unable to function as the sole Ssa1 isoform in yeast cells and also exhibited negative effects on cell growth and

viability. Ssa1 binds to and represses Hsf1, the major transcription factor controlling the heat shock response, and the oxidomimetic Ssa1 failed to stably interact with Hsf1, resulting in constitutive activation of the heat shock response. Consistent with the *in vitro* findings, *ssa1-2CD* cells were compromised for *de novo* folding, post-stress protein refolding and in regulated degradation of a model terminally misfolded protein. Together these findings pinpoint Hsp70 as a key link between oxidative stress and proteostasis, information critical to understanding cytoprotective systems that prevent and manage cellular insults underlying complex disease states.

TABLE OF CONTENTS

| | |
|--|-------------|
| Approval Sheet | i |
| Title Page | ii |
| Cover Art | iii |
| Dedication | iv |
| Acknowledgement | v |
| Abstract | viii |
| Table of Contents | x |
| List of Figures | xii |
| List of Tables | xv |
| Chapter I: Introduction | 1 |
| Cellular chaperones and protein homeostasis | 2 |
| Sensing and response to proteotoxic stress in the cytoplasm | 16 |
| Sensing and transcriptional response to proteotoxic oxidative stress | 22 |
| Chaperones as sensors of proteotoxic oxidative stress | 27 |
| Overview of Hsp70 redox biology using genetic tools | 30 |
| Chapter II: Materials and Methods | 33 |
| Chapter III: In vitro analysis of Ssa1 cysteine modification | 44 |
| Introduction | 45 |
| Results | 48 |
| Discussion | 72 |
| Chapter IV: In vivo analysis of Ssa1 cysteine modification | 75 |

| | |
|--|------------|
| Introduction | 76 |
| Results | 79 |
| Discussion | 110 |
| Chapter V: Explorations of chaperone cysteines within the OxiMouse Database | 114 |
| Introduction | 115 |
| Results | 117 |
| Discussion | 125 |
| Chapter VI: Discussion and Future Directions | 129 |
| Summary of results | 130 |
| Additional explorations concerning Hsp70 and oxidative stress | 140 |
| Hsp70 modulation as a therapeutic tool | 145 |
| Future directions | 148 |
| Bibliography | 152 |
| Vita | 183 |

LIST OF FIGURES

| | |
|---|----|
| Figure 1-1: Structure of the <i>E. coli</i> (DnaK) chaperone | 4 |
| Figure 1-2: Hsp40 and Hsp110 stimulate the hydrolysis and exchange of nucleotide by Hsp70 | 7 |
| Figure 1-3: Ssa has several roles in protein homeostasis | 9 |
| Figure 1-4: Activation and attenuation of the HSR is modulated by Hsp70 | 19 |
| Figure 1-5: Proteotoxic oxidative stress sensing through reactive protein thiols | 25 |
| Figure 1-6: Cysteines are subject to several forms of redox state modification | 29 |
| Figure 3-1: Cysteine substitution mutants reflect states of oxidation | 49 |
| Figure 3-2: Ion chromatography separates Ssa1 subgroups of varying functionality | 51 |

| | |
|---|----|
| Figure 3-3: Purification of Ssa1 variants and co-chaperones | 52 |
| Figure 3-4: Nucleotide binding and hydrolysis are similarly impaired by oxidomimetic substitution in Ssa1-2CD and exogenous oxidation of Ssa1 | 54 |
| Figure 3-5: Nucleotide hydrolysis is similarly impaired by oxidomimetic substitution in Ssa1-2CD and exogenous oxidation of Ssa1 | 57 |
| Figure 3-6: Isolated Ssa1-2CD shows an altered fragmentation profile when incubated with non-hydrolyzable nucleotide | 61 |
| Figure 3-7: Mimicked and exogenous thiol oxidation negatively impacts <i>in vitro</i> protein refolding | 65 |
| Figure 3-8: The deficiency of the oxidomimetic Ssa1-2CD mutant is not caused by dimer formation | 70 |
| Figure 4-1 The oxidomimetic <i>ssa1-2CD</i> mutant is incapable of supporting viability as the sole cytosolic SSA gene | 81 |

| | |
|---|-----|
| Figure 4-2: The thiol oxidomimetic <i>ssa1-2CD</i> allele displays slowed growth | 84 |
| Figure 4-3: Expression of the Ssa1-2CD protein is restricted relative to wild type Ssa1 and Ssa1-2CS | 88 |
| Figure 4-4: Overexpression of <i>ssa1-2CD</i> severely restricts growth | 92 |
| Figure 4-5: Ssa1-2CD fails to bind and repress the heat shock regulator Hsf1 | 95 |
| Figure 4-6: <i>ssa1-2CD</i> is unable to complement <i>ssa1-WT</i> in the folding of <i>de novo</i> proteins. | 98 |
| Fig. 4-7: The <i>ssa1-2CD</i> mutant exhibits multiple deficiencies in proteostasis. | 101 |
| Fig. 4-8: Degradation of the misfolded protein tGND-GFP is chronically impaired in <i>ssa1-2CD</i> cells. | 106 |
| Figure 5-1: Significant oxidation events occur more frequently in Hsp70 than Hsp110. | 121 |

Figure 5-2: Significant oxidation events occur more frequently in constitutively expressed Hsp70s than in stress-induced Hsp70s. 122

Figure 5-3: Cysteine oxidation events within the Hsp70 and Hsp110 proteins of the brain occur more frequently in the NBD than the SBD. 124

Figure 6-1: Yeast Hsp70 cysteine alignment 134

Figure 6-2: Thiol dependent regulation by Hsp70 and Hsf1 136

LIST OF TABLES

Table 1-1: Molecular Chaperone Homologs in Yeast and Humans 13

Table 2-1: Plasmids and strains used in this study 43

Table 5-1: Cysteines of interest in the OxiMouse database 118

Chapter I: Introduction

Note: Portions of this section were originally published in Experimental Cell Research. Santiago A, Goncalves, D., Morano KA. Mechanisms of sensing and response to proteotoxic stress. Exp Cell Research. 2020 Oct 15:395:2.
<https://doi.org/10.1016/j.yexcr.2020.112240> *Elsevier does not require permission to use published materials in one's dissertation:*
<https://www.elsevier.com/about/policies/copyright/permissions>.

Cellular chaperones and protein homeostasis

Protein molecular chaperones assist in the homeostasis of a functional proteome within living cells. This involves ensuring that proteins form and maintain their proper functional conformations, the assembly and disassembly of protein complexes, management of damaged/non-functional proteins, and the transport and localization of proteins within the cell. Imbalances in protein homeostasis can result in chronic accumulation of non-operative and/or aggregated proteins, often correlated with downstream events that lead to adverse neurological states such as Alzheimer's disease, Parkinson's disease, and Huntington's disease ¹⁻³. Such disruptions can occur from a broad set of injuries including both excess heat or sub-optimal growth temperatures, metabolic dysfunction, and the introduction of heavy metals.

In several eukaryote models, including the yeast model *Saccharomyces cerevisiae*, a key group of chaperones that modulate many of these functions are the cytosolic Hsp70 chaperone proteins. Hsp70s are responsible for general protein homeostasis in the cell, working in the cytoplasm, nucleus, the mitochondria, and the endoplasmic reticulum (ER) to promote the general functionality of proteins through nearly every compartment of the cell. Hsp70s are involved in several roles that are directly tied to protein homeostasis, operating through all stages of a protein life cycle. Hsp70s interact with substrate by recognizing and binding to hydrophobic regions within proteins and polypeptides that are flanked by charged residues, continually binding and releasing the substrate so long as the hydrophobic/charged motif is present on the cytoplasmic-facing exterior of the conformation ⁴. Hsp70s recognize a

seven residue peptide sequence, with a wide spread of variation in those seven residues ⁵. Within the substrate binding pocket, the central site of binding is referred to as the 0th site, with several subsites on either side (-3, -2, -1, +1, +2, +3) that have the potential for many interactions, but favor positively charged aliphatic residues ⁶. In DnaK, an *E. coli* Hsp70, a model called the NR peptide (sequence: NRLLLTG) was initially used to determine the first atomic level description of substrate binding (Figure 1-1) ⁷. Since then, there has been a progression of predictive algorithms that can interpret and model potential Hsp70 binding sites. BiPPred is a prediction software that is able to predict peptides that are recognized by the ER-localized human Hsp70 BiP, as well as calculate the binding affinity ⁸. LIMBO is another predictive algorithm, which uses scalable clustering of categorical data, which our lab has used to determine potential Hsp70 binding sites within the transcriptional regulator Hsf1 ^{9,10}. Through this binding, Hsp70s protect nascent polypeptides as they exit the ribosome and along the endoplasmic reticulum, shielding them from damage by incorrect folding conformations and by environmental injury, and the assistance with proper conformational folding of said nascent polypeptides ¹¹. They also recognize these same binding motifs within cytosolic proteins that have sustained injury and are thus incorrectly folded. Additionally, Hsp70 proteins assist in the degradation of chronically misfolded proteins, through interactions with the ubiquitination system ¹². Hsp70 proteins are highly conserved. Throughout all domains of life and all cellular compartments, the structure is defined by an amino-terminal nucleotide binding/ATPase domain (NBD) and a carboxyl-terminal substrate binding domain (SBD), connected by a short linker ⁶.

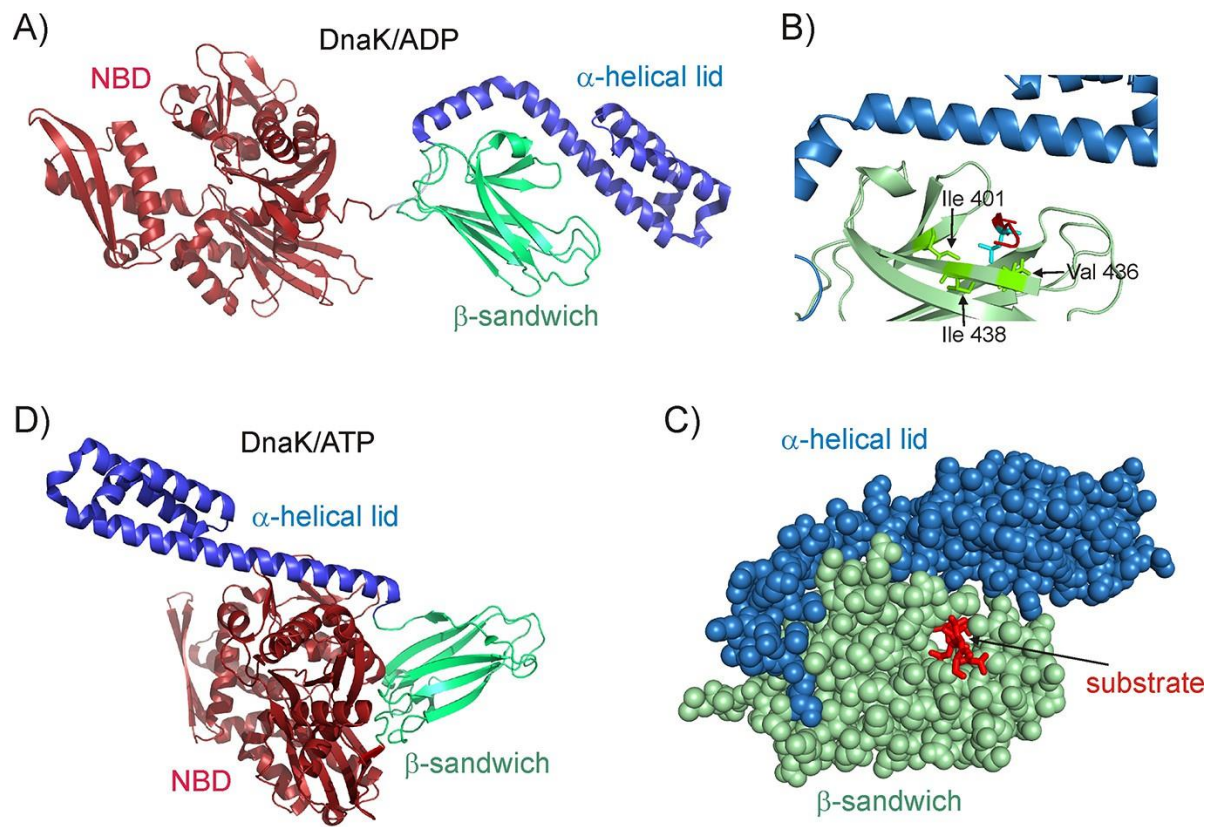
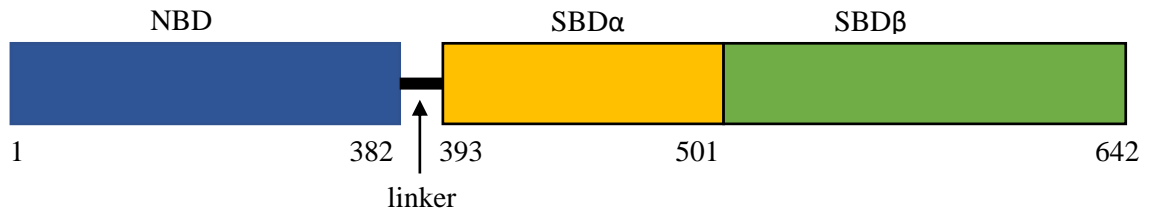


Figure 1-1: Structure of the *E. coli* Hsp70 (DnaK) chaperone

Figure 1-1: Structure of the *E. coli* Hsp70 (DnaK) chaperone (A) Cartoon representation of the NMR structure of DnaK/ADP showing the N-terminal ATPase domain (NBD) and the C-terminal substrate binding domain which consists of a β -sandwich subdomain and an α -helical lid (PDB ID: 2KHO). (B) An enlarged view of the substrate binding cleft showing key hydrophobic residues Ile 401, Val 436 and Ile 438 of DnaK as green sticks forming contacts with the substrate residue that occupies the central binding position (cyan sticks) (PDB ID: 1DKZ). The remainder of the peptide substrate is shown in red. (C) Space filling structure of the substrate binding domain (SBD) with a closed conformation of the helical lid, illustrating the pore that the substrate (red) threads through. (D) The crystal structure of DnaK/ATP in the absence of substrate, showing that upon ATP hydrolysis the α -helical lid becomes docked on the β -sandwich domain concomitant with the undocking of NBD and SBD (PDB ID: 4B9Q). Note: This figure was adapted with permission through a Creative Commons Attribution from: Ashok Sekhar, Algirdas Velyvis, Guy Zoltsman, Rina Rosenzweig, Guillaume Bouvignies, Lewis E Kay (2018) Conserved conformational selection mechanism of Hsp70 chaperone-substrate interactions eLife 7:e32764

The SBD contains two subdomains: the first is composed of a β -sheet formation with a hydrophobic pocket (SBD- β) that recognizes a motif of hydrophobic regions within the protein substrates. The second subdomain (SBD- α) is composed of three α -helices that act as a 'lid', opening and closing over the SBD- β , generating high-affinity binding and reduced substrate release when closed ¹³. The nucleotide binding domain is composed of four rotating lobes that form a nucleotide-binding pocket ¹⁴. The two domains communicate through allosteric interactions, creating two conformations for Hsp70, an 'open' and a 'closed' state ¹⁵. In the open state, the lobes of the NBD rotate due to a conformation change induced by the binding of ATP. This rotation opens a pocket that the linker is then retracted into, bringing the NBD and the SBD closer together ¹⁶. This proximity allows for the interaction between the SBD- α and the NBD, maintaining the upward position of the lid away from the substrate binding pocket of the SBD- β , and allowing protein substrate to dock at the substrate binding site. This shift in conformation is cyclic, going from one to the other in successive iterations with assistance from other highly conserved co-chaperones (Hsp40, which assists in Hsp70/substrate contact; and Hsp110, which assists in nucleotide exchange, as described in detail below) in a process termed chaperone cycling (Figure 1-2) ^{17,18}. This iterative process cycles through the 'open' and 'closed' conformations, binding unfolded substrate to protect it from aggregation, then releasing it to allow for productive folding, but rebinding if productive folding does not occur and the hydrophobic regions are still exposed (Figure 1-3) ¹⁹.

A.



B.

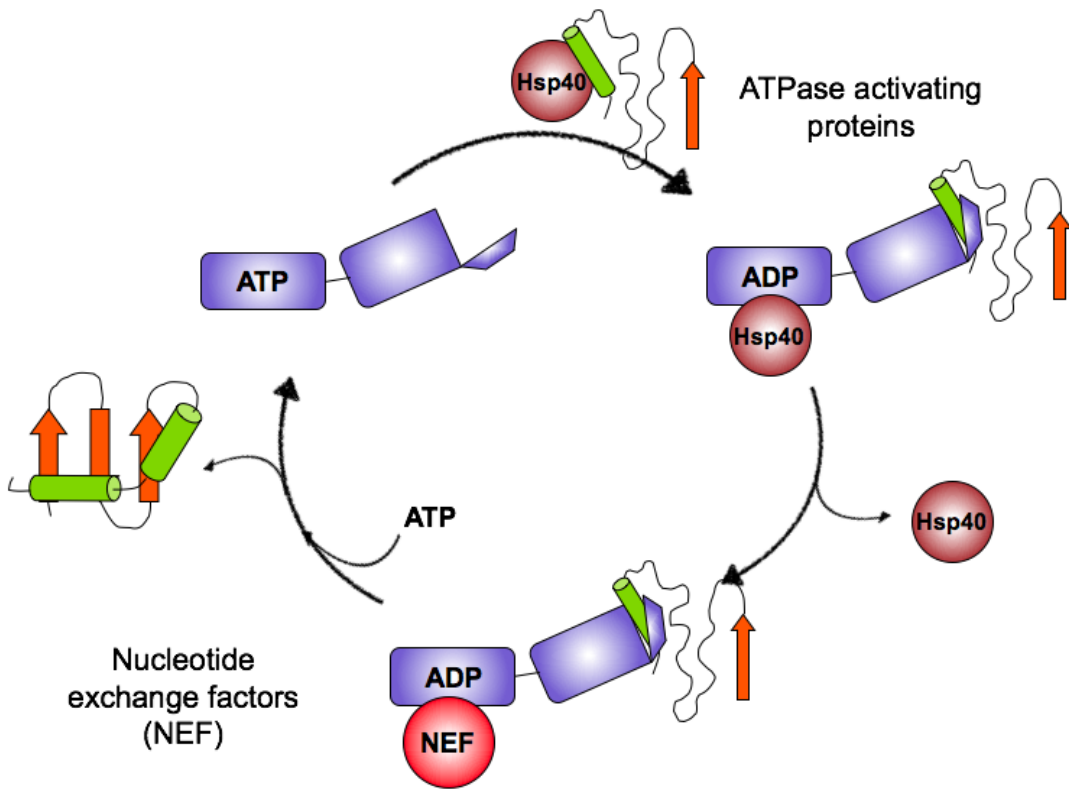


Figure 1-2: Hsp40 and Hsp110 stimulate the hydrolysis and exchange of nucleotide by Hsp70

Figure 1-2: Hsp40 and Hsp110 stimulate the hydrolysis and exchange of nucleotide by Hsp70

(A) The domain structure of Ssa1. (B) The binding of protein substrate (ribbon) to Hsp40 (maroon) is subsequently delivered to Hsp70 (purple) in the open conformation, stimulating the hydrolysis of a bound ATP and a shift into the closed conformation by Hsp70. Hsp110 (red) assists in the release of the ADP molecule, enabling a re-binding of ATP, shifting Hsp70 into the open conformation and continuation of the cycle.

HSR regulation

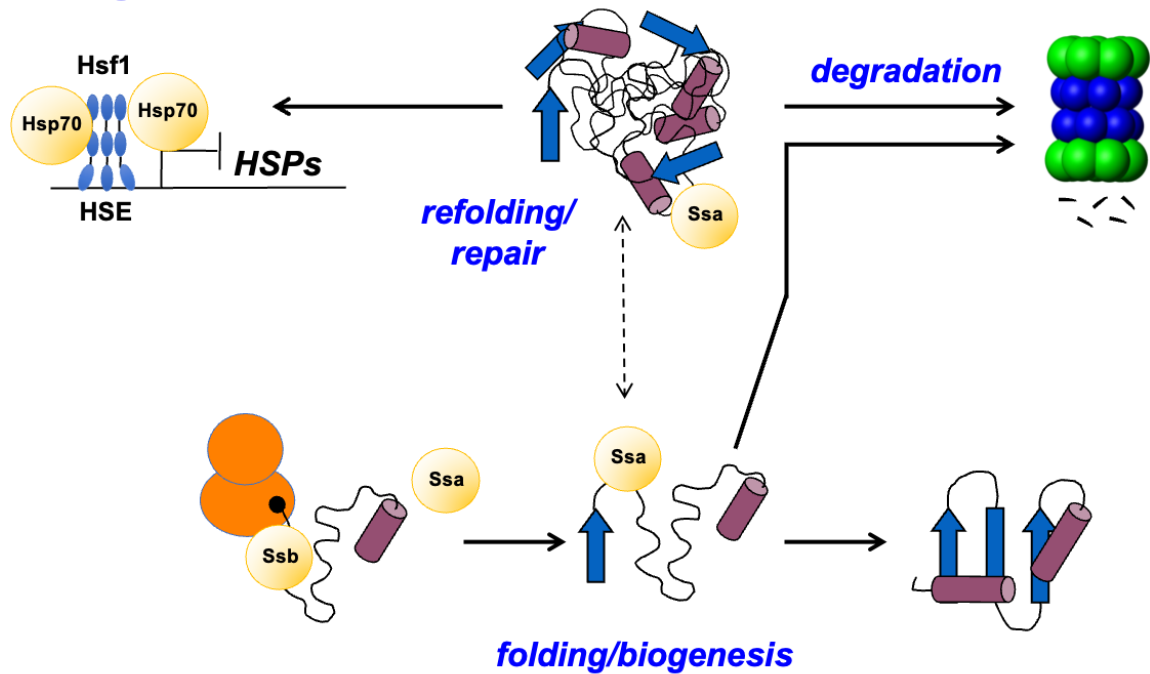


Figure 1-3: Ssa has several roles in protein homeostasis

The protein chaperone Ssa1 maintains protein homeostasis through several functions, including the folding of nascent polypeptides, the refolding of damaged proteins, the assisted degradation of chronically misfolded proteins, and the regulation of stress responses.

Hsp70 proteins also assist in the degradation process for chronically misfolded proteins, through the ubiquitin-proteasome system. In this process, ubiquitin is activated by an E1 enzyme, and conjugated together by an E2 enzyme. E3 enzymes then ligate the ubiquitin to the substrate, tagging it for degradation by the proteasome machinery²⁰⁻²². Ssa1 is involved in the degradation of both chronically misfolded and short-lived proteins through several processes: recognizing and binding the misfolded substrate as noted earlier, maintaining solubility, and escorting and delivering that substrate to the E1 enzyme^{23,24}. The cochaperones Ydj1 and Fes1 were found to be necessary for Ssa1-mediated cytosolic degradation of proteins, as were the ubiquitin conjugating enzymes Ubc4p and Ubc5p^{23,25}. However, the E3 enzyme San1 was shown to be able to recognize and ligate ubiquitin to particular substrates without the presence of Ssa1 in the cell²⁶.

Hsp70 and Hsp40 assist in balancing the rate of intrinsic nucleotide hydrolysis and the binding/release of substrate by Hsp70. Direct interaction between the substrate and the SBD, along with additional stimulation by Hsp40, preempts a conformational cascade that results in ATP hydrolysis within the NBD²⁷. Nucleotide cycling (as defined as the binding, hydrolysis and release of ATP) activity then shifts affinity of the substrate binding domain for the interacting substrates, and also changes the iterative Hsp70 release/binding mechanism that stimulates the folding of proteins (Figure 1-2)²⁸.

Ydj1 and Sis1 are two types of Hsp40 within the yeast cytosol, and belong to the class of chaperones referred to as J-proteins. Named for the first Hsp40 protein discovered in bacteria, DnaJ, Ydj1 is a homologue of the human Hsp40 DNAJB1²⁹.

J-proteins are categorized into two groups, one of which contains a zinc finger region within the carboxyl-terminal domain I. The J-proteins have several highly conserved regions, including a J-domain, carboxyl-terminal domain I and II, a glycine-phenylalanine-rich (G/F) domain, and a dimerization domain³⁰. The J-proteins assist Hsp70 in three ways: the recognition and transfer of substrate to Hsp70, the inducing of conformational change within Hsp70 that stimulates the hydrolysis of ATP, and the localization within cellular compartments, which recruits Hsp70 to those locations³¹. The J-domain facilitates the interaction between Hsp40 and Hsp70, through the conserved histidine-proline-aspartic acid (HPD) region, which directly induces an increased capacity for hydrolysis of ATP by Hsp70³⁰. Ydj1 also assists Hsp70 in the protection of nascent polypeptides as they form their final conformations³².

Hsp110s function as nucleotide exchange factors due to their ability to increase the rate of ADP dissociation from an Hsp70 molecule after hydrolysis^{33–35}. This release continues to drive the iterative cycling of conformational shift between ‘open’ and ‘closed’ states of Hsp70. Hsp110s are distant members of the Hsp70 family, possessing similar domain architecture, save for unstructured additional sequence extensions in the substrate binding domain and at the carboxyl-terminus¹⁵. Of interest, our lab recently showed that this extended carboxyl-terminus possesses a previously unknown substrate binding capacity that was able to suppress aggregate formation³⁶. Hsp110s interact with lobes I and II of the Hsp70 protein, as well as the α -helical ‘lid’ domain, which stabilizes the interaction³³. Sse1 is a member of the Hsp110 family, which act as co-chaperones to both Hsp70 and Hsp90³⁷. The nucleotide exchange factor Sse1 is the major cytosolic Hsp110, and

assists directly in the removal of ADP from the nucleotide-binding domain of Ssa1. Although the homologue Sse2 is present as well, deletion of *SSE2* has no resultant phenotype, while deletion of *SSE1* results in temperature sensitivity, and a synthetic lethality when combined with a deletion of *YDJ1*³⁴. However, deletion of both *SSE1* and *SSE2* is lethal^{38,39}.

The budding yeast *Saccharomyces cerevisiae* has served as a tractable genetic model to study chaperones for decades, as there is a high degree of similarity between the chaperone components and regulation between that of budding yeast and the higher eukaryote counterparts. Within human cells, flies, nematodes, and mice, there exist homologous counterparts of the Hsp70s, the Hsp110s, the Hsp40s, as well as several other major protein chaperones (Table 1-1)⁴⁰⁻⁴². Hsp70s were first discovered as a clathrin-uncoating protein, using power derived from ATP hydrolysis to disassemble the protein complex⁴³. We now know how ubiquitous and crucial the proper function of Hsp70 proteins is for survival. *S. cerevisiae* expresses four Hsp70s in the cytosol, of which Ssa1 (human homolog HSPA1A) is the most prominent, constitutively expressed homolog. Yeast additionally possesses another constitutively expressed homolog (Ssa2), and two stress-induced homologs (Ssa3/4), whose expression is maintained at relatively low levels until environmental stress signals are detected⁴⁴. However, presence of any one of the four Ssa isoforms is sufficient to sustain life^{41,45}. Additionally, several Hsp70 members are restricted to subcellular localizations, such as Ssz1 and Kar2 in the ER (Table 1-1). Ssb1/2, though close in structure and homology to Ssa1/2, are bound to the ribosome and specialize in the protecting and folding of nascent polypeptides⁴⁶⁻⁴⁸. One clear

distinction between the Ssb's and Ssa's is the increased expression of the Ssa family and decreased expression of the Ssb family during cytotoxic stress imbalance, likely due to the wider specialization of the former to combat stressors and the decreased ribosomal activity resulting from stress making the Ssb proteins less useful to prevent injury ⁴⁸. In humans, there are more than 12 representatives of the Hsp70 family, with identical domain architecture, and similar sequences and functionality ⁴⁹. Similar to yeast Hsp70s, the human homologs also work to monitor protein folding, aggregate recovery, assembly of multi-protein complexes, and transport of protein components throughout the cell ⁵⁰. Hsp70 research in yeast has been instrumental for informing the biology of chaperones in human cells.

Table 1-1: Molecular Chaperone Homologs in Yeast and Humans

| Chaperone | Human | Yeast | Localization |
|------------------|-----------------|--------------|---------------------|
| Hsp70 | Hsc70/Hsp70 | Ssa1,2,3,4 | Cytosolic |
| | | Ssb1,2 | Ribosomal |
| | BiP/Grp78 | Kar2 | ER |
| | Hsp70L1 | Ssz1 | Ribosomal |
| Hsp110 | Apg-1/2 | Sse1,2 | Cytosolic |
| | Hsp105 α | | Cytosolic |
| Hsp40 | Hdj2/DNAJ1A | Ydj1 | Cytosolic |
| | Hdj1/DnaJB1 | Sis1 | Cytosolic |
| HSF | Hsf1,2,3,4 | Hsf1 | Cytosolic/nuclear |

Note: Table 1-1 adapted with permission from: Yakubu, Unekwu. (2021). *Deciphering the role of Hsp110 chaperones in diseases of protein misfolding*. Doctoral dissertation: The University of Texas MD Anderson Cancer Center UTHealth Graduate School of Biomedical Sciences.

The expression of the chaperone network is modular, and often tuned to the presence of stressors or non-functional protein aggregates ⁵¹. When exposed to a challenging environment, the production of chaperone system components is ramped up, an example of which is Ssa3 and Ssa4, mentioned above. Cells in log phase generally express Ssa1/2 at >150,000 molecules/cell, while Ssa3/4 are expressed at <20,000 molecules/cell, but during the heat shock response, Ssa3/4 concentrations can increase more than 10-fold ^{52,53}. The stress responses are also checked and attenuated by several measures, such as a much different half life in stress-activated Hsp70 proteins. Specifically, the half-lives are as follows: 20.2 hours for Ssa1, 14.9 for Ssa2, 11.0 for Ssa3, and more than 100 for Ssa4 ⁵⁴. This attenuation allows the stress response to be terminated once the indications of stress have been resolved, and relieve the cell of an over-abundance of chaperone, which has the propensity to be detractive for cellular growth, which is thought to be in part due to the competition for co-factors, as toxicity of Ssa1 overexpression has been relieved by simultaneous overexpression of Sse1 ⁵⁵.

The yeast stress response also involves the function of two additional protein families, the small heat shock proteins (sHSPs) and the disaggregases. Within yeast,

the cytosolic protein disaggregase is called Hsp104, and it is a member of the Hsp100 chaperone family and the AAA+ ATPase superfamily⁵⁶. Hsp104 is a homohexameric structure, with each subunit containing an amino-terminal domain, a nucleotide binding domain, a middle domain, a carboxyl-terminal nucleotide binding domain, and a carboxyl-terminal domain⁵⁷. The disaggregase Hsp104 works by generating motive force through the hydrolysis of ATP, using the force of motion to solubilize aggregates by translocating individual polypeptide components through its central pore^{56,58,59}. Hsp104 then passes the polypeptide to Hsp70 for proper refolding. In humans, there is no direct homolog for Hsp104, however several AAA+ ATPase family members have been implicated in the response to protein aggregation, such as RuvbL1 and RuvbL2⁶⁰.

Small heat shock proteins constitute the broadest and most diverse family of molecular chaperones present in all kingdoms of life⁶¹. With affinity for early-misfolded proteins, sHSPs play significant roles in the maintenance of cell proteostasis under stress conditions as the first line of chaperone defense^{62,63}. sHSPs are present in the cytosol and the nucleus of eukaryotic cells⁶⁴. sHSPs are structurally characterized by their low molecular weight (12-43 kDa) and presence of an α -crystalline domain (ACD)⁶⁵. The ACD is composed of a β -sandwich structure with seven to eight antiparallel β -sheets, flanked by disordered N- and C- terminal extensions⁶⁶. sHSPs act by sequestering misfolded proteins and forming large, soluble assemblies, often prior to refolding by ATP-dependent chaperone complexes. The mechanism involves the interaction of the sHSPs with intermediately folded

proteins through surface exposed hydrophobic residues, stabilizing the substrate and preventing further misfolding and/or aggregation^{67,68}.

sHSPs can form dimers and oligomers bound by weak interactions that give shape and adaptability to these assemblies⁶⁹. In addition to oligomers, some sHSPs can form heterocomplexes (e.g., the human HspB4/HspB5), an uncommon feature that is speculated to give evolutionary diversity of function for sHSPs. *S. cerevisiae* expresses two sHSPs (Hsp42 and Hsp26) that do not form mixed assemblies and therefore fulfill different functions in the proteostasis network^{70,71}. Although sHSPs are expressed at low concentrations under normal growth conditions, under stress conditions, sHSPs are strongly upregulated through stress-responsive transcription factors.

Sensing and response to proteotoxic stress in the cytoplasm

The subject of how elevated temperature that challenges folding of nascent protein chains emerging from the ribosomal exit tunnel is sensed by cells and how that signal is transduced into a response has been an ongoing area of research for some time. This “heat shock response” (HSR) in yeast and other organisms’ scales with the severity of temperature exposure. Shift to elevated temperature (37°C–42°C for yeast) sustains the transcriptional response for an extended time, changing expression of over 3,000 genes^{72,73}. The transcription factor HSF1 (Hsf1 in yeast) is generally recognized as the master regulator of the HSR in eukaryotes. Hsf1 is recruited to promoters of genes comprising the HSR regulon by binding at genome

sequences termed heat shock elements (HSEs) (reviewed in Morano *et. al*(2012) ⁷⁴). Pincus and collaborators recently mapped genome binding sites for Hsf1 in yeast, determining a total of 74 sites, 69 of which are bound under heat shock (HS). In non-stress conditions, Hsf1 basally binds 43 loci, but under stress, Hsf1 cooperates with chromatin remodeling complexes to reveal HSEs occluded by nucleosomes ⁷⁵. The relatively small number of binding sites directly bound by Hsf1 determined in this recent study, compared to the larger number of genes generally affected by general heat shock, may be due to separate downstream factors initiated by Hsf1, but individually distributing and amplifying the HSR activation signal into branching pathways. Additionally, other transcription factors in yeast are responsible for increases in expression of a significant number of stress-induced genes, such as Yap1 responding to oxidative stress and Msn2/4 as a general stress responder ⁷⁴. The structure of Hsf1 itself is dynamic and thermosensitive. Hsf1 is composed of several conserved structural elements, consisting of a DNA-binding domain, a leucine zipper motif domain required for trimerization, a serine-rich regulatory domain, and transcriptional activation domains at both the N- and C-termini. At elevated temperature, the regulatory domain unfolds while the trimerization domain zips together ⁷⁶. To attenuate the HSR signal, re-monomerization is managed by the entropic pulling action of chaperone cofactors ⁷⁷. Variability in Hsf1 potency, and thus the extent of activation of its downstream targets, is linked to the level of phosphorylation. While not necessary for basal activation, increasing levels of phosphorylation act in a non-specific manner to positively tune the intensity or “gain” of HSR activation by Hsf1 ⁷⁸. Fluctuation in the degree of Hsf1 phosphorylation was

recently shown not to be uniform cell-to-cell but instead provides plasticity in the HSR that appears to be beneficial at the population level. In a micro-Darwinian scenario, each cell's response varies and provides Hsp90-mediated adaptability that increases the likelihood of survival ⁷⁹. Several other mechanisms of Hsf1 post-translational modifications that impact activation, duration, and magnitude of the HSR also exist in eukaryotes, including acetylation and sumoylation ^{80,81}.

Interaction between Hsf1 and select protein chaperones was long thought to be a key tenet of HSR regulation, although compelling data to bolster this model were a long time coming ⁸². Decreased Hsf1 activity results in a significant decrease in expression of key chaperones, including Hsp70 and Hsp90, resulting in global cytotoxicity associated with protein aggregation ⁸³. The relationship between Hsp70 and Hsf1 has been thoroughly examined of late, as Hsp70 emerges to play a key role as a stress sensor for Hsf1. Hsp70 recognizes hydrophobic patches in polypeptides, which are typically only exposed in intrinsically disordered proteins or when a protein has been misfolded or damaged. Hsp70 was only recently found to specifically recognize both the previously defined transcriptional regulatory CE2 (conserved element 2) site in the Hsf1 C-terminal transcriptional activation domain and a newly identified site within the N-terminal activation domain, dually suppressing Hsf1's ability to activate gene expression and thus the HSR ^{10,51}. Under heat shock conditions, newly synthesized proteins are highly susceptible to damage by misfolding; indeed, misfolded proteins were demonstrated to titrate cytosolic/nuclear Hsp70 (Ssa1 in yeast) from Hsf1, thereby activating the HSR (Figure 1-4) ⁷⁸.

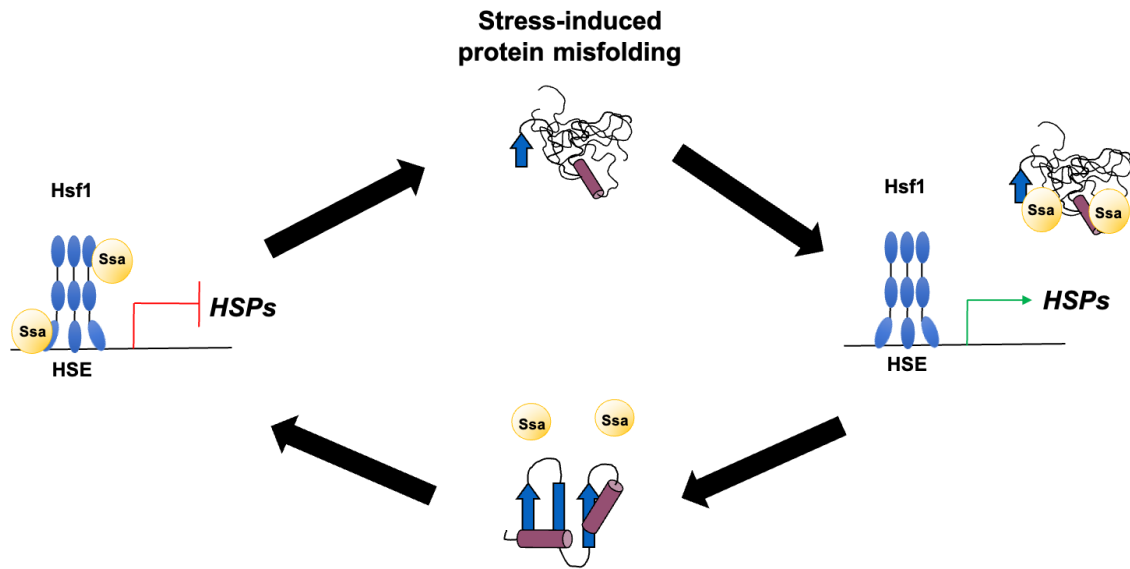


Figure 1-4: Activation and attenuation of the HSR is modulated by Hsp70

Hsp70 binds and represses activation of the heat shock response by binding to several regions within Hsf1. Upon titration away by misfolded protein substrate, Hsp70 releases Hsf1, activating the heat shock response. Upon resolution of misfolded proteins, Hsp70 returns to the Hsf1 binding regions and attenuates the stress response.

Hsp70 was shown to decrease association with Hsf1 by 77% under elevated temperature, and by nearly 100% when exposed to the proline analog compound azetidine 2-carboxylic acid (AZC) ⁸⁴. It thus appears that the prominent protein chaperone Hsp70 plays a direct feedback inhibitory role in its own production as well as governing a significant percentage of the stress- induction of the proteostasis network. As an added layer of regulation, Hsp70 is subject to several types of post-translational modifications that alter its activity and thereby affect control of the HSR through Hsf1. AMPylation, found in other eukaryotes but not yeast, was introduced into *S. cerevisiae* and shown to induce a strong cytoplasmic Hsf1-mediated HSR, similar to outcomes observed in humans and worms ⁸⁵. AMPylation was shown to reduce the ATPase functionality of cytoplasmic Hsp70 and resulted in an interesting and unexplained scenario where an increase in aggregation of α -synuclein and A β was documented, but without the usually associated cytotoxicity ⁸⁶. Deacetylation of four lysine residues within Hsp70 was also shown to occur under heat shock conditions, altering the interactome of Hsp70, activating Hsf1, and enhancing cellular thermotolerance ⁸⁷. In human HeLa cells, Hsp70 was shown to be glutathionylated on multiple cysteines, perturbing a key structural domain and resulting in diminished contact with the substrate ⁸⁸. Our lab and others have previously shown that alkylation or genetic oxidomimetic substitution of key conserved cysteine residues within Hsp70 activates Hsf1 ^{89,90}. In addition to the direct effects these modifications may have on Hsp70-dependent biology, a secondary effect on the Hsp70-Hsf1 regulatory circuit provides yet another layer of HSR control.

Recent advances have been made understanding HSR regulatory pathways outside of the canonical chaperone mechanism. As a crucial component of the translation process, tRNAs are a key factor in protein biogenesis. tRNA supply can be modified both pre- and post- synthesis to selectively manage the synthesis of specific proteins. Stress response genes are enriched in codons for rare tRNAs, meaning that under basal conditions, the production of proteins encoded by these genes is limited. Through an unknown sensing mechanism, cells increase the abundance of these rare tRNAs under stress conditions, allowing for increased synthesis of rare tRNA-containing genes ⁹¹. Existing tRNAs can also be modified, such as by thiolation. Cells deficient in a tRNA-thiolation pathway showed a constitutively activated HSR, while HS in a wild type cell showed decreased levels of thiolated tRNA compared to basal levels ⁹². This relationship may confer stress protection by decreasing translation, as tRNA thiolation is a contributing factor in the control of protein synthesis. Gene expression can also be modulated spatially by the three-dimensional organization of chromatin, changing the accessibility of genes to be bound by their co-factors. Heat shock protein genes were seen to coalesce into foci under heat stress, forming closely apposed regions of high transcription activity ⁹³. Interestingly, the dynamic reorganization is transcription factor- selective, as genes associated with Hsf1 coalesced and interacted under thermal stress, while constitutively active genes and genes under the control of another stress transcription factor, Msn2, did not ⁹⁴. The Hsf1-based HSR is thus uniquely responsive to multiple control modalities that sense changes in cellular properties ranging from translational

potency, the folding status of the proteome, physiological perturbations in temperature, and redox state, and even genome architecture.

Sensing and transcriptional response to proteotoxic oxidative stress

Due to both endogenous processes and exogenous compounds, all organisms are exposed to reactive oxygen species (ROS). ROS are generated by the partial reduction of oxygen and can lead to formation of highly reactive molecules such as hydrogen peroxide and hydroxyl radicals. Despite being a common by-product of metabolic processes, ROS can cause extensive damage to several cellular components, such as lipids, proteins, and DNA ⁹⁵. The likely primary source of endogenous ROS is via leakage of electrons from the respiratory chain in the mitochondria during the production of ATP by oxidative phosphorylation ⁹⁶. Exposure to elevated levels of these harmful compounds can overload the redox management network that cells use to maintain ROS at a tolerable threshold, and this imbalance activates an elaborate response network called the oxidative stress response (OSR), upregulating proteins that mitigate the stress via detoxification and/or increased resistance. The inefficiency or inability of the cellular machinery to neutralize ROS compounds is intimately associated with the development of several diseases such as cancer and cardiovascular diseases, along with being heavily intertwined with the cellular aging process ⁹⁵. Current research trends are focused on processes by which cells sense an imbalance in the redox environment and respond accordingly through selective changes in transcription and translation. As an example, genes classified

by their involvement in 'ATPase function', 'proteasome', and especially 'oxidation-reduction process' are significantly over-represented under heavy oxidative stress in yeast, from a pool of over 300 genes that are transcriptionally altered ⁹⁷.

Many ROS-specific regulatory mechanisms are based on the oxidation state of protein cysteine residues, in part due to the multiple oxidation states that cysteine can maintain, general reversibility, and ease of reactivity, making this residue a versatile redox sensor ^{98,99}. For example, in yeast cells experiencing hydrogen peroxide stress, cysteines in the glutathione peroxidase Gpx3 form a disulfide bridge with a cysteine of Yap1, the major positive regulator of the OSR (Fig. 1-5) ¹⁰⁰. Yap1 contains two distinct cysteine-rich domains that differentially sense oxidants to confer varying responses to stresses, such as inducing TRX2 transcription in response to H₂O₂, versus the thiol oxidant diamide as well as other thiol-chelating stressors such as heavy metals ¹⁰¹. In both scenarios, activated Yap1 translocates from the cytoplasm into the nucleus to activate expression of antioxidant genes. An analogous OSR transcriptional circuit in mammalian cells is based on the transcription factor nuclear factor-erythroid factor 2 (Nrf2). Nrf2 is regulated primarily by interaction with Kelch-like ECH-associated protein (KEAP1) that both retains the transcription factor in the cytoplasm and promotes its rapid degradation ¹⁰² (Fig. 1-5). KEAP1 is a cysteine-rich protein and multiple cysteine residues have been documented to act as sensors for oxidants and thiol-reactive electrophiles ¹⁰³. Cysteine modification ultimately results in inability to complex with Nrf2, promoting the latter's DNA binding and activation of an array of antioxidant genes that in humans play important roles in inflammation, chronic disease, and detoxification ¹⁰⁴. Msn2/4, another key positive

regulator of the OSR in yeast, is indirectly dependent on the thiol status of a zinc-coordinating cysteine residue in the thioredoxin Trx2. Oxidation of this cysteine results in a conformational change and zinc release which mediates localization of the transcription factor Msn2/4 to the nucleus through an unknown mechanism ^{105,106}. Hsf1 also responds to redox imbalance and ROS via Hsp70 in yeast and directly through reactive cysteine residues as demonstrated in mouse ^{39,89,107}. In sum a common theme is clear – ROS and other thiol-reactive molecules are sensed by multiple regulators of gene expression via protein thiols to enable rapid and specific transcription of antioxidant defense proteins. However, the sensors need not be proximal as chaperones or dedicated accessory proteins can fulfill this role to transduce the activation signal.

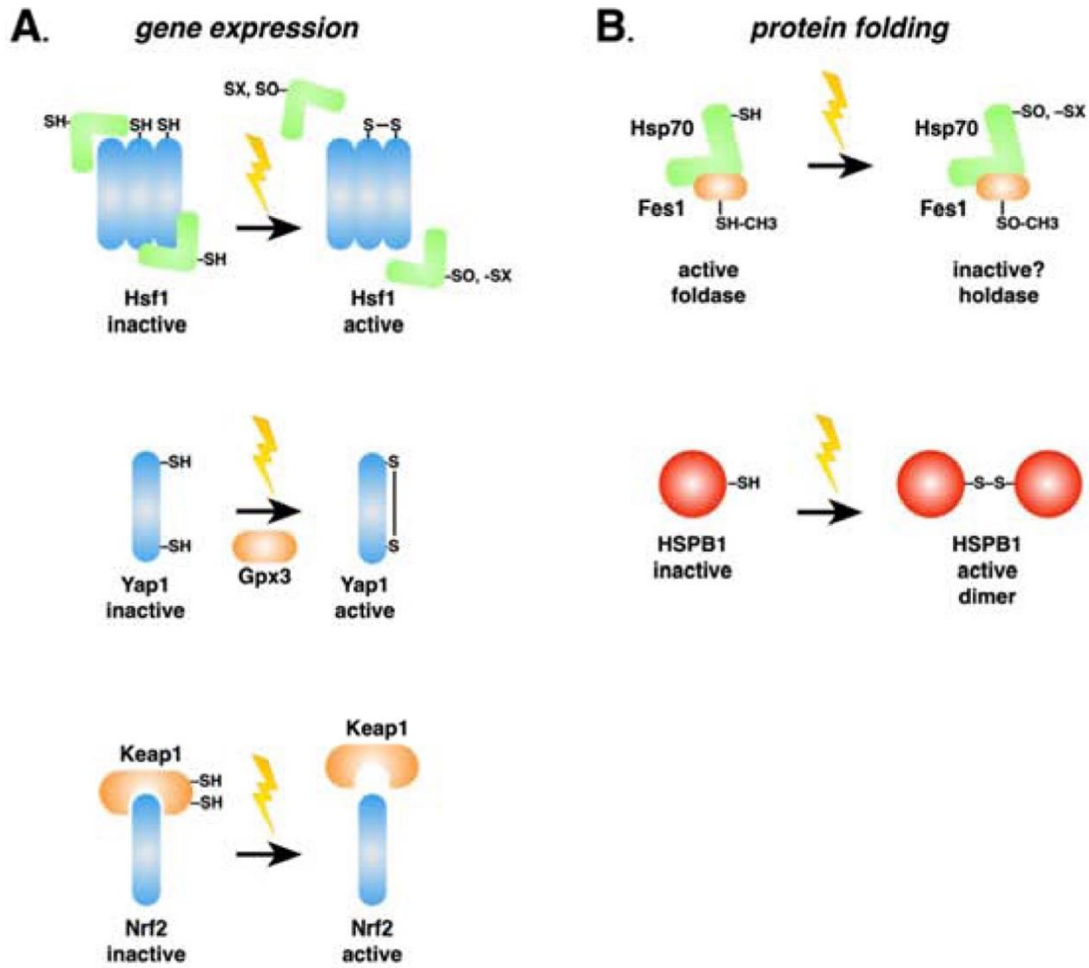


Figure 1-5: Proteotoxic oxidative stress sensing through reactive protein thiols

Figure 1-5: Proteotoxic oxidative stress sensing through reactive protein thiols

Reactive oxygen species, xenobiotics, electrophiles and heavy metals (indicated by the lightning bolts) cause protein misfolding, generating stress signals. Additionally, cytoprotective responses against these insults are induced at the levels of gene expression (A, left) and protein folding (B, right). (A) Transcriptional oxidative stress response pathways in yeast (Yap1), humans (Nrf2), or both (Hsf1) are activated via different mechanisms that share a common theme of reactive cysteines in partner proteins sensing ROS and initiating functional changes in transcription factor activity. Of note, human HSF1 possesses reactive cysteines and is capable of directly sensing ROS, while yeast Hsf1 does not and relies on Hsp70 as indicated. (B) As described in the text and as demonstrated in the case of Hsf1 regulation by Hsp70, protein chaperones are being revealed to directly sense ROS through similar means utilizing either cysteine or methionine residues. Although many questions remain unanswered, a trend of stabilizing the passive “holdase” function of chaperones is emerging, perhaps indicative of a survival strategy based on preventing further proteotoxic stress during ROS exposure and delaying refolding and repair until the danger passes.

Chaperones as sensors of proteotoxic oxidative stress

Several chaperone proteins responsible for maintaining proteostasis are directly influenced by the redox environment. Thiols can be modified in several ways, including through oxidation and nucleophilic attack (Figure 1-6). Bacterial and yeast cytosolic Hsp70 chaperones are heavily impacted by oxidation or adduction of several conserved thiols^{108–110}. Within the ER, a normally oxidizing environment, the Hsp70 BiP (Kar2 in yeast) is modified on cysteine residues based on the thiol redox state to shift from a “folding” to a “holding” chaperone¹¹¹. Fes1, an Ssa1 co-chaperone, was additionally shown to have altered function regulated by methionine oxidation (Fig. 1-5)¹¹². The yeast peroxiredoxin Tsa1 was also shown to alter behavior under redox stress, wherein hyper-oxidation of Tsa1 was a necessary component for recruitment of Hsp70 and Hsp104 to redox-damaged and aggregated proteins during aging⁹⁸. In humans, sHSPs play an important role in sensing ROS. HspB1 (or HSP27), HspB5, HspB6, and HspB8 are known to be upregulated in response to oxidative stress and hyperosmotic stress in rat hippocampal neurons [79]. HSPB1 acts as a redox-sensitive molecular chaperone through the residue Cys137. It has been proposed that Cys137 in HSPB1 modulates protein function by existing in either its oxidized (disulfide) or reduced (thiol) form (Figure 1-5)¹¹³. Although HspB1 is present in the cell as a monomer, dimer, or oligomer, it appears that HspB1 is most active as a chaperone in its dimeric form and that mutations in the intrinsically disordered region are linked with neuropathies¹¹⁴. Our lab found that two yeast sHSPs that function as misfolded protein “sequestrases” mobilize into stable compartments in yeast cells defective in redox balance due to deletion of the

gene encoding thioredoxin reductase (*trr1Δ*), suggesting that redox and proteostatic balance are deeply interconnected (Goncalves and Morano, unpublished results). Some un-liganded metal ions can be harmful due in part to their propensity to bind to free thiols as well as protein cysteine thiols, and the so-called soft metals or metalloids such as cadmium, arsenic, and chromium are highly toxic even at low micromolar concentrations and are potent inducers of the OSR ^{115–117}. Our laboratory recently showed that in experiments with yeast, cadmium induces aggregation of newly synthesized triose phosphate isomerase (Tpi1) in both yeast and human cancer cells and activates Hsp70-based recognition and sequestration of misfolded proteins ¹¹⁸. Cadmium was also shown to impair protein folding in the ER, with subsequent induction of the UPR ¹¹⁹. The presence of toxic metals can also be sensed by intermediate signal transducers as recently demonstrated for arsenic activating the transcription factor Yap8 via coordination with thiols in the MAP kinase Hog1 ¹²⁰.

Together, these results demonstrate that in addition to significant changes in gene expression of antioxidant defense proteins, various forms of redox stress are sensed directly by the main defense proteins themselves for quick-acting responses to mitigate cellular damage. How cells sense and deal with oxidative stress extends beyond maintenance of the redox state of a single cell and may also be governed at the population level. A recent study observed a bi-modal distribution of oxidation state even within a population of yeast cells of the same age ¹²¹. The transition from reduced to oxidized status could be a threshold-based phenomenon that leads to the emergence of at least two distinct cell subpopulations with different growth and survival potential in the face of chronic redox imbalance.

A.

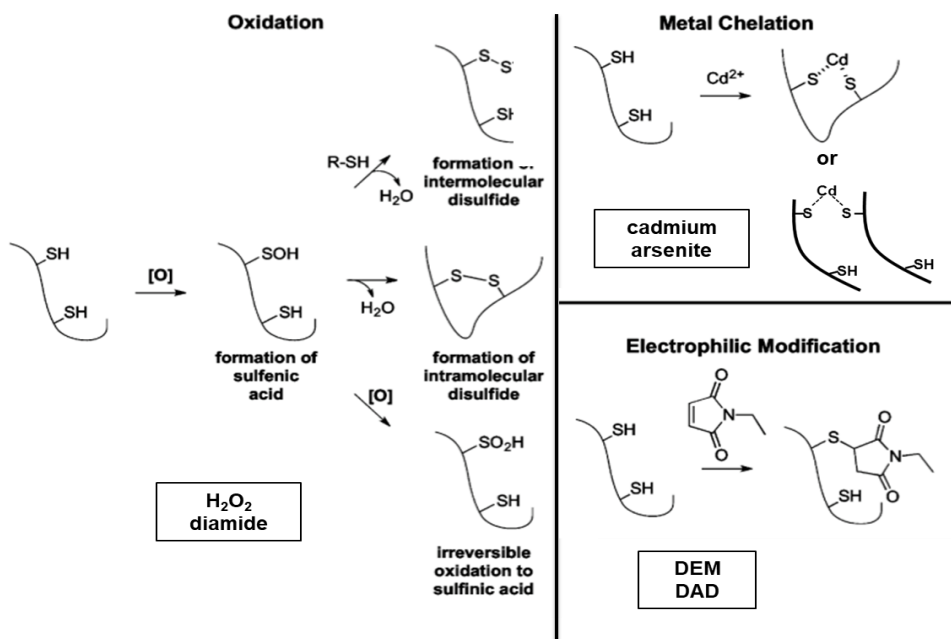


Figure 1-6: Cysteines are subject to several forms of redox state modification

Cysteines present within proteins are susceptible to several distinct forms of modification. The oxidation state of cysteine progresses through the sulfenic, sulfinic, and sulfonic states as oxidative state increases. Cysteine modification also occurs through electrophilic modification and metal chelation. (DEM=diethyl maleate, DAD=diethyl acetylene dicarboxylate). This figure was obtained with permission from West, J., Wang, Y., Morano, K.A. (2008). Small molecule activators of the heat shock response: chemical properties, molecular targets, and therapeutic promise. *Chemical Research in Toxicology*. 25, 2036-2053.

Overview of Hsp70 redox biology using genetic tools

The modelling of cysteine thiol oxidation using genetic techniques has let several groups probe the consequences of cysteine modification within chaperone proteins while reducing broad off-target effects of incubation with exogenous oxidative compounds. Particular genetic substitutions, using amino acids like aspartic acid, were used to effectively mimic the steric and electrostatic changes that occur in thiol oxidation. Oxidation-mimicking substitutions within the inducible Hsp70 of humans (HSPA1A) culminated in changes to the structure of the nucleotide binding pocket within the chaperone, resulting in deficiencies that were both enzymatic and behavioral ⁹⁰. Similarly, an unpaired cysteine residue positioned adjacent to the nucleotide binding pocket of Hsc70, a constitutive human Hsp70, had negative effects when substituted with tryptophan. Tryptophan is an aromatic amino acid, which the Sevier lab (the authors of that work) refer to as a 'bulky amino acid', as they do with aspartic acid. Tryptophan has a six sided benzene ring that was shown to produce steric changes in the surrounding residues when substituted for C17 of Hsc70 ¹⁰⁹. The crystal structure of the C17W mutant showed that a critical Mg²⁺ ion was displaced by ~2Å, due to the loss of a stabilizing water molecule from the nucleotide binding pocket. The C17W mutant was found to be heavily deficient for ATP hydrolysis ¹⁰⁹. As the platform for my work, previous work from our lab detailed how substitution of two cysteine residues (C264, C303) with aspartic acid generated a stimulation of the heat shock response in cells, even when under non-stressed conditions, and resulted in a slowed growth phenotype ⁸⁹. Aspartic acid mimics the

structural and electrical characteristics of sulfinic acid, an oxidized thiol form. Meanwhile, substitution of the same cysteines with the non-modifiable amino acid serine did not stimulate the same constitutive stress response activation, but also did not demonstrate a cytoprotective response when exposed to 600 μ M Cd²⁺ followed by an elevated heat shock, as the wild type cysteines were able to ⁸⁹. This work also found that substitution of C15 destabilized the Ssa1 protein and that response to thiol-reactive compounds was largely abolished in the C264S, C303S mutant, suggesting that C15 does not play a significant role in oxidative sensing.

Oxidomimetic mutations also altered the behavior of the endoplasmic reticulum-localized Hsp70 protein BiP from that of a protein-maturation assisting 'foldase' into a less functional, enzymatically reduced holdase state, passively binding substrates for increased time, without regulated release. This functional modulation promoted an increased cell survival rate under conditions of oxidative stress, but had negative consequences for growth under non-stress conditions ¹¹¹. While increased interaction between this oxidomimetic form of BiP (C63D) and misfolded polypeptide substrates promoted a protective behavior against oxidative stress, a C63H substitution that mirrors the steric bulkiness but not the electric charge of a sulfinic acid was demonstrated to have a dominant negative effect in non-stress conditions, possibly from an increased holdase activity that did not allow proper folding and secretion of protein substrates ¹²². The enzymatic consequences of oxidative mimics using amino acid substitution mirror the deficiencies in nucleotide interactions, ATP hydrolysis activity, and protein refolding seen from exogenously added oxidizing or alkylating compounds ^{90,123,124}. Glutathionylation of cysteines within the Hsp70s of

HeLa cells caused disturbances in substrate recognition and binding, again supporting the concept that Hsp70 cysteines are both highly reactive and functionally vulnerable amino acids ⁸⁸.

This work is a continuation of the work previously established in our lab, detailing the elevated stress response in *S. cerevisiae* cells that carried a C264D, C303D mutation in the *Ssa1* gene, as detailed above. To better detail the functions of C264 and C303 within *Ssa1* as oxidative stress sensors and susceptible targets, as well as the downstream consequences of thiol stress on general *Ssa1*-dependent proteostasis, I performed an approach that made use of both biochemical tactics and genetics. In Chapter 3, I use isolated *Ssa1* WT proteins, as well as the non-reactive *Ssa1*-2CS and the dual sulfinic acid mimic *Ssa1*-2CD (C264D, C303D) to determine the effects of these substitutions on a variety of critical Hsp70 roles *in vitro*, including nucleotide binding, ATP hydrolysis, and the refolding of chemically denatured protein. Exogenous oxidation was then performed to address WT behavior under oxidant exposure. In Chapter 4, I use the same genetic mutations *in vitro*, detailing the impact of thiol oxidation mimicking on several *Ssa1*-mediated proteostatic roles in the more complex system of a living organism. In Chapter 5, I analyze data within the OxiMouse database to explore events of cysteine oxidation in murine Hsp70s across various tissue types and age groups. As a whole, this work gives evidence to a model wherein cysteines within the primary, constitutive cytosolic Hsp70 chaperone are susceptible to modification by oxidative stressors that detractively impacts protein homeostasis but also simultaneously activates the heat shock response to promote a cytoprotective cascade.

Chapter II: Materials and Methods

This research was originally published in the Journal of Biological Chemistry. Santiago A, Morano KA. Oxidation of two cysteines within yeast Hsp70 impairs proteostasis while directly triggering an Hsf1-dependent cytoprotective response. J Biol Chem. 2022 Aug 25:102424. doi: 10.1016/j.jbc.2022.102424. © the American Society for Biochemistry and Molecular Biology or © the Author(s). *JBC does not require permission to use published materials in one's dissertation:* <https://www.elsevier.com/about/policies/copyright/permissions>.

Strains, plasmids and yeast cultivation

Yeast strains were derived from either DS10 (*MATa ura3-52 lys1 lys2 trp1-1 his3-11,15 leu2-3112*) or BY4741 (*MATa, his3Δ1; leu2Δ0; met15Δ0; ura3Δ0*) parent strains. The *ssa1Δssa2Δ* strain (*SL314, MATa ura3-52 lys1 lys2 trp1-1 his3-11,15 leu2-3112 ssa1::HIS3, ssa2::LEU2*) was generously provided by the Craig laboratory and is isogenic with DS10⁴¹. Complementation of the lethal *ssa1Δssa2Δ ssa3Δssa4Δ* strain was conducted using a standard yeast plasmid shuffle technique, with a *URA3*-based *SSA1*-expressing plasmid (a kind gift from the Truman laboratory). The *SSA1* allele plasmids (p413TEF, p413CYC and p423GPD) were constructed by PCR mutagenesis and amplification of the *SSA1* ORF using standard cloning methodology with 5' *SpeI* and 3' *XhoI* restriction sites. All mutants were confirmed using DNA sequencing. All plasmids were transformed into yeast using the rapid yeast transformation protocol¹²⁵. The FLAG-tagged Hsf1-expressing plasmid was used as previously published¹⁰. The pTHD3HA-tGND-GFP plasmid was a kind gift from Dr. Randolph Hampton, University of California, San Diego. The HSE-lacZ plasmid was reported previously¹²⁶. The p425MET25-FFL-GFP-leu2::URA3 plasmid was used as previously described¹²⁷. The 6XHis-Smt3-SSA1 plasmid was kindly provided by Dr. Nadinath Nillegoda (Monash University, Australia). *S. cerevisiae* strains were cultured in yeast extract, peptone, dextrose medium (YPD) or synthetic complete (SC) medium (Sunrise Science, San Diego, CA). For growth curve analysis, cells were grown overnight at 30°C. Cells were then sub-cultured and grown to mid-log phase ($OD_{600}=0.6-0.8$), then diluted to $OD_{600}=0.1$ in fresh media. Growth was monitored using a Synergy MX (BioTek, Winooski, VT) microplate reader for 16 hours

with shaking at 30°C. Petri plate growth analysis was for two days at 30°C. Cells containing the HSE-*lacZ* reporter were grown to log phase, and diluted to OD₆₀₀=0.8. 50uL of Beta-Glo reagent (Promega, Madison, WI) and 100 uL of liquid culture was added to each well in a 96-well microplate and measured for beta galactosidase activity using the Synergy MX (BioTek) microplate reader.

Protein purification

Proteins were isolated as previously described, with several alterations ¹²⁸. Briefly, *SSA1* coding regions were amplified from p413TEF plasmids and subcloned into the pSUMO vector with a 6XHis-Smt3 tag (gifted from the Nillegoda laboratory) ^{128,129}. Plasmids were transformed into BL21(DE3) *E. coli* additionally containing the pRARE plasmid and grown overnight in LB Amp/Kan at 37°C. Subcultures were then grown to log phase (OD₆₀₀=0.6) and expression was induced with 0.5 mM IPTG (MilliporeSigma, St. Louis) for 3 hr at 30°C, then cells were collected by centrifugation, washed, and flash frozen for storage at -80°C. The following day, cells were lysed in 30 mL Buffer K (50 mM HEPES-KOH, pH 7.5, 750 mM KCl, 5 mM MgCl₂) with DNase, RNase, protease inhibitors (PI), and 1 mM PMSF. Suspensions were sonicated on ice to lyse, and cell debris was removed by centrifugation for 10 min at 12,500 RCF at 4°C. Supernatant was removed, and the suspension was again centrifuged. The supernatant was brought up to 30 mL with Buffer K and nutated for 1 hr at 4°C with 1 mL bed volume of Buffer K-equilibrated His-Pur cobalt resin (Thermo Scientific), adding 30 uL fresh PI, 1 mM PMSF, and 50 uL of 100 mM ATP (pH 7.5). The suspension was centrifuged at 4°C for 10 min at 9,000 RCF, and supernatant was

removed. The resin was washed twice with 30 mL of Buffer KC (50 mM HEPES-KOH, pH 7.5, 750 mM KCl, 5 mM MgCl₂, 30 mM imidazole) plus fresh PI and PMSF. Washes consisted of resuspension and hand nutation for 30 sec, 3 min on ice, a 2 min spin at 5,500 RCF in chilled rotors, 3 additional min on ice, followed by supernatant removal. Final supernatant was removed, and the resin was incubated three times with 500 uL of Buffer KE (50 mM HEPES-KOH, pH 7.5, 750 mM KCl, 5 mM MgCl₂, 300 mM imidazole), centrifuged for 30 sec at 6,000 RCF and supernatant was passed through a filter column to elute proteins. All elutions were then concentrated by Vivaspin column (Cytiva) and placed into dialysis tubing, then incubated overnight with stirring in 1 L of chilled Buffer KL (50 mM HEPES-KOH, pH 7.5, 30 mM KCl, 5 mM MgCl₂) to remove imidazole. The SUMO protease Ulp1 (lab isolated) was added to the dialyzed protein sample and incubated at room temperature for 1 hr. 500 uL of Buffer KL-equilibrated resin was added, and the mixture was nutated at 4°C for 1 hour. A filter column was used to separate beads from cleaved protein isolate. 10% glycerol was added and proteins were either frozen at -80°C or immediately further purified using an AKTA pure ion exchange chromatography system (Cytiva) and HiTrap Q HP columns (Cytiva), testing fraction activity by quantifying ATP hydrolysis. Proteins were again concentrated with 10% glycerol, separated into aliquots and snap-frozen at -80°C. Isolated Ydj1 was a generous gift from Elizabeth Craig and Sse1 was from a previously isolated laboratory stock³⁴. Purified Hsp104 protein was a kind gift of the Tsai laboratory (Baylor College of Medicine).

ATP binding assay

For each respective protein sample, 25 μL of ATP-agarose (MilliporeSigma) bead volume was washed three times with 1 mL chaperone buffer (50 mM HEPES-KOH, pH 7.5, 50 mM KCl, 5 mM MgCl_2 , 5 mM DTT) in a siliconized tube. Beads were resuspended in 500 μL chaperone buffer with 1 μM final concentration of protein isolate. Suspensions were nutated at 4°C for 30 minutes and washed five times with 1 mL chaperone buffer + 1.5% Triton X-100 (30 sec spin at 6,000 RCF, on ice in between). After removing supernatant, beads were transferred to a new siliconized tube to negate tube-bound protein and 50 μL of chaperone buffer plus 50 μL of 2X SDS-PAGE sample buffer were added, followed by incubating at 65°C for 20 min prior to gel loading to elute proteins.

ATPase assay

ATP hydrolysis was determined using a malachite green-based assay (MilliporeSigma) to measure phosphate release. Purified Ssa1 was diluted to 0.1 μM , with or without 0.2 μM Ydj1, in 20 μL total volume of reaction buffer in a 96-well plate. 10 μL of 4mM ATP was added to each well, and the plate was incubated with a cover for 90 min at 30°C, followed by the addition of 150 μL of the malachite green reagent. The colorimetric reaction proceeded for 30 min at room temperature before measuring absorbance. Absorbance values were read and converted to picomoles of phosphate using a standardized phosphate curve. Values are reported as specific activity (pmol ATP/ μg Hsp70/min).

in vitro firefly luciferase recovery assay

Refolding of denatured FFL was assessed as reported previously, with slight alteration¹²³. In short, 200 μ M FFL protein was incubated 1:1 with denaturing buffer (50 mM HEPES-KOH, pH 7.5, 50 mM KCl, 5 mM MgCl₂, 5 mM DTT, 3 M guanidinium HCl) at room temperature for 30 min to denature. Denatured FFL (1 μ M) was added to a chaperone mixture containing the respective Ssa1 (0.1 μ M), Ydj1 (0.2 μ M), Sse1 (0.05 μ M), 5 mM ATP, and Hsp104 when applicable (0.1 μ M), then brought to a final reaction volume of 100 μ L with chaperone buffer. 5 μ L of reaction mixture was diluted into a well containing 200 μ L of chaperone buffer prior to measurement. To measure activity of properly folded luciferase, 20 μ L of luciferin (222 μ M) was added to 10 μ L of chaperone buffer, and 10 μ L was auto-injected into each well and chemiluminescence signal measured. Activity was determined at indicated time points, and raw numbers were converted to a percentage through comparison to activity of a non-denatured control in the same volume.

Treatment of chaperones with hydrogen peroxide

A hydrogen peroxide oxidation regimen was amended from a previously described protocols⁹⁰. Ssa1 proteins (5 μ M) were incubated with 1 mM hydrogen peroxide for 1 hr at 37C, followed by 50-fold dilution to final assay concentration. For subsequent reduction, WT was incubated with 20 mM DTT after hydrogen peroxide treatment, and the mixture allowed to incubate at room temperature for 10 min, as previously described¹²⁴.

Trypsin digestion

Chaperones were subjected to trypsin digestion as previously described¹³⁰. In short, 1.5 ug of Ssa1 was incubated with 1 mM of the respective nucleotide for 10 min at room temperature. Trypsin (1 mg/mL) was then added and reactions incubated for 20 min at room temperature, before stopping the reaction by adding 6X SDS-PAGE sample buffer.

Preparation of cell extracts and immunoblotting

Cells were grown overnight, sub-cultured and grown to mid-log phase ($OD_{600}=0.6-0.8$). Proteins were extracted by glass bead lysis as previously described¹³¹. Proteins were analyzed by separation on SDS-PAGE gels (8-12%) and transferred to polyvinylidene difluoride (PVDF) membrane (EMD Millipore). Immunoblots were imaged using an anti-Ssa1/2 polyclonal antibody at a 1:10,000 dilution, anti-FLAG mAb at a 1:4,000 dilution (MilliporeSigma), or anti-GFP at a 1:5,000 dilution (Roche) using a previously described procedure¹³¹. Blots were sprayed with WesternBright ECL-spray (Advansta) and imaged using the ChemiDoc MP Imaging System (Bio-Rad). Bands were quantified using Image Studio Lite (LI-COR Biosciences). To monitor chaperone stability, 100 ug/mL cycloheximide was added to log phase cultures.

Hsf1 immunoprecipitation

Immunoprecipitation was performed as previously described¹⁰. In short, 30 mL of cells were lysed by glass beads, and total lysate was co-incubated with anti-

FLAG M2 Affinity gel (MilliporeSigma) in a total volume of 700 μ L of TEGN buffer (20 mM Tris-HCl, pH 7.9, 0.5 mM EDTA, 10% glycerol, 50 mM NaCl), plus protease inhibitors (PI), nutating for 2 hr at 4°C. Beads were washed eight times using 750 μ L of TEGN + PI, followed by elution of proteins using 40 μ L of FLAG peptide (200 μ g/mL) at room temperature for 25 min. 6X SDS-PAGE sample buffer (350 mM Tris-HCL, pH 6.8, 36% glycerol, 10% SDS, 5% beta-mercaptoethanol, and 0.012% bromophenol blue) was added to samples and incubated at 65°C for 20 min to elute.

Fluorescence microscopy

For all experiments, yeast live cells were imaged as described previously¹¹⁸. In short, cells were wet-mounted on slides and imaged using the 100x objective of an Olympus IX81 microscope, using a FITC filter to visualize GFP. For each experiment, identical exposure times were used. For foci counts, strains were grown overnight in SC-HIS-URA and late growth stage cells were imaged.

In vivo FFL assays

FFL-GFP *de novo* assays were carried out as previously specified¹²⁷. Briefly, indicated strains containing the 413TEF *SSA1*-expressing plasmid and p425MET25-FFL-GFP-leu2::URA3 were grown overnight in SC-URA-HIS at 30°C. 100 μ L additional methionine was added to repress plasmid expression. Cells were sub-cultured in fresh media to log phase $OD_{600}=0.8$, 5 mL of cells were harvested by centrifugation, and washed to remove all methionine. Cells were resuspended in 5

mL of SC-URA-MET to induce FFL-GFP expression and activity was measured at the indicated time points by adding 10 μ L of 222 nM luciferin in a microplate reader. Refolding assays were performed similarly to *de novo* FFL activity assays, but after 1 hr of induction, 100 mg/mL of cycloheximide was added to stop protein synthesis. Cells were then subjected to heat denaturing at 42°C for 15 min, then incubated at 30°C for recovery. FFL-GFP activity was measured by adding 10 μ L of 222 nM luciferin in a microplate reader or imaged for foci.

tGND-GFP protein turnover

Steady state levels of the terminally misfolded protein tGND were performed essentially as described ¹³². In brief, BY4741 *ssa1 Δ ssa2 Δ* cells containing the pTHD3HA-tGND-GFP plasmid and relevant p413TEF *SSA1* allele plasmid were grown to early log phase in SC-HIS-URA ($OD_{600}=0.5$). 1 mL of cells were collected, washed, resuspended in 177 μ L of 1.85 M NaOH and left on ice for 10 min. 177 μ L of cold 55% trichloroacetic acid was added, and the sample incubated on ice for an additional 10 min. Cells were centrifuged in a cold room at 7,200 RCF for 1 min and supernatant removed. The pellet was resuspended in 500 μ L of ice-cold acetone and centrifuged. The supernatant was removed and 100 μ L per OD of 2X urea buffer (1 % SDS, 8 M Urea, 10 mM MOPS, 10 mM EDTA, pH 6.8, 0.01 % bromophenol blue, 1 mM PMSF) was added. Suspensions were sonicated for 5 min and samples placed at 65°C for 20 min, followed by an additional 5 min of sonication. Cells were again centrifuged and supernatant was moved to a new tube and frozen prior to SDS-PAGE separation and immunoblot. For microscopy, cells were grown to early log phase

(OD₆₀₀=0.5) in SC-HIS-URA and 100 ug/mL cycloheximide was added to cultures. Cells were imaged for foci at relevant time points.

OxiMouse Database Analysis

The OxiMouse database was accessed through the searchable portal at <https://oximouse.hms.harvard.edu/sites.html>. Search terms included 'Hsp70, Hsc70, 70kDa, and Hsp110, and 110kDa'. All data was extracted into Microsoft Excel and cysteine oxidation events were divided into groupings of single proteins with all relevant cysteine sites within that protein in a single group. Significant events were quantified by dividing the % population of each singular cysteine site between old mouse/young mouse, with a minimum threshold of 1.5. All ten tissue types were examined.

Statistical analysis

Student's *t*-test was used to analyze mean differences between conditions. Prism 9 (GraphPad Software) was used to analyze averages of end point measurements of each time point and calculate standard error of the mean. For all significant tests, **p*=0.05; ***p*=0.005; ****p*=0.0005; *****p*=0.00005.

Table 2-1: Strains and plasmids used in this study

| <u>Strain</u> | <u>Source</u> |
|--|------------------|
| DS10 (<i>MATα</i> , <i>-leu2</i> , <i>trp1-1</i> , <i>ura3</i> , <i>his3</i> , <i>lys2</i> , <i>GAL2</i>) | Lab of E. Craig |
| DS10 ssa1Δssa2Δ (<i>MATα</i> , <i>ura3-52</i> , <i>lys1</i> , <i>lys2</i> , <i>trp1-1</i> , <i>his3-11,15</i> , <i>leu2-3112</i>) | Lab of E. Craig |
| BY4741 (<i>MATα</i> , <i>his3Δ1</i> , <i>leu2Δ0</i> , <i>met15Δ</i> , <i>ura3Δ0</i>) | Lab of K. Morano |
| BY4741 ssa1Δssa2Δssa3Δssa4Δ pURA3-SSA1-WT (<i>MATα</i> , <i>his3Δ1</i> , <i>leu2Δ0</i> , <i>met15Δ</i> , <i>ura3Δ0</i>) | Lab of A. Truman |
| <u>Plasmid</u> | <u>Source</u> |
| 413-TEF-HSF1-GFP-FLAG | Peffer, 2019 |
| 413TEF-ssa1-WT | This study |
| 413TEF-ssa1-2CS | This study |
| 413TEF-ssa1-2CD | This study |
| 413CYC-ssa1-WT | This study |
| 413CYC-ssa1-2CS | This study |
| 413CYC-ssa1-2CD | This study |
| 423GPD-ssa1-WT | This study |
| 423GPD-ssa1-2CS | This study |
| 423GPD-ssa1-2CD | This study |
| 6XHis-Smt3-SSA1-WT | Nillegoda, 2016 |
| 6XHis-Smt3-SSA1-2CS | This study |
| 6XHis-Smt3-SSA1-2CD | This study |
| pTHD3HA-tGND-GFP | Singh, 2020 |
| p425MET25-FFL-GFP-leu2::URA3 | Abrams, 2014 |
| 416TEF-HSE-lacZ | Trott, 2008 |

Chapter 3: In vitro analysis of Ssa1 cysteine modification

This research was originally published in the Journal of Biological Chemistry. Santiago A, Morano KA. Oxidation of two cysteines within yeast Hsp70 impairs proteostasis while directly triggering an Hsf1-dependent cytoprotective response. J Biol Chem. 2022 Aug 25:102424. doi: 10.1016/j.jbc.2022.102424. © the American Society for Biochemistry and Molecular Biology or © the Author(s). *JBC does not require permission to use published materials in one's dissertation:* <https://www.elsevier.com/about/policies/copyright/permissions>.

Introduction

Chaperone cycling between an Hsp70 and the co-chaperones Hsp40 and Hsp110 can be segmented into three distinct phases. These phases rely on an inter-dependent relationship between nucleotide, chaperone-chaperone interactions, and the conformation of the chaperones themselves. Categorically, these phases can be defined loosely as binding, conformational interaction, and release. Initially, Hsp40 recognizes and binds substrate delivering it to the substrate binding domain of the Hsp70⁵⁸. For this first step to occur, it is imperative that the SBD of Hsp70 be open and ready to receive substrate, which only occurs after the binding of ATP¹⁴. The docking of Hsp40 to Hsp70 stimulates ATP hydrolysis, in conjunction with the binding of substrate itself. The catalytic activity of Ssa1 is $k_{cat}=0.031$, but when incubated individually with the respective co-chaperones, Ydj1 stimulates the rate of Hsp70 ATPase activity by a factor of at least 10.2, and the Hsp40 Sis1 stimulates ATPase activity by a factor of 8.1¹³³. Hydrolysis alters the conformation of Hsp70, closing the 'lid' of the SBD and pulling the linker into a docking position, causing interaction of the NBD and SBD⁴, forming the 'closed' position. Hsp70 will remain in this position until the release of the ADP molecule and subsequent binding of a new ATP molecule. To continue the cycle, an Hsp110 NEF aids in the release of the ADP, allowing a new ATP to bind³⁵.

In this study, I wanted to understand the effects that genetically mimicked and exogenous oxidation of the two cysteines in question, C264 and C303, had on Ssa1 enzyme activities and cellular roles. Miyata et. al. performed an *in-silico* modelling of homologous cysteine oxidation mutants in the human stress-inducible Hsp70 protein,

finding that there was a potential conformational change within the NBD that shifted critical residues away from being able to properly stabilize the phosphates within a bound ATP⁹⁰. This impaired stabilization was predicted to result in reduced capacity to properly interact with nucleotide. Their mimicked and exogenously oxidized Hsp70 experiments, through incubation of isolated proteins with both hydrogen peroxide and methylene blue, showed a reduction in ATP hydrolysis and alterations in several other chaperone behaviors due to cysteine oxidation. Using mass spectrometry, the researchers found that the modified cysteines were C267 and C306, homologs of the cysteines that my work is exploring. In the following set of experiments, I perform similar *in vitro* assays to determine the role of cysteine oxidation within Ssa1 on each step of the chaperone cycling process to assess whether the functional consequences of cysteine modification are conserved. I examined ATP binding, ATP hydrolysis, limited trypsin digestion, and functional refolding of chemically denatured FFL to assess each stage of chaperone cycling and the resultant chaperone capabilities of Hsp70, using both exogenous oxidation and mimicked oxidation. Interactions between Hsp70 and its co-chaperones are also critically important, so I took additional consideration to alter the ratios and presence of co-chaperones in several experiments, to determine whether cysteine oxidation extended beyond Hsp70 and has inter-protein effects.

Obtaining the proteins to perform the *in vitro* experiments was no small feat, as several months were spent in determining the optimal method of protein expression and extraction. Initially, yeast proteins were used to over-express Ssa1, as a natively-expressed protein would be subjected to the correct post-translational

modifications. However, an overexpression of Ssa1 is detrimental to yeast growth, so the resulting protein yields were limited. Alternatively, *E. coli* was used to express the Hsp70s to a much greater extent, but the extracted Hsp70s were less enzymatically active than previously reported in literature. After this initial attempt of mine, Yoo et. al. published a paper that described a fractionation of *E. coli*-derived Ssa1 proteins via ion chromatography, in which two populations of Ssa1 were isolated. A larger subgroup that was less enzymatically active, and a smaller subgroup that was able to hydrolyze ATP at previously reported levels ¹³⁴. They were able to separate the two subgroups using ion chromatography. I mirrored their protocol, and found that my isolated protein was similarly able to hydrolyze ATP to the expected amount, but that it greatly reduced the yield of overall protein that I was able to isolate. This functional subgroup formed the chaperone pool that allowed me to perform the following assays. The following chapter details my work into exploring the enzymatic and functional impacts of mimicked and exogenous oxidation on cysteines C264 and C303 *in vitro*. I found that the Ssa1-2CD protein was significantly hindered in the ability to bind and hydrolyze ATP, as well as to refold chemically denatured substrates. These effects were mirrored by exogenous oxidation of the Ssa1-WT protein, but were largely not seen in the Ssa1-2Cs protein. Additionally, it was observed that the tryptonization profile of Ssa1-2CD was different compared to Ssa1-WT and Ssa1-2CS when incubated with a non-hydrolyzable nucleotide analog, and that the presence of Hsp104 did not remedy the Ssa1-2CD substrate refolding deficiency.

Results

Ssa1 oxidation reduces ATP binding and hydrolysis

The conformational changes between the NBD and SBD that allow Hsp70 chaperones to iteratively bind and release substrate are dependent on allosteric signals from interactions with nucleotide, substrate, and co-chaperones. This process was previously shown to be disrupted by exogenous treatment with thiol-reactive compounds¹²³. The sulfhydryl alkylating reagent *N*-ethylmaleimide negated the ability of yeast *Ssa1* to bind ATP-agarose, as well as to hydrolyze ATP¹²⁴. Human Hsc70 and Hsp70 were also both shown to be susceptible to thiol modification, with detrimental effects on ATP hydrolysis^{90,109}. To continue exploring the Hsp70/nucleotide relationship and to confirm the relevancy of thiol modification, I generated and purified to homogeneity recombinant *Ssa1* proteins with the wild type cysteines, serine substitutions (*Ssa1*-2CS), or aspartic acid substitutions (*Ssa1*-2CD) at cysteines 264 and 303^{89,128} (Fig. 3-1). Because binding of ATP within the NBD generates an allosteric signal to induce conformational change of Hsp70, I hypothesized that modification of C264 and C303 would alter the ability of *Ssa1* to interact with nucleotide, similarly to what was found by Miyata, *et. al.* when they modelled the oxidation of the homologous stress-induced human Hsp70 *in silico*⁹⁰. Originally, I attempted several protocols for yeast and bacterial expression of plasmids obtained from our stock library, including both a thrombin-cleavable *E. coli* expression plasmid and a FLAG-tagged yeast expression plasmid.

A

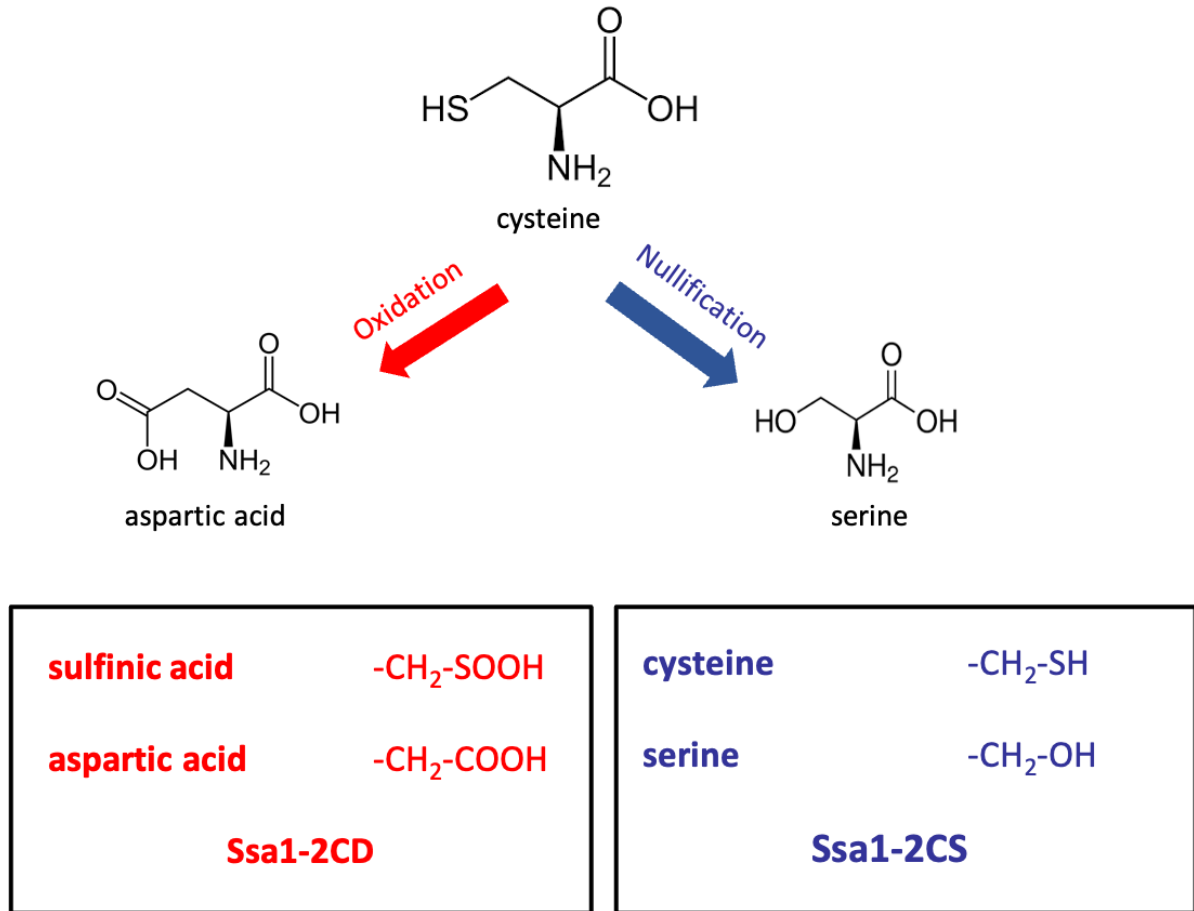


Figure 3-1: Cysteine substitution mutants reflect states of oxidation

Substitution of cysteines C264 and C303 within the NBD of Ssa1 reflect the potential oxidation states of cysteine. Substitution of cysteine with aspartic acid structurally reflects the secondary oxidation of a cysteine, sulfinic acid (red). Substitution of cysteine with serine structurally reflects a cysteine that is non-reactive to thiol modification (blue).

The yeast expression vector was not able to produce effective levels of protein on a practical timeline, and the thrombin cleavable plasmid product was not fully cleaved in my attempts. I settled on a His₆-SUMO-tagging plasmid that allowed for high levels of expression and very clean purifications due to ease in the tag removal process. Haniel Yoo, of the Drummond lab at the University of Chicago, published a finding that documented how anion-exchange ion chromatography of *E. coli*-derived Ssa1 protein was able to separate two populations of Ssa1, one more enzymatically active and one less enzymatically active. I repeated her ion chromatography protocol and found that I also had two distinct populations, one that approached 10 pmol phosphate/ug Hsp70/min, and a less-active population that had a 10-fold reduction in activity (Figure 3-2). The first peak, accounting for the majority of the isolated protein, was not optimally functional for ATP hydrolysis. Ssa1 collected from the second, smaller, peak, exhibited ATPase activity similar to reported levels. The two peaks are indicative of possible different net charge of the two populations, as each peak is subsequently released from the positively-charged anion-exchange chromatography column as the ionic concentration increases. For this approach, I used a gradient increasing gradually from 0 to 1 M NaCl, and this indicates that the second, relatively more functional peak, had a higher degree of binding strength to the chromatography column. Once the fractions were separated, I found that our isolations also reported values of ATP hydrolysis that were comparable to published Hsp70 values (~8 pmol phosphate/ug Hsp70/min⁹⁰) and repeated the process for the 2CS, and the 2CD mutant isolations (Figure 3-3).

A

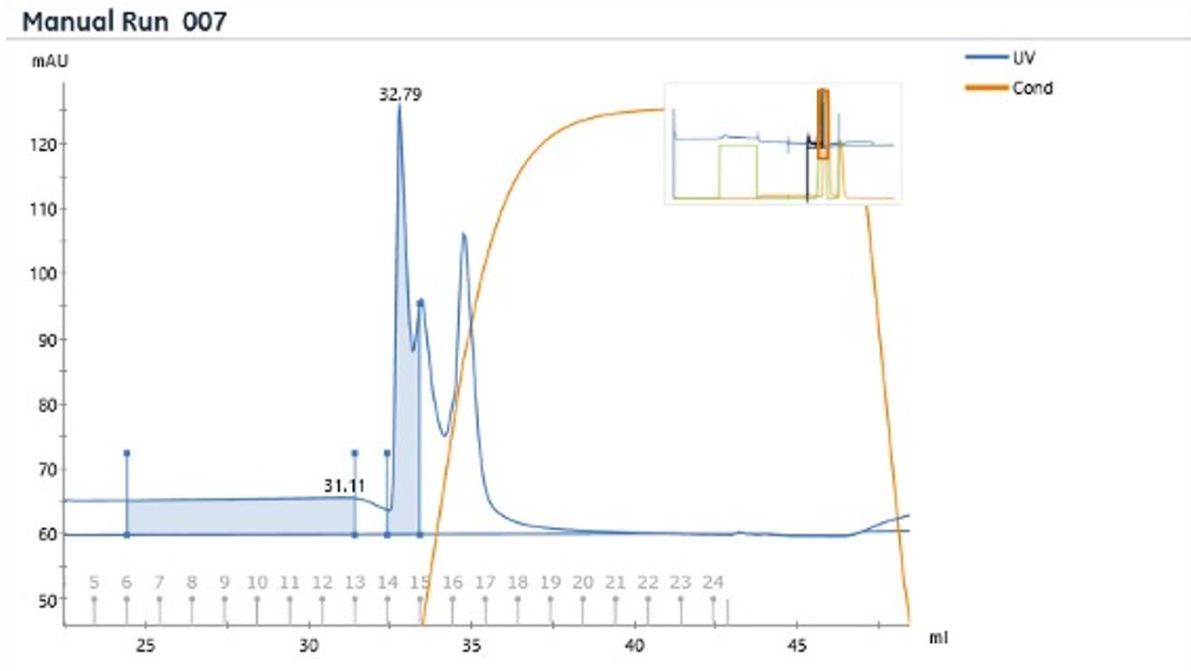


Figure 3-2: Ion chromatography separates Ssa1 subgroups of varying functionality

(A) Using a Hi-Trap Q anion-exchange chromatography column, isolated Ssa1 mutant proteins were separated using a gradient of 0M-1M NaCl in Chaperone Buffer. The 0.5mL fractions of separation are listed at the bottom. The orange line indicates conductivity, and the blue line is a measure of ultraviolet absorbance, indicating protein concentration.

A.

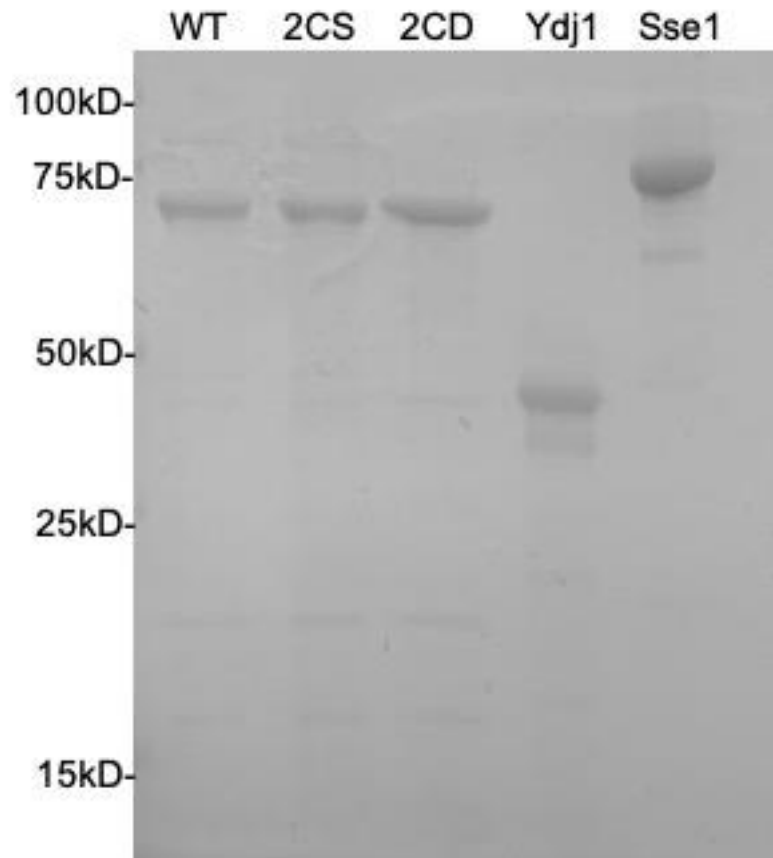
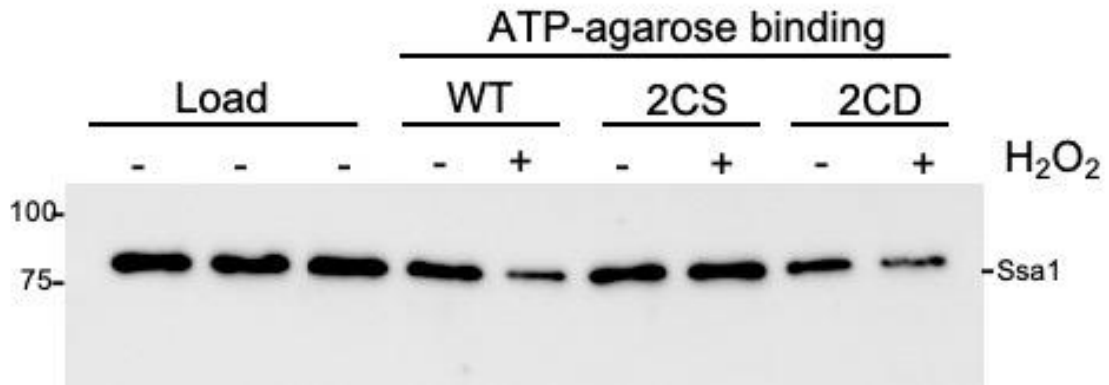


Figure 3-3: Purification of Ssa1 variants and co-chaperones

(A) Isolated Ssa1 proteins containing wild type cysteine, cysteine to aspartic acid mutations, and cysteine to serine mutations are stable in isolation. Previously isolated co-chaperones Ydj1 and Sse1 are also shown. Each well contains between 2.5 and 8 μ g of isolated protein, suspended in an SDS-PAGE gel and stained with One-Step Blue protein stain (Biotium).

The first category of Ssa1 functionality that I wanted to measure was ATP-binding ability. If the findings of the homologous cysteines in the human stress-inducible Hsp70 modelling were also reflected in an Ssa1 protein with similar mutations, I expected the ability to bind nucleotide to be altered due to the misalignment of critical residues within the nucleotide binding pocket. To test this hypothesis, I measured nucleotide binding ability using ATP-agarose chromatography. Purified proteins were incubated with ATP-agarose, followed by several washes and elution with sample buffer and immunoblot. Initial tests proved to be contaminated by residual protein which had bound to the inner surface of the microcentrifuge tube. The strength of binding also proved to be unexpectedly strong, and iterative levels of Triton X-100 detergent were added until protein began to release from the column. Additionally, the proteins were found to take less than expected amounts of time to bind the column. Initial extended incubation times of one hour in a refrigerated setting did not result in more bound protein than a 20-minute incubation time, suggesting very rapid binding, as well as decreasing the amount of spontaneous release that may happen with extended incubation. Comparable amounts of Ssa1 (WT) and Ssa1-2CS were eluted from the ATP-agarose beads after incubation, while the Ssa1-2CD protein was unable to bind to the same extent (Fig. 3-4A, quantitated in Fig. 3-4B). Hydrogen peroxide was added as an exogenous oxidant, to monitor the effects of WT cysteines that were receptive to modification. Incubation of an isolated protein with an exogenous oxidant actively reflects the exposure of Ssa1 to an abundantly oxidized cellular environment, and the results I found lend credibility to the genetic substitution mutant.

A.



B.

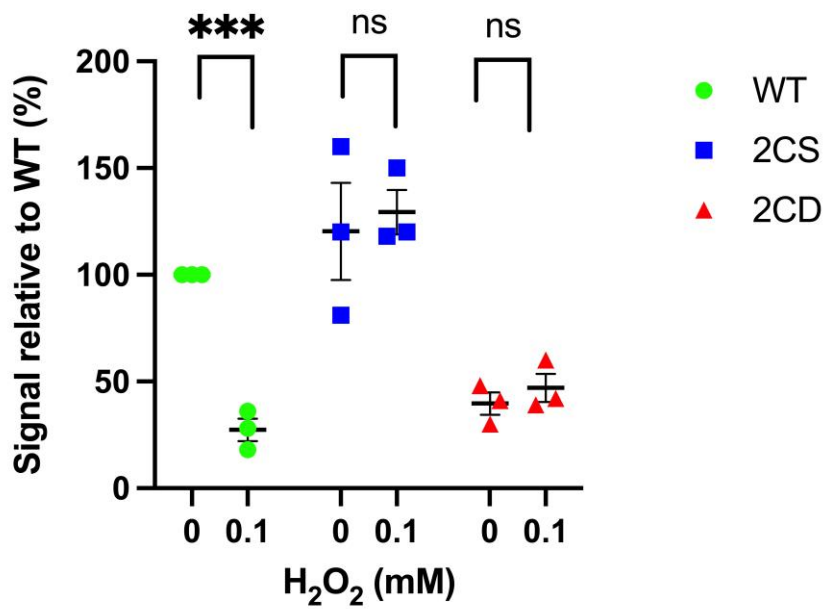
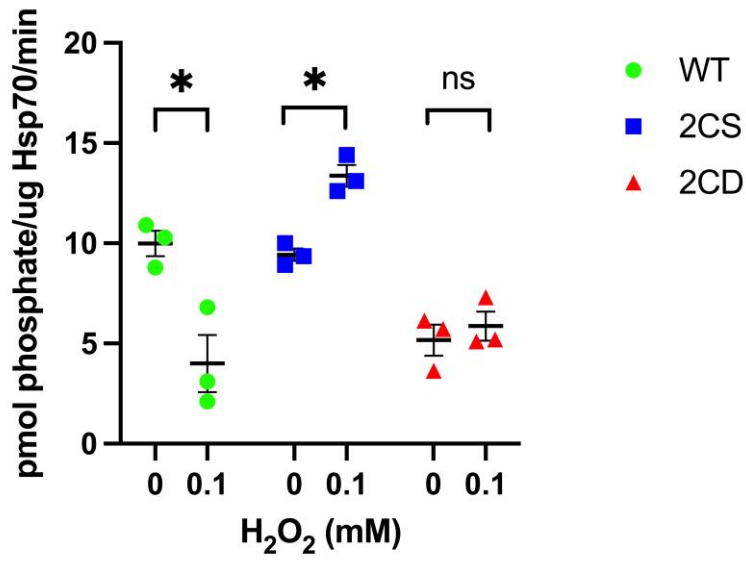


Figure 3-4: Nucleotide binding and hydrolysis are similarly impaired by oxidomimetic substitution in Ssa1-2CD and exogenous oxidation of Ssa1

Figure 3-4: Nucleotide binding is similarly impaired by oxidomimetic substitution in Ssa1-2CD and exogenous oxidation of Ssa1 (A) Immunoblot displaying elution fraction of 25 uL ATP-agarose bead volume incubated with 1 uM total respective protein treated or not with 1 mM hydrogen peroxide. (B) Quantification of the signal in A converted to relative percentage of untreated Ssa1 and normalized for load. Bolded horizontal bars indicate mean, and error bars indicate SEM.

Addition of 1 mM hydrogen peroxide prior to incubation with the beads significantly reduced the signal of eluted Ssa1, while Ssa1-2CD ATP binding remained low and nearly identical to untreated sample, as averaged over three experiments (Fig. 3-4B). Importantly, Ssa1-2CS retained full ATP binding capacity regardless of hydrogen peroxide treatment, suggesting that reduced nucleotide binding is a functional consequence of oxidation of cysteines 264 and 303. To assess whether the reduced binding interaction resulted in a downstream change in catalytic activity, I tested the ability of each isolated protein to hydrolyze ATP using a malachite green assay to quantify released phosphate. Akin to nucleotide binding, Ssa1 and Ssa1-2CS exhibited comparable levels of specific activity, while Ssa1-2CD demonstrated significantly reduced hydrolysis. (Fig. 3-5). Treatment with hydrogen peroxide also drastically reduced ATP hydrolysis of the Ssa1 but not Ssa1-2CS protein, while Ssa1-2CS retained full and even slightly elevated activity. Hydrolysis of ATP in the NBD is stimulated by Hsp40. It was noted that the hydrolysis deficiency of Ssa1-2CD may only affect the basal Ssa1 ATPase activity, and that the ATPase stimulation of Hsp40 may be able to compensate for the decreased activity. I therefore wanted to determine if stimulation by Hsp40 could overcome the basal hydrolysis deficit of Ssa1-2CD. Similarly, Hsp110 is also able to assist in ATP hydrolysis by Hsp70, so it was also a consideration as to whether the presence of Hsp110 was able to compensate for the deficiency of Ssa1-2CD. Interestingly, the addition of the Hsp40 Ydj1 and the Hsp110 Sse1 equally stimulated all Ssa1 isolates, but was not able to rectify the deficiency in hydrolysis from Ssa1-2CD (Fig. 3-5B).

A.



B.

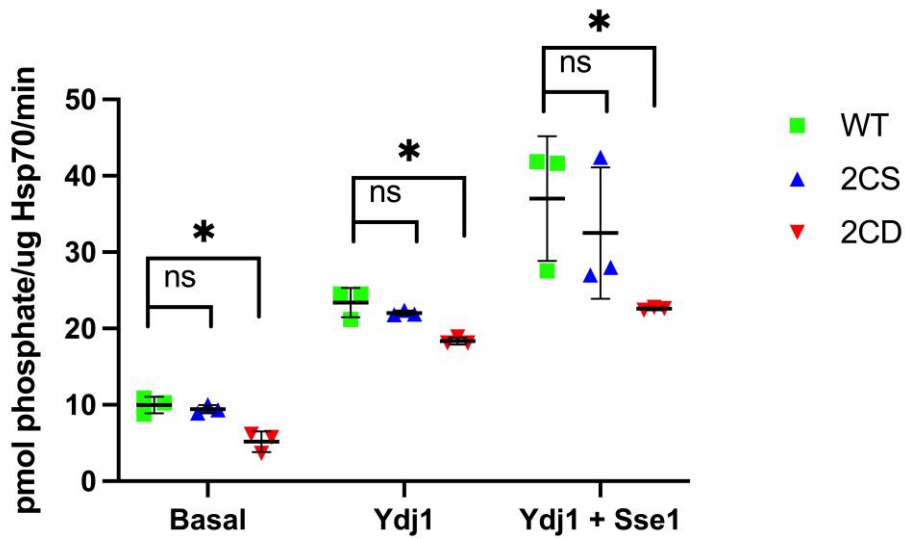


Figure 3-5: Nucleotide hydrolysis is similarly impaired by oxidomimetic substitution in Ssa1-2CD and exogenous oxidation of Ssa1

Figure 3-5: Nucleotide hydrolysis is similarly impaired by oxidomimetic substitution in Ssa1-2CD and exogenous oxidation of Ssa1

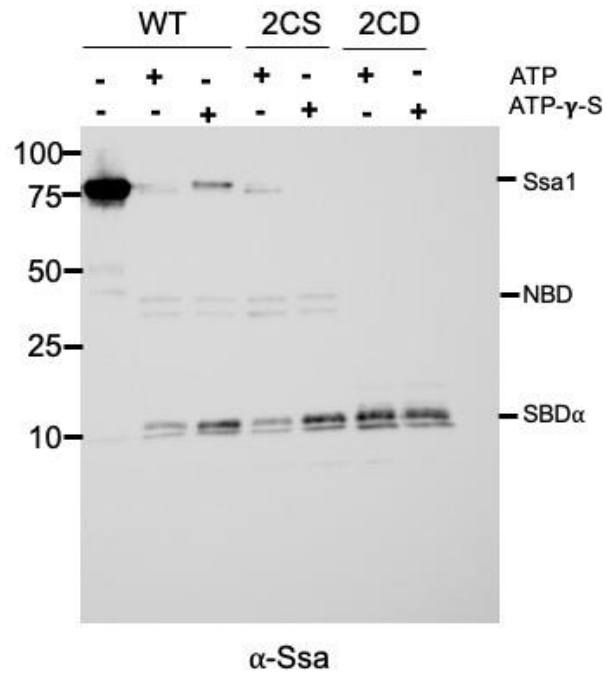
(A) Rate of ATP hydrolysis by a 0.1 μ M suspension of respective proteins, treated or not with 1 mM hydrogen peroxide. (B) ATP hydrolysis by WT and mutant Ssa1 proteins, basal and stimulated by 0.2 μ M Ydj1. Bolded horizontal bars indicate mean, and error bars indicate SEM. *, $p < 0.05$; ns, not significant.

Together, these data indicate that modification of cysteines, by both exogenous oxidation and oxidomimetic mutation, results in an altered relationship between Ssa1 and nucleotide resulting in reduced ability to bind and hydrolyze ATP. Disruption of nucleotide interaction within the NBD of Hsp70 has negative implications for the allosteric conformational changes signaled through the linker to the SBD, possibly affecting substrate interaction¹⁶. The allosteric signaling could also work in the reverse, whereby signals from the SBD are not correctly transduced through to the NBD. Allostery of Hsp70 results in conformational shifts of the domains in concert, and these shifts are the crucial action that drive the Hsp70 roles in proteostasis. I then hypothesized that if the 2CD/nucleotide relationship was altered, it may be due to altered conformation status in the presence of nucleotide, relative to WT.

To assess differential NBD conformational status, I performed limited trypsinization of isolated Ssa1 variants as used previously to interrogate NBD structure by monitoring proteolytic fragmentation patterns of Hsp70.¹³⁰ I incubated each chaperone mutant with either ATP or the non-hydrolyzable ATP- γ -S analog, followed by limited trypsin digestion. Interestingly, I observed increased and nucleotide-independent generation of what I believe to be the SBD α 'lid' domain (10 kDa) in the 2CD mutant based on visually observed molecular mass, as compared to WT and 2CS (Fig. 3-6)⁷. I inferred that this may be due to 2CD being locked into one conformation for a longer period of time, stabilizing the SBD α in a more exposed state. In the 'open' conformation, the NBD is either bound to ATP or does not have nucleotide in the pocket at all, and the lid domain is directly interacting with the outer

face of the NBD. In the 'closed' state, ADP is bound within the NBD and the lid sits over the substrate bound in the SBD. An altered relationship with nucleotide has the propensity to disrupt the signals passed through the domains to achieve conformational end-states, possibly leaving critical residues exposed to solvent for increased amounts of time, or protecting easily digestible protein sections through increased intra-protein interactions.

A.



B.

Time(m) t0 t5 t10 t15 t20

100 kDa
75 kDa
50 kDa
25 kDa
10 kDa

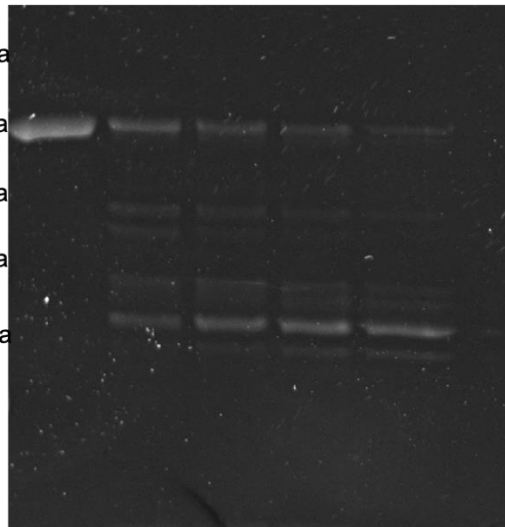


Figure 3-6: Isolated 2CD shows an altered fragmentation profile when incubated with non-hydrolyzable nucleotide

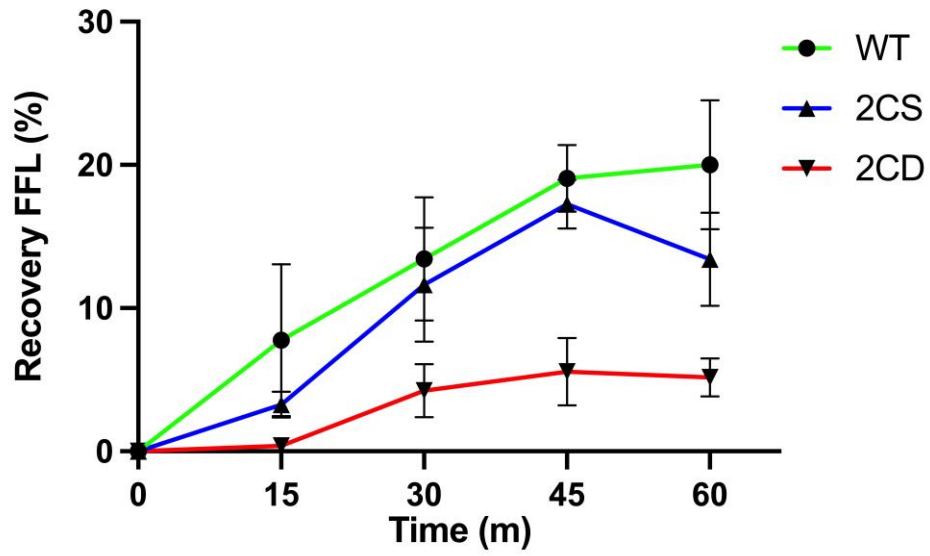
Figure 3-6: Isolated 2CD shows an altered fragmentation profile when incubated with non-hydrolyzable nucleotide

(A) Limited trypsin fragmentation profile of each indicated Ssa1 incubated with the respective nucleotide. 1.5 ug of Ssa1 was incubated with 1 mM of the respective nucleotide for 10 min at room temperature. 1 mg/mL of trypsin was then added and reactions incubated for 20 min at room temperature. (B) Time course of limited trypsin digestion.

To determine the consequences of impaired nucleotide interaction on protein folding by Hsp70, I utilized recombinant firefly luciferase (FFL) as a substrate for Ssa1. The enzymatic activity of properly folded FFL to produce chemiluminescence in the presence of the substrate luciferin has been previously used to measure substrate refolding by yeast chaperones *in vitro*^{135–137}. I therefore reconstituted the Hsp70 folding triad that includes Hsp70 (Ssa1), Hsp40 (Ydj1), and Hsp110 (Sse1) to examine refolding of chemically denatured FFL *in vitro*. Ssa1 and the cysteine-null Ssa1-2CS were found to have comparable basal ability to refold FFL post-exposure to guanidinium hydrochloride, while the yield of active enzyme produced by Ssa1-2CD was dramatically reduced (Fig. 3-7A). To determine if the refolding deficiency of Ssa1-2CD is a product of reduced aggregation resolution or an inherent deficiency, I then elected to include the yeast disaggregase Hsp104, an important factor in aggregate resolution *in vivo*, to assist Hsp70 and Hsp40 in the reactivation of aggregated proteins⁵⁸. After addition of this disaggregase to the chaperone mixture, I found that while Hsp104 approximately doubled the final yield of FFL recovered for all strains, there was still a significant defect in folding by Ssa1-2CD as compared to Ssa1-WT and Ssa1-2CS (Fig. 3-7B). An equitable increase in the system as a whole suggested that Hsp104 aided in the resolution of the aggregation resolution system, possibly giving the Hsp70s more access to polypeptide strands, but that the inherent deficiency of 2CD to properly assist in refolding was still a limiting factor. I again used hydrogen peroxide as an oxidative stressor to examine the effects of unbalanced oxidative stress that chaperone proteins may encounter in a cell. To determine the effects of exogenous oxidation on refolding, I measured the final yield of recovered

FFL after pre-exposure of Ssa1 alone to 1 mM hydrogen peroxide, and found that there was a significant decrease in recovery by SSA1-WT after oxidation, while Ssa1-2CS and Ssa1-2CD interestingly exhibited increased folding with respect to their untreated matched samples (Fig. 3-7C). I hypothesize that this may be due to a secondary effect that shifts the conformation of Ssa1, such as oxidation of cysteine 15 or a previously unidentified methionine residue, but further inquiry is necessary. However, because the observed increases occurred in both the serine and aspartic acid mutants, these effects are likely independent of cysteines 264 and 303. The oxidation state of thiol is reversible in the sulfenic acid state, reversible in the sulfinic state with the help of a sulfiredoxin, and non-reversible at the sulfonic acid state of maximum oxidation ¹³⁸. To examine the reversibility of the hydrogen peroxide-incubated proteins, I also attempted to recover the refolding abilities of WT after exogenous oxidation by treatment with the reductant dithiothreitol (DTT). I did not observe significant restoration of refolding, possibly due to hyperoxidation of the thiol moiety by hydrogen peroxide to a sulfinic or sulfonic acid, the former of which is genetically modeled by the 2CD mutation (Fig. 3-7D).

A.



B.

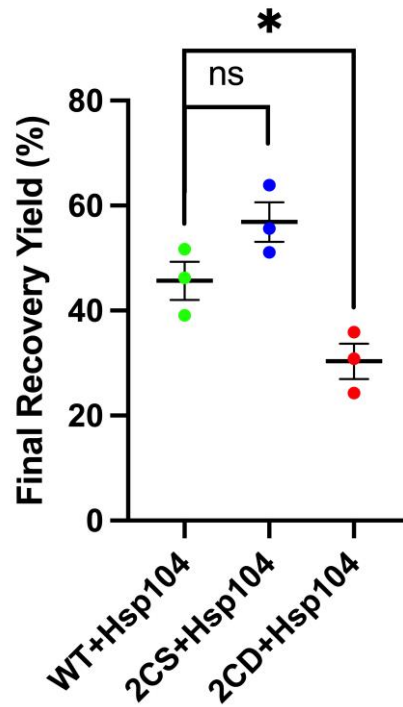
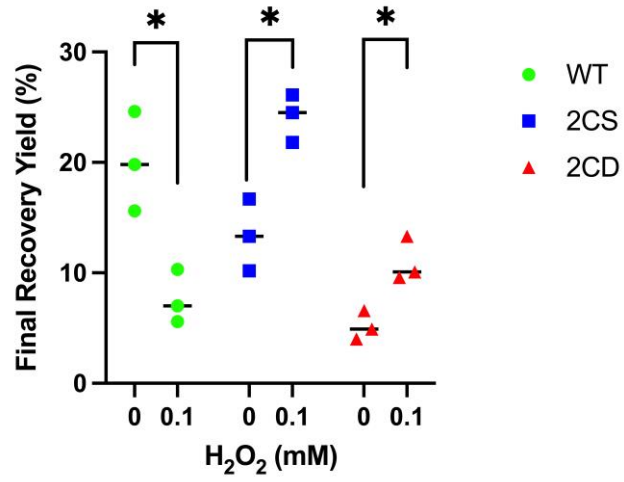


Figure 3-7: Mimicked and exogenous thiol oxidation negatively impact *in vitro* protein refolding

C.



D.

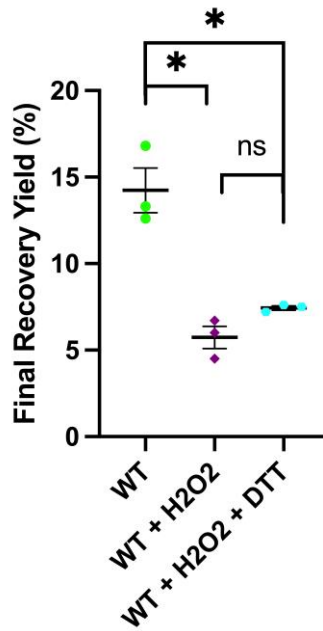


Figure 3-7: Mimicked and exogenous thiol oxidation negatively impact *in vitro* protein refolding

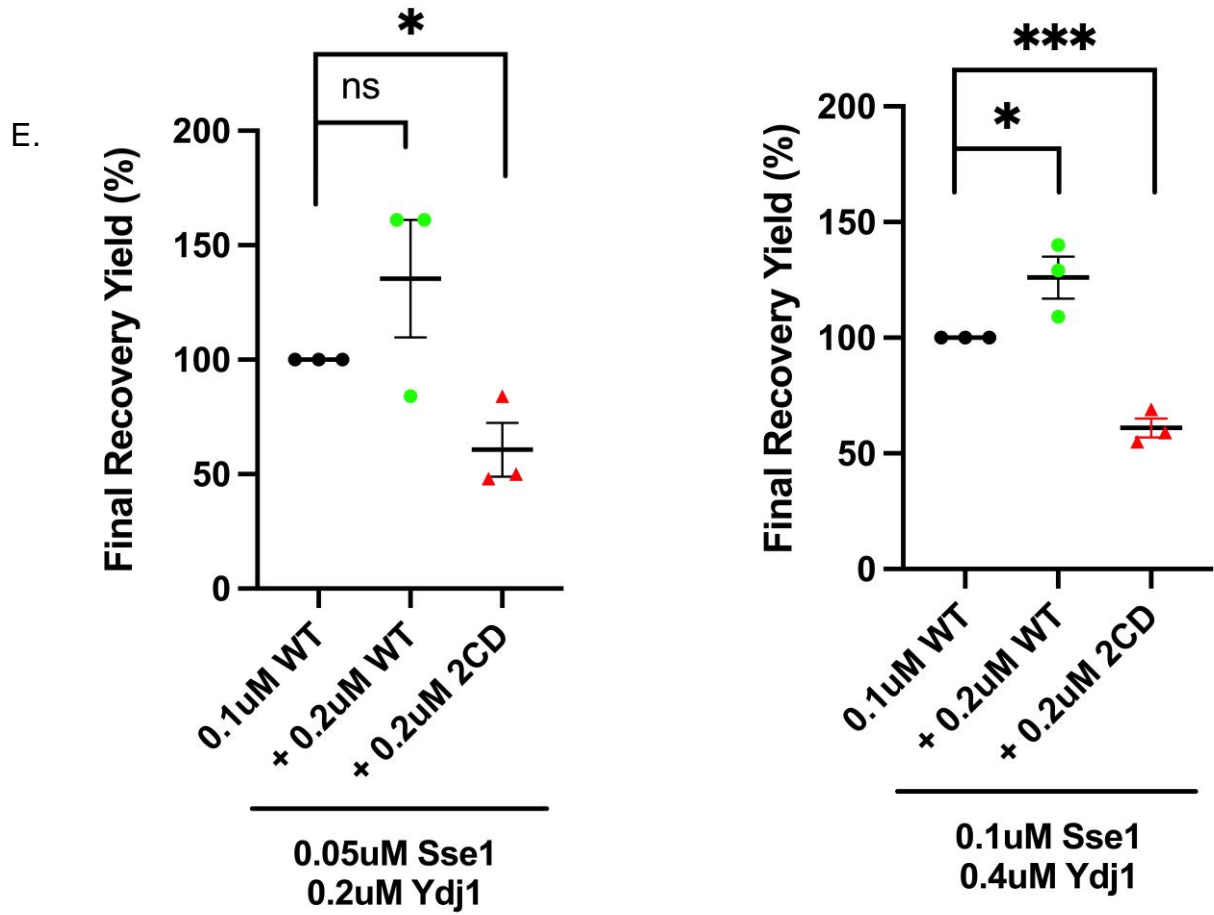
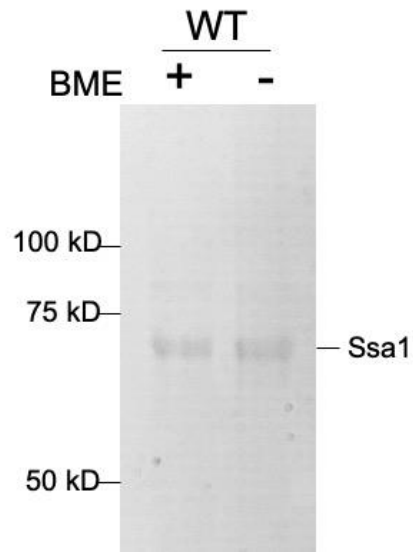


Figure 3-7: Mimicked and exogenous thiol oxidation negatively impact *in vitro* protein refolding

Figure 3-7: Mimicked and exogenous thiol oxidation negatively impact *in vitro* protein refolding (A) Firefly luciferase (FFL) recovery over time in the presence of 0.1 μ M of the indicated Ssa1 protein and co-chaperones Ydj1 (0.2 μ M) and Sse1 (0.05 μ M), as described in detail in *Materials and Methods*. (B) End point measurements of folding reactions including addition of 1 μ M Hsp104. (C) End point measurements of folding reactions using Ssa1 variants treated or not with 1 mM hydrogen peroxide. (D) End point measurements of folding reactions, indicating the respective protein and subsequent addition of exogenous compounds. (E) End point measurements of folding reactions, indicating the respective protein additionally added to reactions as in (A). Bolded horizontal bars indicate mean, and error bars indicate SEM.

In at least two prior reports, thiol modification or oxidomimetic substitution in Hsp70 chaperones has generated increased holdase capacity, binding substrate without ATP-regulated release, and therefore resulting in a negative effect on protein refolding^{122,123}. To assess the possibility that a C264/C303 oxidomimetic displays similar negative properties, I titrated 0.2 μ M additional Ssa1 or Ssa1-2CD into a pre-existing chaperone cocktail containing 0.1 μ M Ssa1, as well as subsequently doubling co-chaperone ratios to ensure that competition was not a limiting factor. I found that compared to Ssa1 alone, the Ssa1/Ssa1-2CD pool was hindered in refolding ability (Fig. 3-7E). This suggests that the Ssa1-2CD oxidomimetic may non-productively bind substrate and inhibit refolding. Dimerization of the proteins, caused by inter-protein formation of disulfide bonds, may also cause a complication in determining Hsp70 functionality, due to potential steric hinderance and limited mobility. To assess the potential of Ssa1 dimerization via oxidative disulfide bond formation, I subjected Ssa1 to treatment with 1mM hydrogen peroxide, but no altered migration in a non-reducing SDS-PAGE gel, indicative of dimer formation, was observed (Fig. 3-8A). To ensure that the altered relationship between Hsp70 and nucleotide was inherent to Ssa1, it was imperative to rule out the possibility that the cysteine oxidation was alternatively affecting the interaction between Hsp70 and the co-chaperone Sse1 and explore the possibility that basal Ssa1-2CD may refold protein as well as Ssa1-WT. To do so, I tested whether reduced interaction with the NEF Sse1 contributed to the deficiency in 2CD activity, but determined that even in reactions lacking Sse1, Ssa1-2CD was unable to refold FFL as efficiently as Ssa1 (Fig. 3-8B).

A.



B.

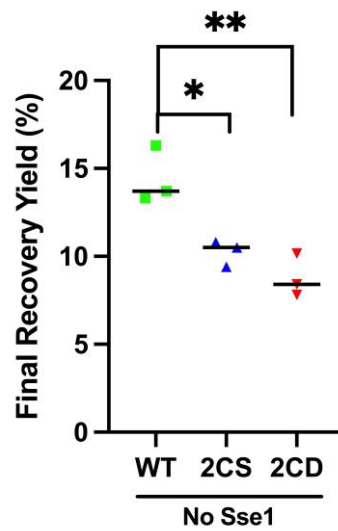


Figure 3-8: The deficiency of the oxidomimetic Ssa1-2CD mutant is not caused by dimer formation

Figure 3-8: The deficiency of the oxidomimetic Ssa1-2CD mutant is not caused by dimer formation

(A) Coomassie staining of Ssa1 WT after exposure to exogenous oxidants as described in *Materials and Methods*, incubated both with and without the reductant beta-mercaptoethanol (BME). (B) Firefly luciferase (FFL) recovery over time in the presence of 0.1 uM of the indicated Ssa1 protein and the co-chaperone Ydj1 (0.2 uM), as described in detail in *Materials and Methods*. Bolded horizontal bars indicate mean, and error bars indicate SEM. *, $p < 0.05$; ns, not significant.

Discussion

Using genetic mimics unlocks the ability to create a chronic impairment within the isolated *in vitro* system that mirrors a modified thiol state. Those findings were then corroborated by exogenous oxidation, a finding that boosted our confidence in the genetic substitution model. Initial attempts to isolate proteins were unsuccessful for several reasons, even when using expression plasmids and bacterial strains that had been published as previous protocols. Even more interesting, it was found that only a small portion of the eventual isolation pool was properly functional, but that this was not acknowledged in several predecessor publications utilizing identical tools. The unusable pool was able to be separated by anion exchange, suggesting that the difference between the pools was inherent to the proteins and resulting in an unknown modification or property that increased ionic binding strength. *E. coli*-expressed proteins are not always a suitable method for large scale isolations of yeast proteins, at least not without secondary assurances of function. With more than 400 potential post-translational protein modifications, techniques such as mass spectrometry, ion chromatography, and enzymatic assays may be employed to determine isolated protein quality ¹³⁹.

The data from chapter 3 directly implicate oxidative modification of cysteines with the functionality of Ssa1. I was able to show a decrease in both nucleotide binding and hydrolysis, as well as the inability to fully refold denatured protein substrate. These deficiencies did not result from a disulfide bridge homodimer that limited Ssa1 mobility, nor from the interaction with Sse1, suggesting that the deficiency was due to an intra-protein malfunction. The sustained refolding deficiency

in the presence of Hsp104 also suggests that it is not related to an impairment in aggregate dissolution.

The difference in trypsinization profile between Ssa1-WT and Ssa1-2CD suggests that each respective protein is conformationally different, in a way that protects the SBD α lid domain. The Ssa1-2CD profile mirrored what Ssa1-WT looked like when bound to the non-hydrolyzable analog, in which Ssa1-WT would be in the open conformation. If Ssa1-2CD is less able to bind ATP and when it does bind, also to hydrolyze it, it stands to reason that Ssa1-2CD would spend a greater amount of time in the open conformation even in the presence of ATP. In the open conformation, the lid domain is interacting with the NBD, which perhaps protects several residues that may be subjected to trypsinization, either by direct interaction or by lowered exposure of the Hsp70-interacting face to the environment. Alternatively, the *in-silico* modelling mentioned above shows the altered position of several key residues involved with hydrolysis. It is also foreseeable that the amount of time involved in the hydrolysis reaction increases in the Ssa1-2CD mutant, leading to a lowered total threshold for hydrolysis capacity in a given time frame, a potentially looser attachment to the ATP molecule, or an increased amount of time spent in the interim between ATP binding and full ADP hydrolysis. Depending on conformational specifics, this may cause conformations in Ssa1-2CD to be either open or closed, or perhaps in a middle zone, where the lid domain is trypsinized as a whole and not degraded to further sections due to intra-protein interactions, leading to stronger signal.

I was able to show that there is the opportunity for reversibility of oxidized cysteines through thiol reduction, by a relatively increased refolding rate in Ssa1-WT

treated with 20mM DTT after exposure to 1mM hydrogen peroxide. However, the refolding deficiency was not fully recovered, suggesting that a large quantity of the protein fraction was not recoverable after treatment with DTT. This lends credence to the importance of reversibility in a stress-sensing system that utilizes cysteines. Over-oxidation can result in irreversibility, which is toxic for substrate folding behaviors. The prevention of over-oxidation by assistive chaperones and other stress-response methods could be the difference between whether a cell recovers from injury or succumbs to toxicity.

Altogether, the data in chapter 3 exhibit the effects of Ssa1 cysteine modification in a closed system, resulting in a negative impact for several behaviors that are directly linked to Ssa1's role as a chaperone protein. In the following chapter, I will expand on the role of Ssa1 cysteine modification in a living organism, using the yeast model *Saccharomyces cerevisiae*.

Chapter IV: In vivo analysis of Ssa1 cysteine modification

This research was originally published in the Journal of Biological Chemistry. Santiago A, Morano KA. Oxidation of two cysteines within yeast Hsp70 impairs proteostasis while directly triggering an Hsf1-dependent cytoprotective response. J Biol Chem. 2022 Aug 25:102424. doi: 10.1016/j.jbc.2022.102424. © the American Society for Biochemistry and Molecular Biology or © the Author(s). *JBC does not require permission to use published materials in one's dissertation:* <https://www.elsevier.com/about/policies/copyright/permissions>.

Introduction

Although it is important for isolating the phenotype of mutants to reduce compounding factors, *in vitro* experiments lack the complexity of a fully adaptive living system. Thus, I extended the cysteine-to-serine and cysteine-to-aspartic acid mutations into living yeast cells. Due to the ease of genetic manipulation in yeast, the wealth of preceding work regarding yeast chaperone cysteine oxidation, and the lab's history of experience performing yeast assays, *S. cerevisiae* was an ideal choice. Building upon the work of both our lab and the David Pincus laboratory at the University of Chicago that elucidated the interactions of Hsf1 and Hsp70 and the consequences for the heat shock response, this body of work also provided the opportunity to find the mechanism of action of a result obtained by previous student Yanyu Wang, which determined that the Hsp70 cysteines C264 and C303 were responsible for triggering a previously known elevated heat shock response to oxidative stress^{51,78,89}.

The yeast model also allowed the measurement of several protein-specific functions of Ssa1, including the folding of nascent proteins, the refolding of damaged proteins, and the degradation of chronically misfolded proteins. I leveraged the reporter strain FFL-GFP for both enzymatic quantification and for visual determination of protein aggregation, shown by GFP foci. This versatile reporter is useful for both enzymatic quantification and visual imaging, as the firefly luciferase (FFL) protein produces chemiluminescence when in the presence of the substrate luciferin and ATP, and the GFP protein is a fluorescent tag that can be seen under a microscope. FFL is also susceptible to heat denaturation and chemical denaturation, making it a

helpful proxy for understanding cellular protein dynamics. FFL-GFP has been utilized by our lab and by many others in nascent folding, refolding, and localization experiments, as the chemiluminescence is a quantifiable reporter of protein functionality and the GFP tag allows for visual determination of the protein location in a cell ^{35,127,140–143}. Additional tags can be added to FFL-GFP, such as nuclear export and nuclear localization tags, that further increase the versatility of FFL-GFP ¹⁴⁴.

As mentioned above, nascent proteins are especially susceptible to environmental damage, as they have not yet formed the tertiary conformations that internally envelope and protect hydrophobic residues from water molecules. Hsp70 recognizes a hallmark of these nascent proteins: a hydrophobic patch of residues flanked by charged residues. Hsp70 then binds these patches and sterically shields them from the environment. The binding, release, and subsequent rebinding of the Hsp70 is also thought to assist in the folding of the protein itself, by introducing activation energy into the folding system. That activation energy is also useful in the refolding of proteins, through introduction of a pulling force called ‘entropic pulling’ ¹⁴⁵. When proteins aggregate, Hsp70 can shield incorrectly folded patches within misfolded proteins and by releasing the substrate, allow them to reform in a potentially more functional state. That entropic pulling mechanism is dependent on the repeated cycling of Hsp70, which the *in vitro* experiments suggest may be deficient.

As discussed in the introduction, Hsp70 interacts with the ubiquitination machinery to assist in the degradation of proteins, by delivering chronically misfolded substrate to Ubr2 (an E3 enzyme). Interestingly, recent literature showed Ssa1 to have altered levels of degradative assistance efficiency, depending on substrate ¹³².

Several substrates were not affected by Ssa1 presence or deletion, leading us to choose the Ssa1-dependent substrate tGND-GFP for our degradation assays.

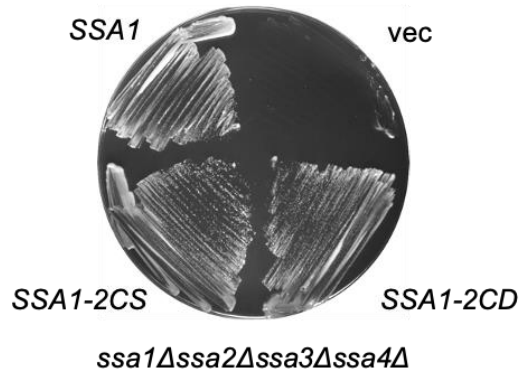
Oxidative stress is constitutively present in the environment, predominantly due to the processes of the mitochondria leaking ROS into the cytoplasm. Exploration of the consequences of oxidative stress within the cytoplasm is therefore a pertinent necessity for understanding a circumstance that exists in humans, healthy or otherwise. Relating that exploration to chaperone proteins and their functions in protein homeostasis can serve as a foundation to understanding of the risks threatening protein function. Non-functional proteins have the propensity to form aggregates, and through connecting the dots between oxidation, protein management systems, and protein health, I can better understand the environment that creates protein-related disorders, such as Alzheimer's disease and Parkinson's disease, both of which feature protein aggregation as a tenet of disease. In this chapter, I determine the consequences of mimicked oxidation of Ssa1 cysteines C264 and C303 using the *ssa1-2CD* mutant and find that the resulting yeast are deficient in the nascent folding and refolding activity of FFL-GFP, unable to interact with and repress Hsf1, and constitutively show elevated levels of chronically misfolded substrate.

Results

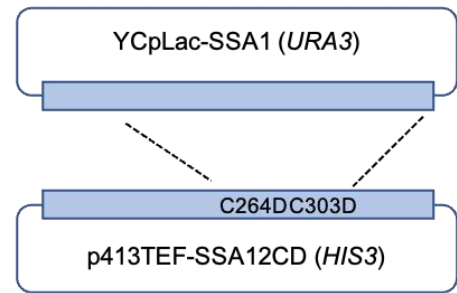
To complement our *in vitro* studies, I addressed consequences of Ssa1 oxidation through the genetic cysteine null and oxidomimetic Ssa1 mutants. I initially attempted to express *ssa1-2CD* as the sole cytosolic SSA gene in a quadruple *ssa1Δssa2Δ ssa3Δssa4Δ* deletion background¹⁴⁶. The quadruple deletion strain contained a wild type copy of *SSA1* on a *URA3*-selectable plasmid and was subsequently transformed with a *HIS3*-selectable plasmid expressing wild type *SSA1* or the *ssa1-2CS* or *ssa1-2CD* mutants. A plasmid shuffle technique was used to selectively isolate colonies that possessed only the *HIS3* plasmid via plating on 5-fluoroorotic acid (5-FOA) media. Any colonies that possessed the *URA3* gene would be able to create a toxic by-product from 5-FOA present in the media and limit their own survival, ensuring that only colonies that no longer contained the *URA3*-selectable plasmid and only the *HIS3*-selectable plasmid would be obtained. Surprisingly, all recovered yeast colonies expressing *SSA* alleles after this selection process grew at identical rates when plated (Fig. 4-1A), inconsistent with the slow-growth phenotype previously reported for the *ssa1-2CD* mutant⁸⁹. This occurrence caused us to probe further into the genotypes of transformants to ensure proper transformation. Sequencing of the recovered *HIS3*-marked plasmid revealed that the *ssa1-2CD* allele had converted to the wild type sequence encoding the original cysteine residues (Fig. 4-1B). I hypothesize that this unexpected genotype was due to a recombination event between the two plasmids, whereby the likely inability of *ssa1-2CD* to function as the sole expressing cytosolic SSA gene resulted in selection for rare allele exchange events (Fig. 4-1C). The occurrence of this event was

interesting, as I had also noticed that colonies that I had expected to contain the *ssa1-2CD* allele (but actually contained the wild type allele) usually did not appear for multiple days after the *ssa1-2CS* allele transformants, suggesting that the increased time was necessary to increase the likelihood of the assumed event. After several attempts resulting in either no viable colonies or only allele-exchanged colonies, I concluded that the *ssa1-2CD* allele is incapable of sustaining viability as the sole cytosolic SSA isoform due to the functional defects demonstrated in Chapter 3.

A.



C.



B.

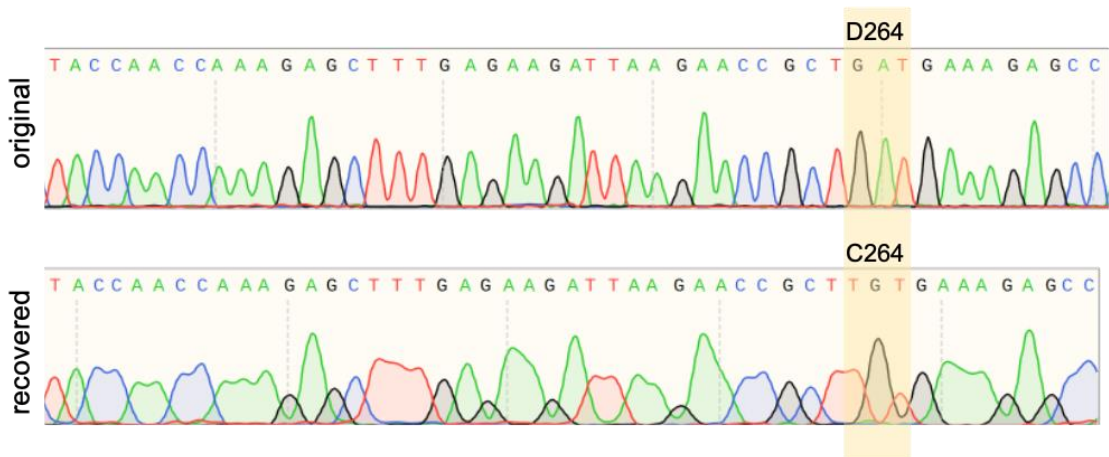
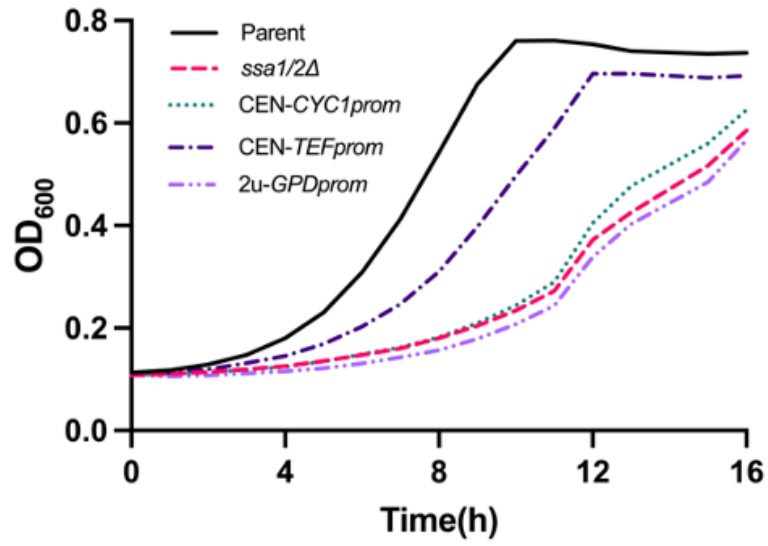


Figure 4-1: The oxidomimetic *ssa1-2CD* mutant is incapable of supporting viability as the sole cytosolic SSA gene

Figure 4-1: The oxidomimetic *ssa1-2CD* mutant is incapable of supporting viability as the sole cytosolic SSA gene (A) 48-hour 5-fluoroorotic acid (5-FOA) plate growth of the indicated *HIS3*-selective plasmid, in an *ssa1Δ ssa2Δ ssa3Δ ssa4Δ* deletion background demonstrating unexpected wild type growth for the *ssa1-2CD* mutant. (B) Sequencing analysis of the introduced *HIS3*-selective plasmid (original) and the recovered plasmid extracted from the colonies shown in (A), demonstrating reversion of the aspartic acid-encoding codon GAT to the original cysteine-encoding codon TGT. Only the region surrounding C264 is shown for simplicity. (C) Proposed recombination mechanism to explain the gene reversion event during the plasmid shuffle process.

I elected to continue with oxidomimetic expression *in vivo* in an *ssa1Δ ssa2Δ* deletion background, where Ssa3/4 are present at low levels to support viability, but cell growth is still significantly impaired in non-stressed conditions ⁸⁹. This genetic background had also been utilized previously ⁸⁹. I additionally wanted to ensure that expression of the wild type and mutant alleles best represented natural levels and examined different heterologous promoters for suitability. I found that *SSA1* allele expression from the weak *CYC1* promoter on centromeric (*CEN*) yeast expression vectors resulted in diminished growth for all genotypes, suggesting general Ssa protein insufficiency. However, expression from the stronger *CEN-TEF* vector backbone resulted in normal growth for *SSA1* and *ssa1-2CS* strains, while the *ssa1-2CD* and empty-vector control both grew at stunted rates that were similar to each other and consistent with previous reports (Fig. 4-2A, 4-2B and 4-2C) ⁸⁹.

A.



B.

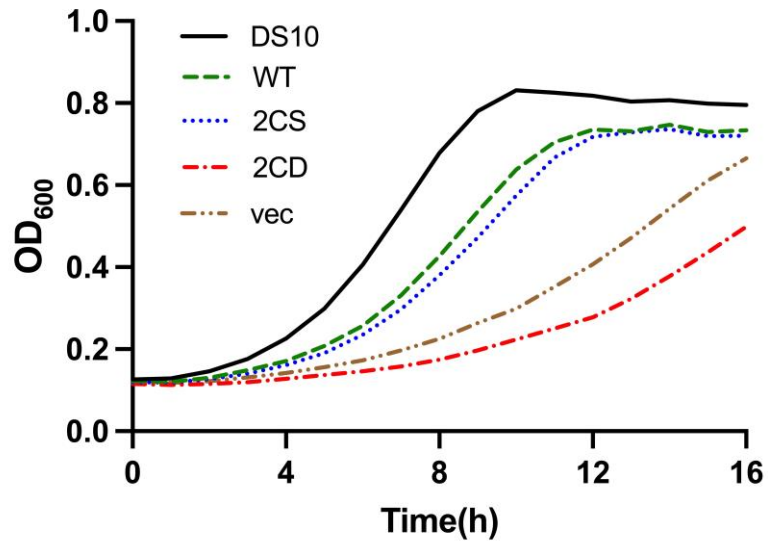


Figure 4-2: The thiol oxidomimetic *ssa1-2CD* allele displays slowed growth

C.

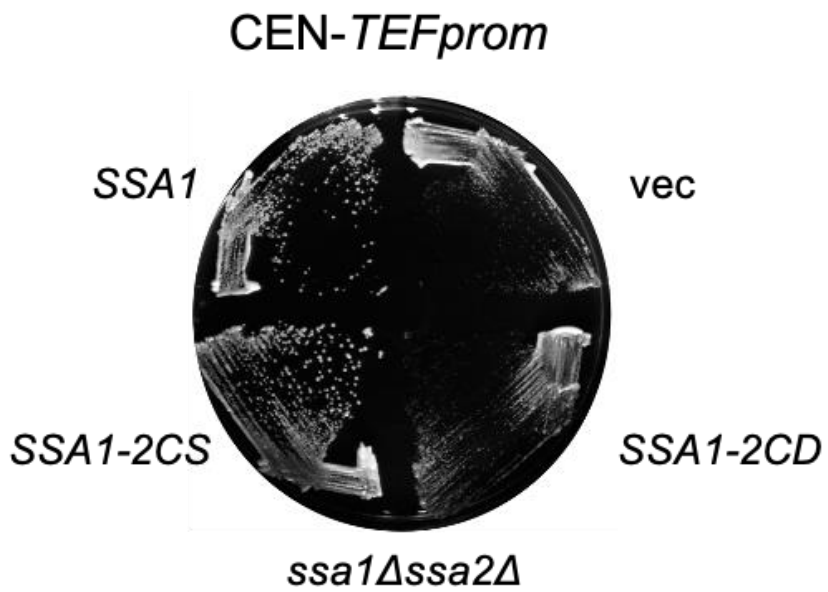
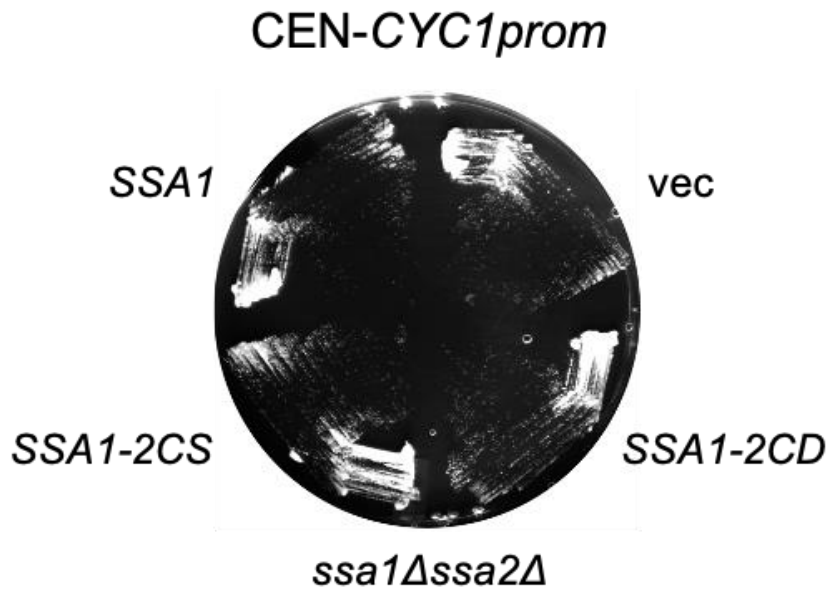


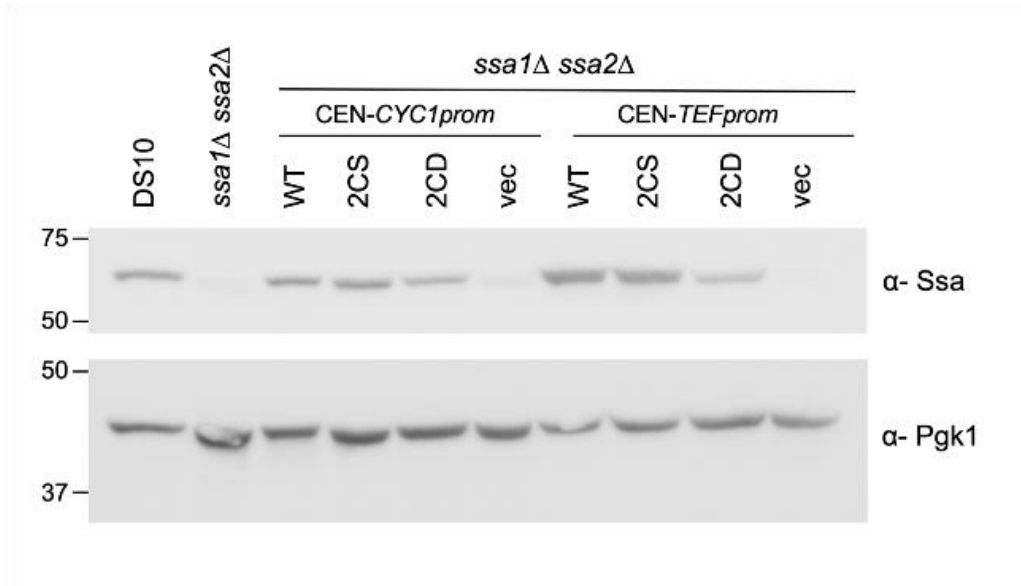
Figure 4-2: The thiol oxidomimetic *ssa1-2CD* allele displays slowed growth

Figure 4-2: The thiol oxidomimetic *ssa1-2CD* allele displays slowed growth (A)

16-hour growth curve of parent strain DS10, *ssa1Δ ssa2Δ*, and wild type *SSA1* driven by the indicated promoter in a *ssa1Δ ssa2Δ* background. (B) 16-hour growth curve of DS10 and indicated *SSA1* allele expression driven by the *TEF* promoter, in an *ssa1Δ ssa2Δ* background. (C) 48-hour plate growth of each indicated *SSA* gene driven from the weak *CYC1* promoter and the stronger *TEF* promoter in the *ssa1Δ ssa2Δ* background.

Immunoblots confirmed that Ssa1 protein levels were expectedly lower driven from the *CYC1* promoter in *ssa1* Δ *ssa2* Δ cells as compared to the DS10 parent strain (Fig. 4-3 A,B). Intriguingly, *TEF*-driven Ssa1 protein levels were similar between *SSA1*, *ssa1-2CS*, and the parent DS10 strains, but the *ssa1-2CD* allele clearly produced lower levels of Ssa1-2CD protein (Fig. 4-3 A,B). I reasoned that Ssa1-2CD expression was either being actively curtailed or that the mutation resulted in a protein more susceptible to degradation. To test protein stability, I treated cells with the protein translation inhibitor cycloheximide and tracked the existing pool of Ssa1 from each allele by immunoblot, finding that Ssa1-2CD was stable over the course of 3 hr (Fig. 4-3C). Additionally, Ssa1-2CD did not partition into the insoluble fraction to an extent greater than Ssa1 or Ssa1-2CS (Fig. 4-3D). Thus, the Ssa1-2CD protein was both stable and non-aggregated in the cytosol relative to wild type Ssa1. These results led us to the conclusion that steady state Ssa1-2CD levels might be restricted in actively growing cells but that the protein itself was not inherently destabilized by the cysteine to aspartic acid substitutions, relative to wild type Ssa1.

A.



B.

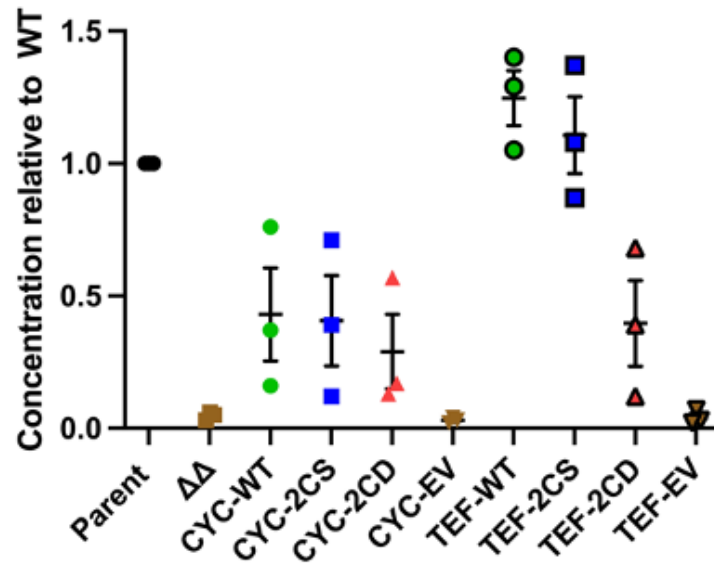
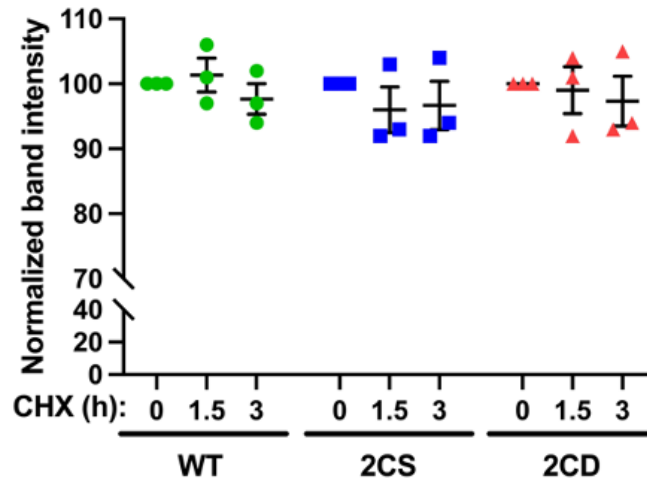


Figure 4-3: Expression of the Ssa1-2CD protein is restricted relative to wild type Ssa1 and Ssa1-2CS

C.



D.

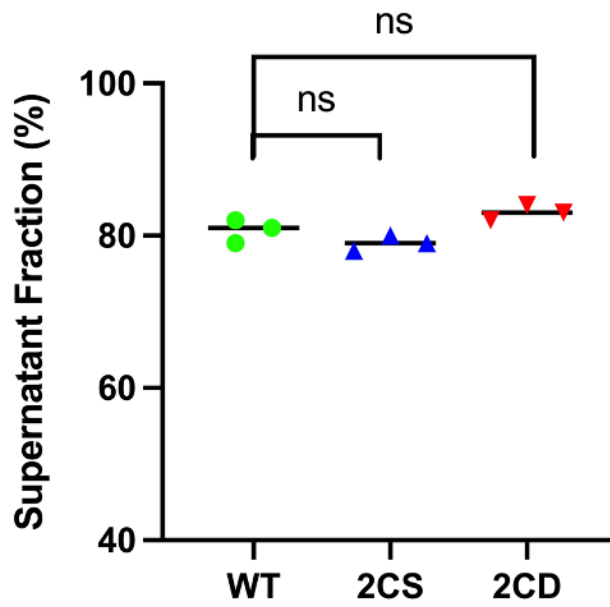


Figure 4-3: Expression of the Ssa1-2CD protein is restricted relative to wild type Ssa1 and Ssa1-2CS

Figure 4-3: Expression of the Ssa1-2CD protein is restricted relative to wild type Ssa1 and Ssa1-2CS (A) Relative protein expression of each indicated Ssa1 protein from the wild type strain DS10, or the respective *CYC1* or *TEF* plasmid in the *ssa1Δ ssa2Δ* background. (B) Quantification of the relative levels of each indicated protein compared to expression in the DS10 background. (C) Immunoblot cycloheximide chase analysis to monitor protein stability over time of each indicated protein driven from the *TEF* promoter, in the *ssa1Δ ssa2Δ* background. Bolded horizontal bars indicate mean, and error bars indicate SEM. (D) Differential centrifugation of the respective Ssa1 protein, reported as percentage of total Ssa1 in the supernatant fraction as assessed by SDS-PAGE and immunoblot.

Our in vitro experiments indicated that Ssa1-2CD inhibited protein folding in the presence of wild type Ssa1. I noted that culture growth rates of the *ssa1-2CD* strain were slower than even the empty vector *ssa1* Δ *ssa2* Δ control strain, suggesting that expression of the Ssa1-2CD protein at even moderate levels was more detrimental than having no Ssa1 at all (Fig. 4-2B). To further explore this phenomenon, I expressed all *SSA1* alleles from the strong *GPD* promoter on a 2 μ vector backbone¹⁴⁷. This level of overexpression of *SSA1* and *ssa1-2CS* reduced growth rates to a level similar to the empty vector background control, consistent with previous reports that chaperone overexpression can be deleterious (Fig. 4-4)⁵⁵. However, overexpression of the *ssa1-2CD* allele resulted in near-total cessation of growth despite the presence of Ssa3/4 in this background, indicating overexpression toxicity beyond the inability to complement loss of Ssa1/2 functions.

A.

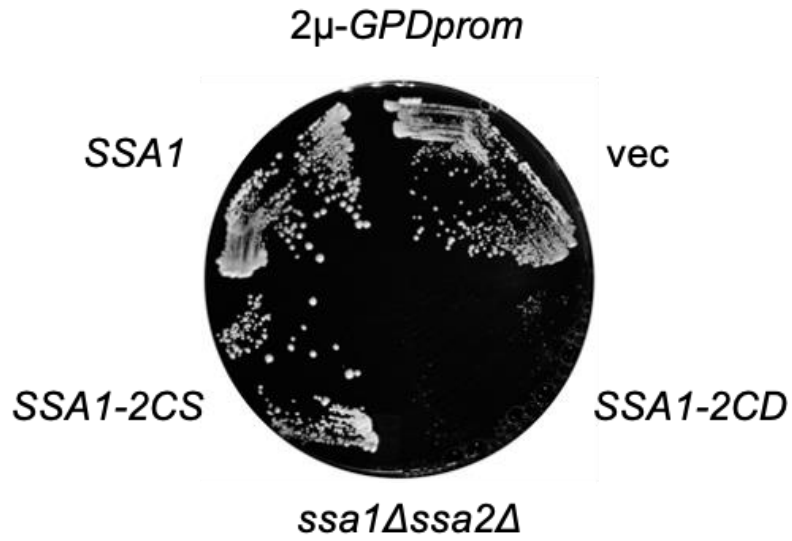


Figure 4-4: Overexpression of *ssa1-2CD* severely restricts growth

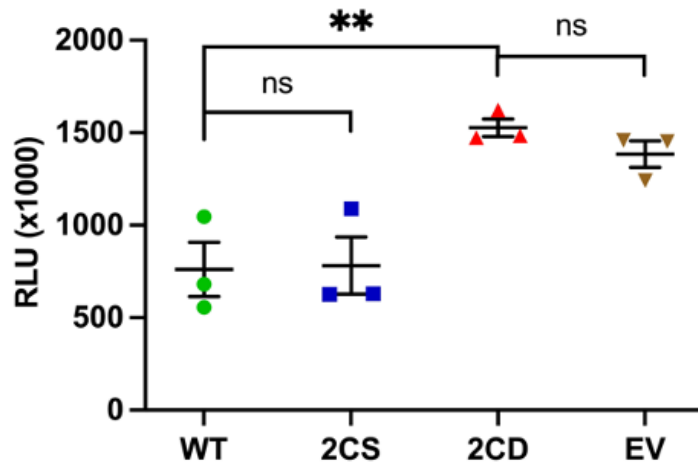
(A) 96-hour plate growth of each indicated SSA gene driven from the strong *GPD* promoter in the *ssa1Δ ssa2Δ* background.

Ssa1 has been recently shown by our laboratory and others to act as a repressor of the heat shock response transcription factor Hsf1 through physical association with both the amino- and carboxyl-terminal transcriptional activation domains^{10,51,78}. Our lab has previously published that thiol-modifying compounds induce a heat shock response in *SSA1*, but not *ssa1-2CS*, cells⁸⁹. Consolidating these findings, I hypothesized that thiol stress alters C264 and C303 within Ssa1, inactivating the chaperone and resulting in release of Hsf1 and subsequent induction of the HSR. This parallels the basic concept of heat shock induction, whereby through a mechanism of Ssa1 alteration, the repressive action of Hsp70 to prevent heat shock gene induction by Hsf1 is lessened, freeing Hsf1 to be activated and express the genes under its control. While the current model assumes indirect de-repression through titration of Ssa1 by what seem to be higher affinity to misfolded protein substrates, our proposed method of action is instead a direct modification of Ssa1.

I first confirmed that the HSR was chronically activated in the *ssa1-2CD* strain utilizing an Hsf1-responsive HSE-lacZ reporter (Fig. 4-5A). This reporter has been utilized in several publications from our lab, and uses a high-resolution Beta-Glo measurement to assure reliable quantification^{10,89,148}. The Beta-Glo reagent is an indicator of beta-galactosidase activity. When beta-galactosidase production is under control of a promoter that contains a heat shock element, it is then an indicator for Hsf1 activity, and a measurable proxy for the heat shock response that can be read using a high-resolution luminometer. Ssa1 represses Hsf1 through the substrate-binding domain, while the cysteine substitutions are within the nucleotide-binding domain, leading me to hypothesize that the interaction between Hsf1 and Hsp70

would not be compromised by our serine substitutions ⁸⁴. As expected, *ssa1-2CS* cells exhibited appropriate HSR repression, verifying that the endogenous cysteines are not required for Ssa1 to function as a repressor of Hsf1. As shown in Figure 4-3, the steady-state expression levels were higher for WT and *ssa1-2CS* when driven by the moderately-expressive TEF promoter, but levels between protein expression were comparable if driven by differentially expressing promoters. Thus, to test our hypothesis that Ssa1-2CD is defective in Hsf1 association, Hsf1-GFP-FLAG was co-expressed in cells containing either *CYC1*-driven *SSA1* and *ssa1-2CS* or *TEF*-driven *ssa1-2CD* alleles to control for differential Ssa1 protein levels, and co-immunoprecipitations were performed. Both Ssa1 and Ssa1-2CS associated with Hsf1, but no detectable signal was observed for Ssa1-2CD (Fig. 4-5 B,C). None of the Ssa1 proteins were found to associate with the GFP-FLAG control, confirming specificity of Hsf1 binding. These data indicate that the oxidomimetic Ssa1-2CD is unable to productively bind the bipartite contact sites on Hsf1 and provide a molecular mechanism to explain oxidative stress sensing by Hsf1 via Cys264/303 of Ssa1. Hsp70 proteins are critical factors for ensuring proteostasis ¹⁸. Their actions are heavily dependent on the conformational cycling ensured by the relationship between Hsp70, its co-chaperones, and nucleotide hydrolysis. Due to the disruption of this relationship demonstrated in Chapter 3, I hypothesized that mimicked cysteine oxidation would have negative consequences for Hsp70 protein surveillance activities.

A.



B.

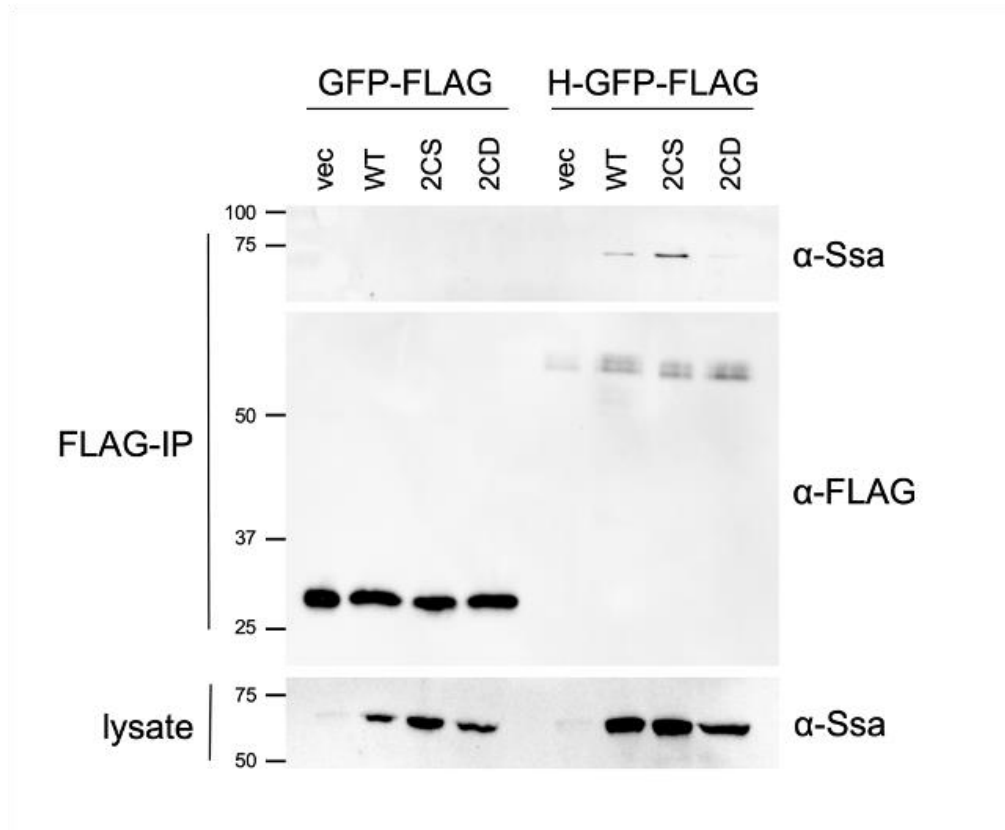


Fig. 4-5. Ssa1-2CD fails to bind and repress the heat shock regulator Hsf1

C.

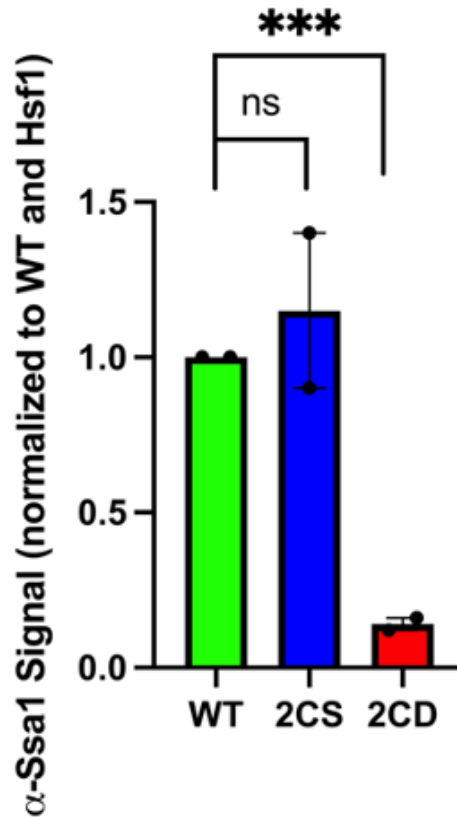
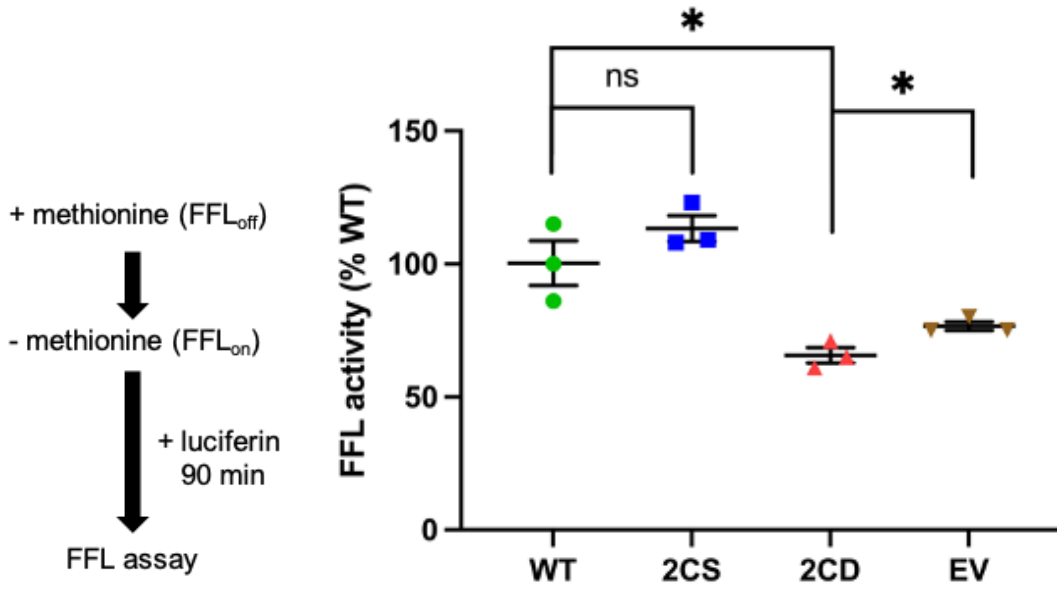


Fig. 4-5. Ssa1-2CD fails to bind and repress the heat shock regulator Hsf1 (A) HSE-lacZ activity of strains containing wild type and mutant *SSA1* alleles grown at 30°C. To normalize Ssa1 protein levels, *SSA1* and *ssa1-2CS* were expressed from the *CYC1* promoter and *ssa1-2CD* from the stronger *TEF* promoter. (B) Co-immunoprecipitation of tagged Hsf1-GFP-FLAG or GFP-FLAG control and the indicated Ssa1 proteins. (C) Quantification of assay detailed in (B), normalized for load and measured as the ratio of signal compared to WT. Bolded horizontal bars indicate mean, and error bars indicate SEM.

Data presented in Chapter 3 demonstrate that the Ssa1-2CD protein or exogenously oxidized Ssa1 are defective in functional protein refolding. To complement the *in vitro* folding assays, I co-expressed with the *SSA1* alleles a previously generated and well documented firefly luciferase (FFL)-GFP fusion protein known to require the Hsp70 chaperone system for folding in living cells^{127,140}. Used in earlier assays, FFL has the benefit of quantitative reporting of function, by measuring the chemiluminescence activity of interaction with its substrate luciferin. Additionally, this fusion protein tagged the FFL with GFP, allowing the visual localization of FFL in live cells without disrupting the chemiluminescent function of the FFL. To monitor *de novo* folding of nascent polypeptides, I utilized the methionine-repressible promoter of the FFL-GFP plasmid to induce expression of FFL in log phase cells, by removing the methionine that halted earlier expression¹⁴⁰. FFL activity was measured by luciferase assay over the course of 90 min. The *ssa1-2CS* mutant was able to fully complement the *de novo* folding defect observed in *ssa1Δ ssa2Δ* cells relative to cells expressing *SSA1* while the *ssa1-2CD* mutant was significantly defective (~ 60% of wild type luciferase activity) (Fig. 4-5A). To account for the lower abundance of Ssa1-2CD, I also examined *de novo* folding activity in a *CYC1-SSA1* strain and found that this reduced level of expression still maintained higher FFL activity than observed in the *TEF-ssa1-2CD* background, indicating that absolute protein levels do not explain the reduced capacity for FFL folding seen with Ssa1-2CD (Fig. 4-6B).

A.



B.

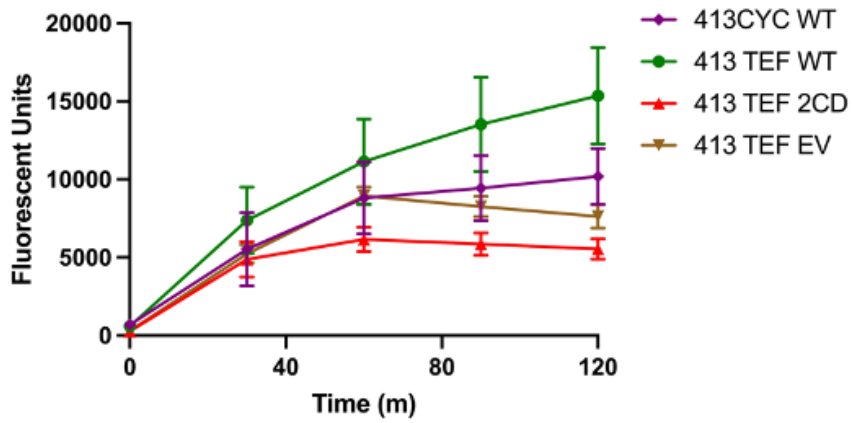
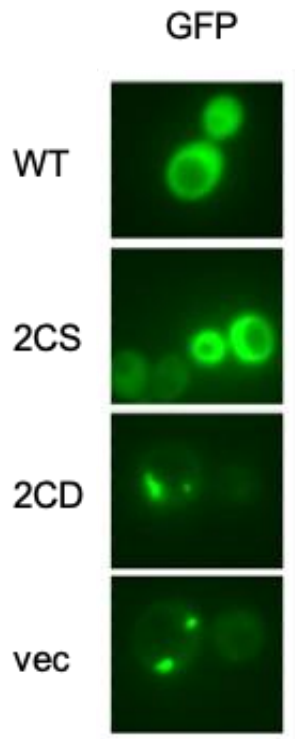


Figure 4-6: *ssa1-2CD* is unable to complement *ssa1-WT* in the folding of *de novo* proteins

Figure 4-6: *ssa1-2CD* is unable to complement *ssa1-WT* in the folding of *de novo* proteins (A) End point *de novo* folding ability of *SSA1* or mutant *ssa1* alleles as measured by luciferase activity assay, monitored over 90 min. (B) *de novo* expression of FFL-GFP. Bolded horizontal bars indicate mean, and error bars indicate SEM.

Misfolded proteins are known to aggregate in concert with protein chaperones, including sequestrases and disaggregases, and can be visualized *in vivo* using fluorescent tagging approaches^{149,150}. To examine the status of properly folded and potentially misfolded FFL, overnight cultures of *SSA1*, *ssa1-2CS*, *ssa1-2CD* and a vector control containing the FFL-GFP expressing plasmid were visualized using fluorescence microscopy. Micrographs displaying representative images show that FFL-GFP was found to be fully soluble in *SSA1* and *ssa1-2CS* strains while *ssa1-2CD* and the vector control exhibited large foci, visible as fluorescent puncta that were present in a significantly higher percentage of cells (Fig. 4-6 A, B). As an additional orthogonal approach to complement our *in vitro* findings, I determined the ability of each strain to refold heat-denatured substrate. Log-phase cells were washed to remove methionine and induce FFL-GFP expression to generate a pool of substrate. Cycloheximide was then added to prevent additional FFL-GFP expression and steady-state luminescence activity was measured. Cellular FFL-GFP was denatured by incubating cultures at 42°C, followed by a recovery period at 30°C. Cells were then visualized by fluorescence microscopy and luminescence was determined. All strains contained puncta immediately after heat shock, and while *SSA1* and *ssa1-2CS* strains resolved FFL-GFP aggregates, *ssa1-2CD* and the empty vector control failed to do so (Fig. 5D). These results were mirrored when FFL enzymatic activity was examined, with the *ssa1-2CD* and the empty vector control only managing to restore approximately 50% of original pre-heat shock FFL-GFP activity (Fig. 5E).

A.



B.

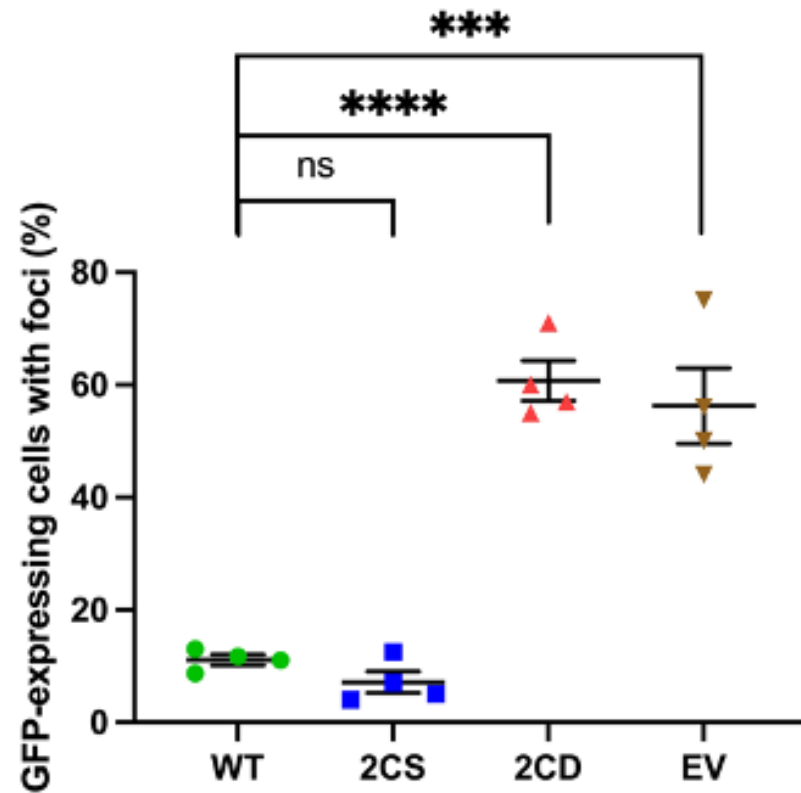


Fig. 4-7: The *ssa1-2CD* mutant exhibits multiple deficiencies in proteostasis

C.

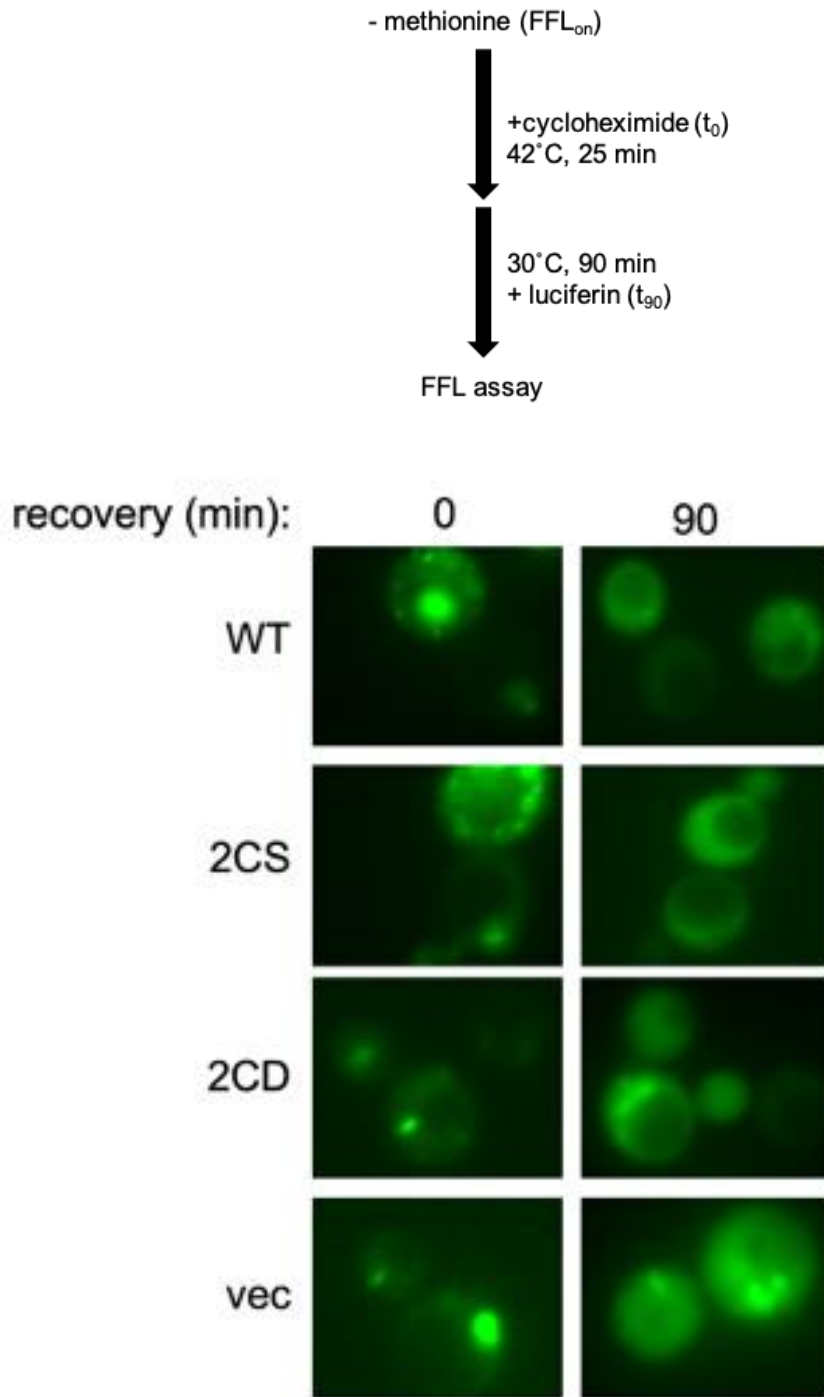


Fig. 4-7: The *ssa1-2CD* mutant exhibits multiple deficiencies in proteostasis

D.

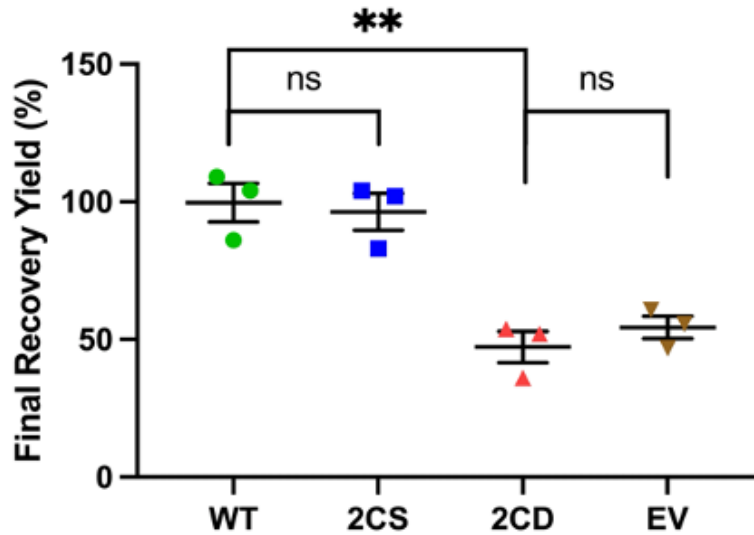


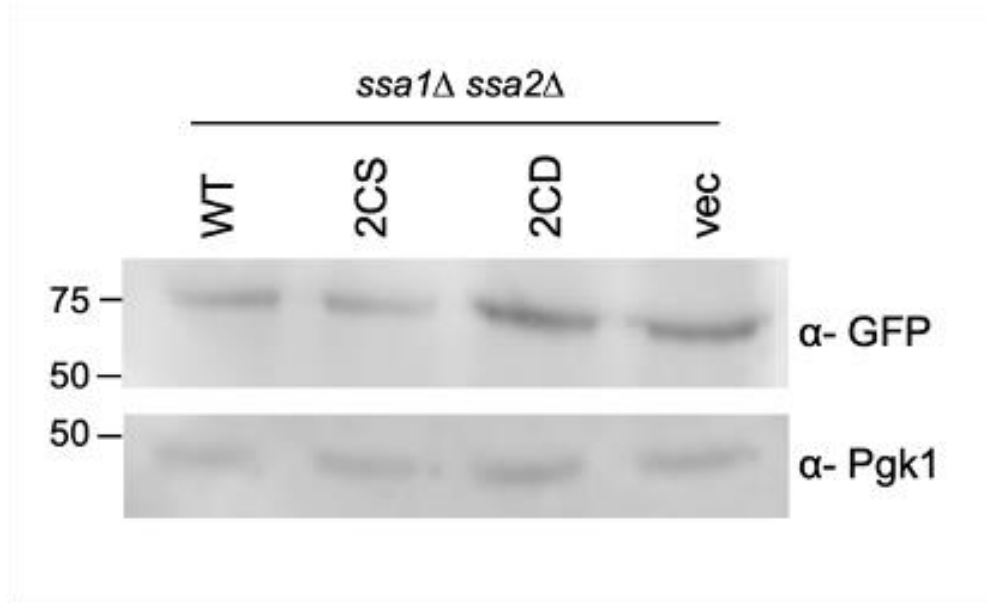
Fig. 4-7: The *ssa1-2CD* mutant exhibits multiple deficiencies in proteostasis

(A) Images representing FFL-GFP fluorescence in *SSA1* or *ssa1* mutant strains grown overnight at 30°C. (B) Quantification of (A) in terms of foci per cell. Each data point represents percentage of cells containing foci from a minimum of 50 cells per replicate. (C) Schematic of FFL-GFP recovery assay and representative micrographs detailing *SSA1* and mutant *SSA1* strains at 0 and 90 min after initiation of cycloheximide chase. Number of cells containing foci are shown as an inset percentage. (D) Quantification of assay detailed in (C), measured as the percentage FFL-GFP chemiluminescence activity at t_{90} in *SSA1* and respective *ssa1* mutant strains, relative to the same sample at t_0 . Bolded horizontal bars indicate mean, and error bars indicate SEM.

Taken together, these data indicate that the mimicking of chronic oxidation of Ssa1 cysteines 264 and 303 dramatically undermines general proteostasis, with negative consequences for the proper folding of nascent translating polypeptides and the re-folding of stress-denatured proteins. Chaperones, most notably the Hsp70s, are tightly integrated into the protein quality control system and selectively regulate protein degradation via presentation of substrate to ubiquitin ligases¹³². Though Hsp70s are not involved in the direct degradation process, their assistance in the degradation system can be measured by proxy using direct protein surveillance techniques. To investigate how thiol modification of Ssa1 cysteines affects degradation of misfolded proteins, I utilized a well-characterized substrate, tGND-GFP^{132,151}. This artificial construct contains a truncated version of the Gnd1 protein fused to GFP that results in an unfoldable substrate with defined kinetics of degradation through the ubiquitin-proteasome pathway^{132,151}. I first attempted several chronically misfolded protein models that did not have an Ssa1 dependence, including CPY-GFP and GFP^{NLS}-VHL (Fig. 4-8E). The Hampton lab published a paper detailing the varied dependence on Ssa1 for degradation of specific substrates, indicating that one chronically misfolded protein substrate with clear Ssa1 dependence was tGND-GFP¹³². I then expressed tGND-GFP in the presence of the *SSA1* alleles and observed a greater than two-fold increase in steady state levels of the substrate by immunoblot in the *ssa1-2CD* and vector control strains (Fig. 4-7A, 4-7B). This indicated that in the absence of stress, the concentration of the chronically misfolded tGND-GFP was more than twice as high in the *ssa1-2CD* strain than in the *SSA1* strain. To determine the status of accumulated tGND-GFP, log phase cells

were treated with cycloheximide to stop further synthesis and imaged by fluorescence microscopy. Representative micrographs show the presence of tGnd1-GFP foci presence in all strains at t_0 , indicating that misfolded protein was sequestered into protein aggregates (Fig. 4-7C). After 90 min, foci remained in a significantly higher amount of *ssa1-2CD* and vector control cells compared to *SSA1* and *ssa1-2CS* cells, where foci were largely eliminated, indicative of impaired substrate processing and degradation (Fig. 4-7C, 4-7D). Taken together, these data support the conclusion that Ssa1 cysteine oxidation, as mimicked by aspartate substitution, renders the chaperone defective in promoting the degradation of terminally misfolded substrates.

A.



B.

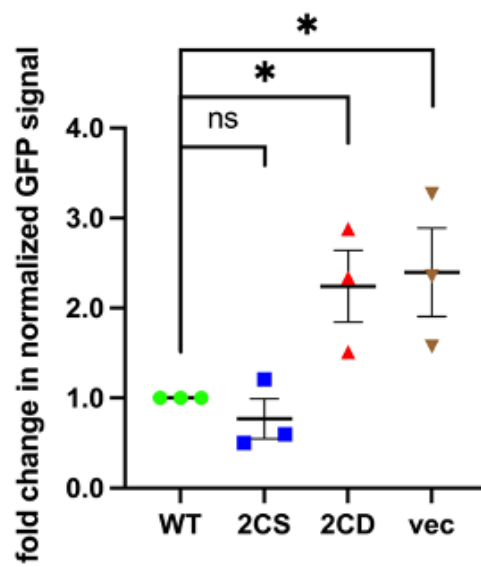
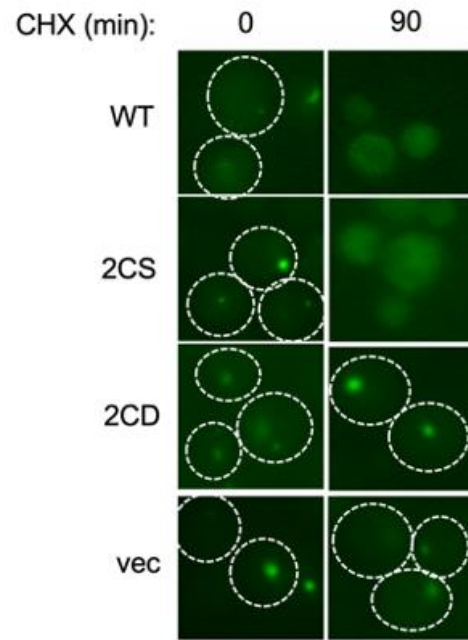


Fig. 4-8: Degradation of the misfolded protein tGND-GFP is chronically impaired in *ssa1-2CD* cells

C.



D.

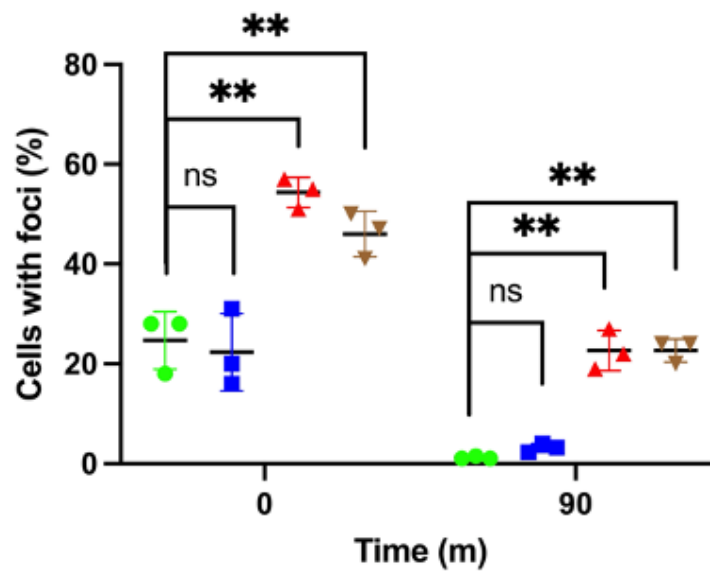


Fig. 4-8: Degradation of the misfolded protein tGND-GFP is chronically impaired in *ssa1-2CD* cells

E.

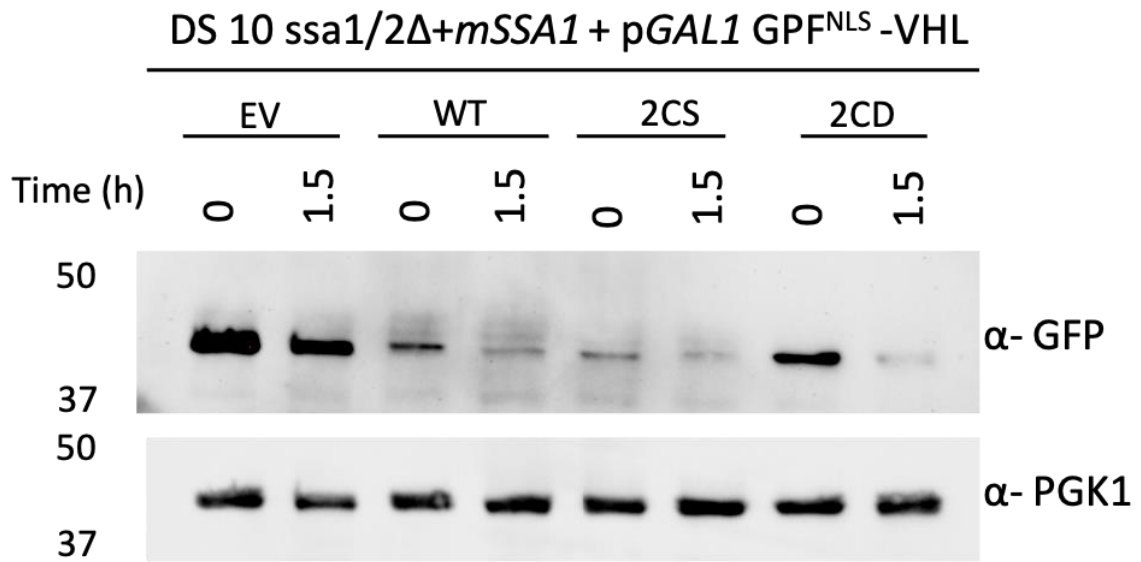


Fig. 4-8: Degradation of the misfolded protein tGND-GFP is chronically impaired in *ssa1-2CD* cells

Fig. 4-8: Degradation of the misfolded protein tGND-GFP is chronically impaired in *ssa1-2CD* cells (A) Western blot analysis of steady state levels of the chronically misfolded protein tGND, co-expressed with *SSA1* or mutant *ssa1* alleles taken from cells in log phase. (B) Quantification of signal in A, measured as fold change of each mutant allele relative to *SSA1*, from three replicate blots. (C) Representative images of cycloheximide chase, monitoring tGND-GFP foci presence over 90 min for each respective allele. (D) Quantification of images in C, with each data point representing a percentage of cells containing foci from a minimum of 50 cells per replicate. Bolded horizontal bars indicate mean, and error bars indicate SEM. (E) Western blot analysis of steady state levels of the chronically misfolded protein GFP^{NLS}-VHL, co-expressed with *SSA1* or mutant *ssa1* alleles taken from cells in log phase.

Discussion

The attempts to isolate Ssa1-2CD were not successful, but it did reveal how detrimental the irreversible oxidation of cysteines 264 and 303 are for the homeostasis of growing cells. When the *SSA1* genes were driven from the *CYC1* promoter, the growth was globally slowed, but also comparable between all strains. When the genes of interest are driven from the *TEF* promoter, the concentration of Ssa1-WT and Ssa1-2CS in the cell were increased, while Ssa1-2CD remains at a comparable level to when it was produced by the *CYC1* promoter. Altogether, this suggests a threshold of Ssa1 protein abundance whereby when the presence of Ssa1 is below that threshold, the cell is not globally affected by the mimicked oxidation of cysteines any more than a reduced cysteine. When only a small amount of Ssa1 is produced, phenotypes are masked by the relatively low amount and potential remediation by intracellular operations, and all strains are identical in growth deficiency. However, when Ssa1 production is above that threshold, the behavior of Ssa1 affects the cell either positively (as with WT and Ssa1-2CS) or negatively (as with Ssa1-2CD), and the implications of the negative behavior are such that the concentration is lowered back below that threshold. As the Ssa1-2CD protein is stable over time (Figure 4-3C) and is not subject to insolubility (Figure 4-3D), it is likely through direct action by the cell that the concentration is lowered below the threshold of affectation.

The inability to fully bind to and repress Hsf1 is a very interesting result. Recent published data explored the link between cytosolic misfolded protein and the titration of Hsp70 away from Hsf1, stimulating the heat shock response. However, the binding

to both Hsf1 and misfolded protein substrates is done by the SBD of Hsp70s. This suggests a higher affinity for misfolded proteins than for Hsf1, which was found by the Andreasson lab to be predominantly the misfolding of nascent proteins⁸⁴. Once there is no more high-affinity substrate, Hsp70 returns to bind Hsf1 and terminates the stress response. Our results mirror this mechanism of action, but stem from a direct Hsp70 modification. Interestingly, it is a modification of the NBD that is affecting the affinity of the SBD to Hsf1. However, the mechanism of action necessitates a release of Hsf1 in order to stimulate the stress response, and several oxidative stressors were shown to directly elevate HSR expression⁸⁹. Our lab first demonstrated how celastrol, a Chinese herb, stimulated the heat shock response as well as a battery of antioxidant defense genes under the control of Yap1, an oxidant defense transcription factor³⁹. Continuing that research, our lab then showed that Hsf1 activity was directly stimulated by several thiol modifying compounds and that the response was ameliorated by excess thiol treatment, also connecting the reactivity of the response to the two cysteines of interest in Ssa1, C264 and C303, which were found to be sensitive to thiol modification⁸⁹. Our lab then expanded the details of Hsf1 regulation by Hsp70 through the identification of a secondary Hsp70 binding site in the N-terminal activation domain, and demonstrated how abolishing these two Hsp70 regulatory sites resulted in dysregulation of the heat shock response¹⁰. Thus, it corroborates the allosteric changes seen in Chapter 3 that an oxidomimetic within the NBD is able to alter the affinity of Hsp70 for Hsf1 through conformational change to the SBD or through altered relationship with nucleotide, affecting binding kinetics. Several similar studies in Ssa1 homologues have argued that Hsp70s with

cysteine modifications have the propensity to go from a 'foldase' that actively promotes protein folding to a 'holdase' that binds to and protects misfolded substrate, drastically slowing the release ^{122,152}. I posit that these examples of NBD modification affecting SBD kinetics mirrors what is also seen in our data, resulting in a lowered Hsf1-binding affinity.

Our *in vitro* data also suggests a deficiency in many primary roles of Hsp70 regarding protein homeostasis. Cells expressing *ssa1-2CD* were significantly less able to correctly fold FFL-GFP *de novo*, or to refold aggregates of the same protein after heat-induced misfolding. Additionally, levels of chronically misfolded protein substrate were constitutively elevated in *ssa1-2CD* cells. Leading from the data, this defect may be multi-pronged in its root cause. The data in Chapter 2 demonstrates a clear deficiency in the ability of Ssa1-2CD to optimally engage with nucleotide, which results in a global lowering of the rate of chaperone cycling, and a slowed ability to go through the iterative conformational cycle that is the cornerstone of Ssa1's role in protein homeostasis. Additionally, the purported transition from a 'foldase' to a 'holdase' may lengthen the time spent binding each individual peptide, slowing the rate of comparative protein folding between the strains. Chronic stimulation of the heat shock response through the inability of the Ssa1-2CD mutant to repress Hsf1 activity also leads to chronically decreased functional transcription through premature termination ¹⁵³. Reversibility of the cysteine sensor is tantamount to proper defense as a non-modifiable Ssa1-2CS may not be able to detect oxidative stress and respond with de-repression of Hsf1, while the Ssa1-2CD is mimicking an irreversible oxidative stress detection signal, which has been linked to elevated unfolded protein response

stimulation in the endoplasmic reticulum in multiple myeloma cells, through overlapping signal pathways ¹⁵⁴. Constitutive induction of the unfolded protein response may lead to cell death through apoptosis ¹⁵⁵. Altogether, the consequences are sub-optimal for exponential growth of a cell, but may be beneficial to a cell that is exposed to stress. By limiting functional protein propagation through the elongated binding of polypeptides, the cell minimizes the chances that incorrectly folded, potentially toxic proteins are formed, which may further exacerbate the stress. The potential reversibility of the cysteine modification allows for reversal of Ssa1's functionality once the redox imbalance has been restored and the cysteine is able to be reduced again, terminating the multi-protein stress response.

**Chapter V: Explorations of chaperone cysteines within the OxiMouse
Database**

Introduction

Oxidation is particularly important to cellular health through the progression of aging, as cells undergo a sudden redox collapse as they advance in lifespan ¹⁵⁶. However, it is not certain as to whether aging is a consequence of oxidative stress, or vice-versa ¹⁵⁷. For many decades, it has been postulated that damage to macromolecules by oxidative stress is sustained to a point of imbalance that is phenotypically seen as the weathering of cells, or 'aging' ¹⁵⁸. Neurodegeneration is also heavily implicated with both aging and imbalance of protein management systems, making the redox state of chaperone systems and thus the impact of redox on function, a link of utmost importance. Understanding the impact of cysteine oxidation state within proteins is critical for research that aims to prevent, protect, or reverse the proteomic damages seen to correlate with aging.

In recent years, databases have been compiled that explore cysteine oxidation within the complete proteome of various organisms, such as compilations of the yeast redoxome by the Jakob lab and the Toledano lab ^{159–162}. The use of labeling techniques, such as ¹⁴C labelling of the thiol-modifying compound NEM and the ¹²C labelling of the thiol-modifying isotope-coded ICAT affinity tag (OxICAT), allows researchers to monitor the redox state of protein thiols in their native environment. However, one detractor in redox identification studies has been the lack of quantification regarding the percentages of oxidized thiols relative to the entire pool of that specific protein ¹⁶³. However, a recently published model of proteomic oxidation, dubbed OxiMouse, has illustrated a comprehensive and quantitative

mapping of the cysteines within the mouse proteome, *in vivo*¹⁵⁹. The OxiMouse system was developed by using non-hydrolyzable, irreversible, cysteine-alkylating phosphate 'warheads' (CPTs), allowing for purification by IMAC¹⁵⁹. To measure percentage of reversible/irreversible oxidation within a specific protein species, the authors used a selective labeling technique coupled with the CPT to discern redox states. The researchers then took the data further by examining the differences in ten different types of tissue, and comparing each between young and old mice. Quantitatively, the researchers isolated 34,000 total unique cysteine sites, in 9,400 unique proteins, in mice that were either 16 weeks or 80 weeks old, in 5 biological replicates, the entirety of which can be found at <https://oximouse.hms.harvard.edu>. I elected to take a deeper look into the OxiMouse database and deduce the redox state of proteins that are relevant to my Ssa1 data. Specifically, I wanted to quantifiably explore the thiol oxidation state of Hsp70 and structurally similar Hsp110 proteins, in regards to young versus old mice, in each tissue type.

Results

Building on the work of the Chouchani lab, I was able to draw conclusions about the *in vivo* redox state of several chaperone proteins in mice that are homologous to the proteins of interest in the previous chapters. I began by parsing through the database and collecting the relevant cysteine information from every Hsp70 and Hsp110 that was present. To deduce which cysteines were significantly more oxidized in old mice versus young (significant cysteine oxidation events), I set a threshold of old/young greater than or equal to 1.5x-fold higher cysteine oxidation for each site (a minimum 50% increase). The cysteines of interest are shown in the table below:

Table 5-1: Cysteines events of interest in the OxiMouse database

| Cysteine of interest | Location | Constitutive/Induced | Protein Family |
|-----------------------------|-----------------------------|-----------------------------|-----------------------|
| HSP1AL C605 | cytosol, nucleus, lysosomes | constitutive | 70 |
| HSPA2 C18 | cytosol, nucleus | constitutive | 70 |
| HSPA2 C191 | cytosol, nucleus | constitutive | 70 |
| HSPA2 C577 | cytosol, nucleus | constitutive | 70 |
| HSPA2 606 | cytosol, nucleus | constitutive | 70 |
| HSPA1B C17 | cytosol, nucleus, lysosome | stress induced | 70 |
| HSPA1B C306 | cytosol, nucleus, lysosome | stress induced | 70 |
| HSPA1B C574 | cytosol, nucleus, lysosome | stress induced | 70 |
| HSPA1B C603 | cytosol, nucleus, lysosome | stress induced | 70 |
| HSPA5 C42 (BiP) | ER | constitutive | 70 |
| HSPA9 C66 | mitochondria | constitutive | 70 |
| HSPA9 C317 | mitochondria | constitutive | 70 |
| HSPA9 C366 | mitochondria | constitutive | 70 |
| HSPA9 C487 | mitochondria | constitutive | 70 |
| HSPA9 608 | mitochondria | constitutive | 70 |
| HSPA4L C140 | cytosol, nucleus | constitutive | 110 |
| HSPA4L C167 | cytosol, nucleus | constitutive | 110 |
| HSPA4L C245 | cytosol, nucleus | constitutive | 110 |
| HSPA4L C270 | cytosol, nucleus | constitutive | 110 |
| HSPA4L C310 | cytosol, nucleus | constitutive | 110 |
| HSPA4L C417 | cytosol, nucleus | constitutive | 110 |
| HSPA4L C540 | cytosol, nucleus | constitutive | 110 |
| HSPA8 C17 | cytosol, nucleus | constitutive | 70 |
| HSPA8 C574 | cytosol, nucleus | constitutive | 70 |
| HSPA8 C603 | cytosol, nucleus | constitutive | 70 |
| HSPA4 C140 | cytosol, nucleus | constitutive | 110 |
| HSPA4 C167 | cytosol, nucleus | constitutive | 110 |

| | | | |
|--------------|--------------------------------|----------------|-----|
| HSPA4 C213 | cytosol, nucleus | constitutive | 110 |
| HSPA4 C245 | cytosol, nucleus | constitutive | 110 |
| HSPA4 C270 | cytosol, nucleus | constitutive | 110 |
| HSPA4 C310 | cytosol, nucleus | constitutive | 110 |
| HSPA4 C417 | cytosol, nucleus | constitutive | 110 |
| | | | |
| HSPA1A C603 | cytosol, nucleus, lysosomes | stress induced | 72 |
| | | | |
| HSPA12A C80 | cytosol, nucleus | unsure | 70 |
| HSPA12A C246 | cytosol, nucleus | unsure | 70 |
| HSPA12A 564 | cytosol, nucleus | unsure | 70 |
| | | | |
| HSPA14 C89 | cytosol | stress induced | 70 |
| HSPA14 C304 | cytosol | stress induced | 70 |
| HSPA14 C335 | cytosol | stress induced | 70 |
| HSPA14 C394 | cytosol | stress induced | 70 |
| HSPA14 C440 | cytosol | stress induced | 70 |
| HSPA14 C492 | cytosol | stress induced | 70 |
| | | | |
| HSPA12B C36 | cytosol, nucleus | constitutive | 70 |
| HSPA12B C194 | cytosol, nucleus | constitutive | 70 |
| HSPA12B C250 | cytosol, nucleus | constitutive | 70 |
| HSPA12B C321 | cytosol, nucleus | constitutive | 70 |
| HSPA12B C365 | cytosol, nucleus | constitutive | 70 |
| HSPA12B C570 | cytosol, nucleus | constitutive | 70 |
| HSPA12B C595 | cytosol, nucleus | constitutive | 70 |

Table 6-1: Cysteines events of interest in the OxiMouse database

Cysteines identified as modified within the Hsp70 and Hsp110 categories of the mouse proteome. Unique cysteine sites are listed, followed by the predominant site of protein localization, the state of protein induction, and the specific protein category (70/110).

The OxiMouse database consists of data from ten tissue types: lung, epithelial tissue (epi), liver, brain, heart, brown adipose tissue (BAT), spleen, kidney, subcutaneous adipose tissue (SubQ), and skeletal muscle tissue (SKM). With our lab fundamentally based in yeast cell biology that links to neurodegeneration, I elected to examine significant oxidation events as a product of Hsp70 vs Hsp110 in each tissue type. Aging impacts the entire organism, but the structural impact of aging and disease presentation is very dependent on tissue type. In 8 out of 10 tissue types, there was a larger number of significant cysteine oxidation events in Hsp70s than Hsp110s, with the only two tissue types had more Hsp110 cysteine oxidation events being the brain and the liver (Figure 5-1). The highest total significant oxidation events occurred in the brain and the epithelial tissue. The lowest total significant oxidation events occurred in the heart and skeletal muscle tissue. Next, I quantified which of the significant oxidation events occurred in constitutively expressed proteins versus stress-induced proteins. The vast majority of oxidation events in all tissue types occurred in constitutive proteins, with no stress-induced oxidation events occurring at all in brown adipose tissue, kidney tissue, and epithelial tissue (Figure 5-2). Single events were seen in heart tissue, spleen tissue, and subcutaneous fat tissue. The most abundant stress-induced events occurred in the brain.

A.

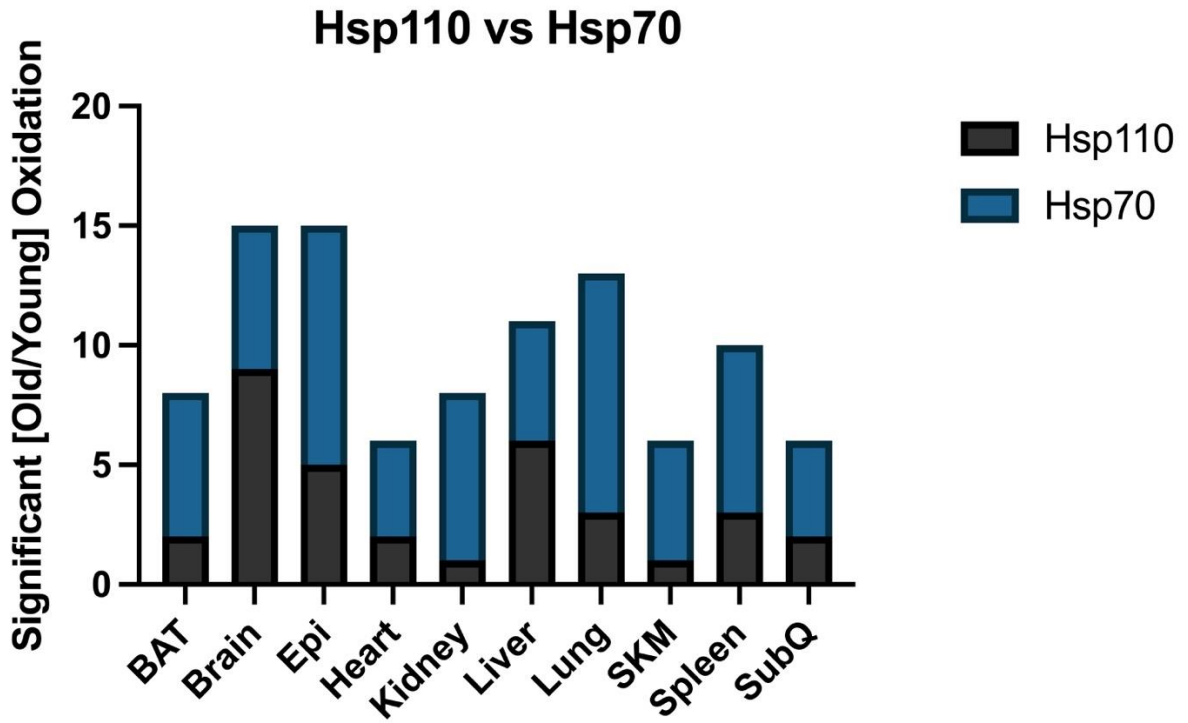


Figure 5-1: Significant oxidation events occur more frequently in Hsp70 than Hsp110 (A) Significant cysteine oxidation events (>1.5-fold increase in young/old populations) in Hsp70s (blue) or Hsp110 (black), for each respective tissue type.

A.

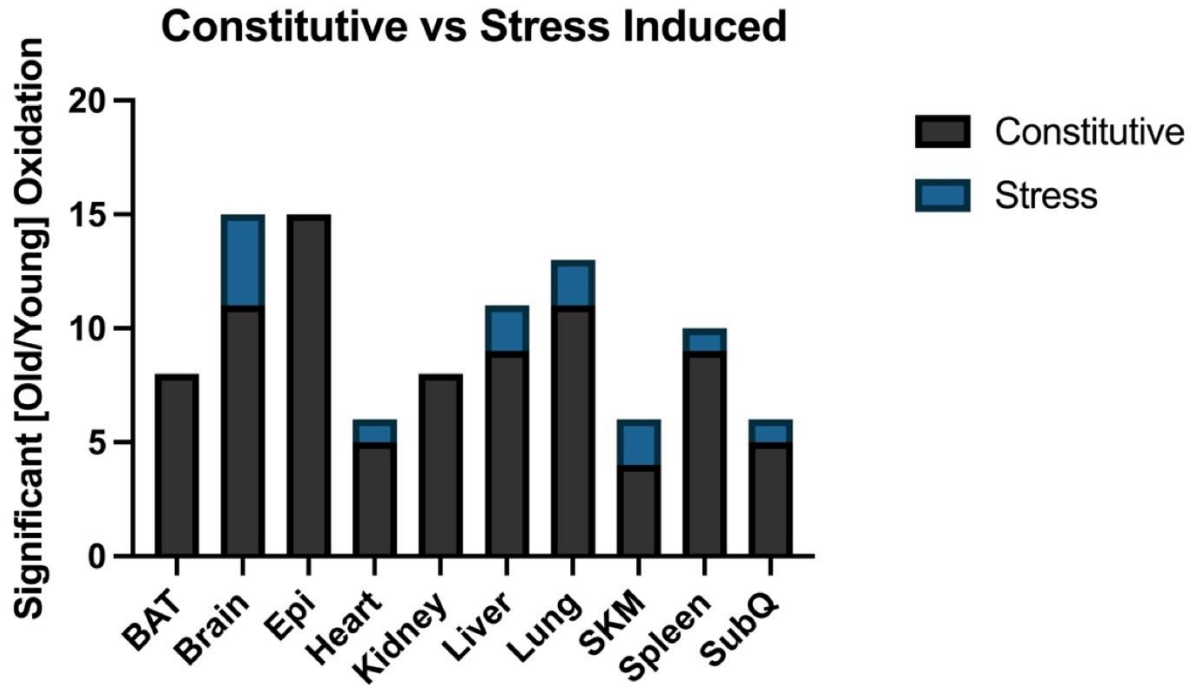
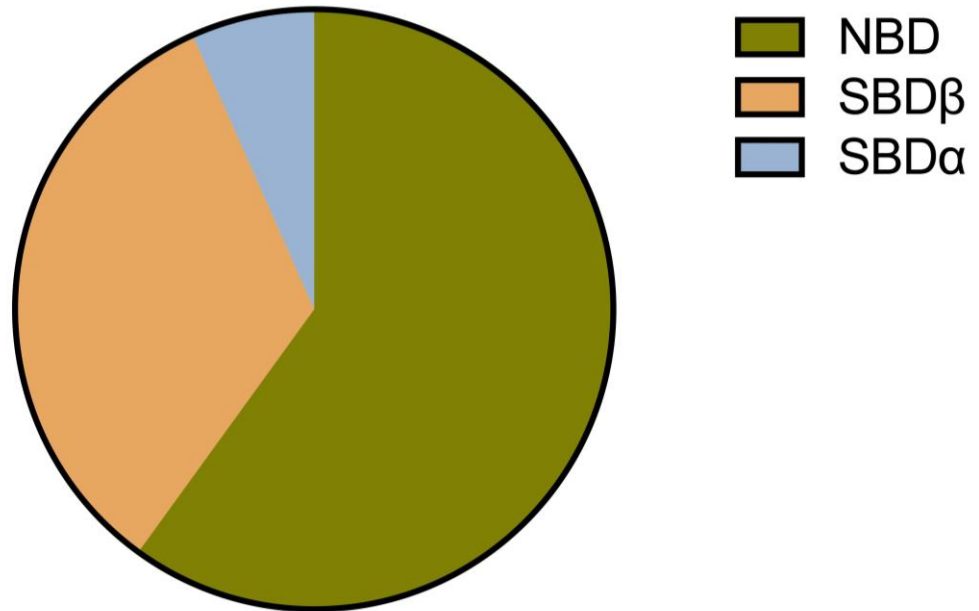


Figure 5-2: Significant oxidation events occur more frequently in constitutively expressed Hsp70s than in stress-induced Hsp70s (A) Significant cysteine oxidation events (>1.5-fold increase in young/old populations) in stress-induced proteins (blue) or constitutively expressed proteins (black), for each respective tissue type.

The Ssa1 cysteines of interest in the previous chapters are both within the nucleotide binding domain. That localization was the premise for the underlying hypothesis that the phenotypic deficiency stemmed from the interaction between Ssa1 and nucleotide. Here, I compared the localization of the significant cysteine events of the brain as a product of the functional domain of the respective proteins, quantifying the number of events in the nucleotide binding domain, and each respective component of the substrate binding domain (Figure 5-3). Hsp70s and Hsp110s have a very similar structure, except for a series of extensions within the Hsp110 family, so comparing their structures may offer insights to how these general domains are affected by cysteine oxidation. By a small margin, there are more oxidation events that occur in the nucleotide binding domain than the entirety of the substrate binding domain, and only a single oxidation event occurs in the SBD α 'lid' domain (Figure 5-3). The total events are: NDB (8), SBD α (1), and SBD β (6).

A.



Total=15

Figure 5-3: Cysteine oxidation events within the Hsp70 and Hsp110 proteins of brain occur more frequently in the NBD than the SBD (A) The total number of cysteine oxidation events occurring in the Hsp70 and Hsp110 proteins of the OxiMouse brain tissue, as categorized by functional domain. Nucleotide binding domain events are shown in green, substrate binding domain- α is shown in blue and substrate binding domain- β is shown in orange.

Discussion

The benefit of a cohesive quantification of an organism's full proteome cannot be overstated. Introducing such complexities as tissue type and age difference creates a diligent assessment of the role that oxidation plays in tissue-specific proteome breakdown and disease manifestation around the body. Specifically exploring Hsp70s and the structurally-similar Hsp110s allows me to draw comparisons between my work and the proteome of other eukaryotes. With neurodegenerative disease being correlated to oxidative imbalance, it is important to understand key sites of oxidation that are present in the proteostatic machinery over time. Exploring the significant oxidation sites of Hsp70s and the structurally similar Hsp110s within mouse tissues creates an in-depth assessment of the oxidative state of resident cysteines, and the effects on the domain architecture that they reside in.

In Figure 5-1, the quantification is diverged in two directions: the number of oxidation events in each tissue type, and the distinction between occurring within an Hsp70 or an Hsp110 for each event. By sheer number, the oxidation events occur much more frequently in Hsp70s than Hsp110s. In fact, there are only two Hsp110 proteins that contain significant oxidation events, compared to ten Hsp70 proteins. There are 84 Hsp70 oxidation events across tissues and 13 Hsp110 events, giving an average of 8.4 events/affected protein for Hsp70s and 6.5 events/affected protein for Hsp110s, a surprisingly comparable metric considering the lower total population of affected Hsp110s.

It is also very interesting to notice the spread of oxidative events across tissue types. Skeletal muscle tissue, heart tissue, and subcutaneous adipose tissue had

lower occurrences of oxidative events than the other tissues, with nearly one third of the occurrences in brain and epithelial tissue. One possible reason for the differing levels in tissue type is the consistent exposure that epithelial tissues get to exogenous oxidants, such as pollutants and environmental organisms, while the brain is highly susceptible to damage and may require additional oxidative-stress sensing ability relative to other organs. Meanwhile, heart has abundances of resting metabolic activity relative to other organs, and the SKM has increased metabolic activity during any non-resting phase, meaning that heightened sensitivity to oxidative stress would result in a constant negative feedback loop ¹⁶⁴.

In Figure 5-2, the data is assembled to visualize the difference between stress-induced proteins and constitutively expressed proteins that contain significant oxidation events. This is especially of interest for the Hsp70 proteins, which constitute a more dedicated 'stress-induced' category. There are only thirteen individual oxidation events in stress-induced proteins, making them the clear minority to events in constitutively expressed proteins. This suggests that constitutive proteins require, or are at least susceptible to, modification by stress. The increased modification likely is a result of more stringent and tunable regulation, allowing the behaviors and effectiveness of proteins present at relatively higher concentrations to adapt more flexibly to environmental injury. Stress-induced proteins are by definition more present in an antagonistic environment, and susceptibility to that environment may negate the behaviors that rectify the injury itself. Thus, a nullification of that regulation may be more evolutionarily advantageous as the stress-induced proteins are not part of the negative feedback loop brought on by the oxidative challenge. This allows the

constitutive Hsp70 proteins to enable the protective 'holdase' behavior in the face of potential injury, while the non-susceptible stress-induced proteins compensate for the necessary 'foldase' behavior.

Additionally, I explored the structural impact of oxidation events by examining in which domain the event occurred (Figure 5-3). Due to the very similar structures of Hsp70s and Hsp110s (30-33% sequence similarity¹⁶⁵), I could define the events in the same categories of nucleotide binding domain (NBD), substrate binding domain alpha (SBD α), and substrate binding domain beta, (SBD β). I found that the categories were nearly split equally, which was interesting in reference to my own data, given that all three cysteines of Ssa1 are located in the NBD. However, in mice chaperone proteins, there is a large occurrence of SBD-localized cysteines, and they are shown to be widely susceptible to oxidative modification in the OxiMouse model. My work in Ssa1 showed a behavior modification brought on by oxidative stress that altered the relationship between Ssa1 and nucleotide, which also shifted the behavioral and conformational aspects of Ssa1 through allosteric shifts. Interestingly, this OxiMouse data suggests that modification, and thus likely regulation, can affect both the intra-protein focused domain (NBD) and the inter-protein focused domain (SBD), likely affecting both to some extent through allostery, as was seen in Ssa1. Directly affecting the cysteines within the substrate binding domain may not only cause conformational shifts that echo throughout the protein, but also may cause a direct steric barrier to substrate proteins that are attempting to bind. Elevated oxidation states of cysteine were mirrored by the Sevier lab by more sterically imposing amino acid substitutes, and were referred to as 'bulky substitutions', due to their space-filling

and conformation shifting characteristics ¹¹¹. The nearly equal spread of NBD and SBD oxidation events seen in the OxiMouse model suggest that a direct steric hinderance within either domain may be one method of regulating chaperone function when faced with an oxidative challenge.

Altogether, this database exploration yielded a number of parallels to my own work and serves to further elaborate on the role that cysteine modification plays in the oxidative stress response.

Chapter VI: Discussion and Future Directions

Note: Portions of this section were originally published in Experimental Cell Research. Santiago A, Goncalves, D., Morano KA. Mechanisms of sensing and response to proteotoxic stress. Exp Cell Research. 2020 Oct 15:395:2. <https://doi.org/10.1016/j.yexcr.2020.112240>. *Elsevier does not require permission to use published materials in one's dissertation:* <https://www.elsevier.com/about/policies/copyright/permissions>.

Summary of Results

In these explorations, I report in detail the functional ramifications of oxidation of two key cysteines in Ssa1 shown prior to be necessary for stimulation of the HSR by thiol-reactive molecules, using both genetic and chemical strategies. Data analysis of isolated proteins showed that Ssa1-2CD, but not the Ssa1-2CS mutant, is deficient or the binding of ATP and subsequent hydrolysis, plus ATP-dependent folding of proteins. Similar consequences were seen after treatment of wild type Ssa1 protein with hydrogen peroxide, corroborating the usefulness of the aspartic acid substitution to mimic the sulfinic acid moiety of the thiol group within the cysteine, post-oxidation. Of interest, the cysteine nullification substitution to serine (Ssa1-2CS) was non-reactive when exposed to hydrogen peroxide at concentrations that reduced Ssa1 enzymatic activity *in vitro*. I have thus determined that cysteines 264 and 303 are solely responsible for the documented behaviors *in vitro* and *in vivo*, given our experimental conditions. Along with these two Ssa1 cysteines which are found on lobe IIB in the nucleotide binding domain, a third cysteine residue is conserved in most Hsp70 homologs buried further within the nucleotide binding cleft (C15 in Ssa1). Our data posits that C15 is not a vulnerable site of oxidation within Ssa1. This finding is at odds with previous findings from the Sevier laboratory in which C63 of the ER-localized Hsp70 Kar2/BiP was shown to be susceptible to oxidation¹⁶⁶. Yet, both the *S. cerevisiae* Hsp70 Kar2 and the mammalian Hsp70 BiP lack homologous cysteines 264 and 303, adding complexity to a direct comparison. Of note, all three cysteines are susceptible to reactivity with the alkylating compound N-ethylmaleimide (NEM); NEM-Ssa1 also demonstrated an identical array range of functional deficiencies as

our oxidomimetic substitute and peroxide-treated Ssa1¹²³. NEM-treated Ssa1 exhibited modified trypsinization profiles and intrinsic tryptophan fluorescence that indicates structural changes in the NBD¹²⁴. In human Hsc70, it was reported that modification of nucleotide pocket-facing C17 sterically shifted a catalytic magnesium ion that is necessary for nucleotide hydrolysis by increasing the separation of that magnesium from several coinciding residues¹⁰⁹. These reported data are also consistent with prior results that the dye compound methylene blue oxidizes cysteines 267 and 306 in the stress-inducible human Hsp70, resulting in deficient ATP binding and hydrolysis⁹⁰. *in silico* modeling from the same published work explained that oxidation occurs in a step-wise fashion, where C306, residing on the outer surface of lobe IIB of the NBD, is primarily oxidized, leading to a conformational shift that displaces the inner lobe cysteine, C267, into a solvent-exposed cleft. This structural shift is noted to increase both accessibility and reactivity of the thiolate anion of cysteine 267 and concurrently disfigure the full NBD, reducing nucleotide binding affinity and downstream enzymatic activities. This model is parallel and sound with a previously reported study from our lab that demonstrated the reaction of C264 in Ssa1 with a 4-hydroxynonenal alkyne and subsequent derivatization via click chemistry that was lost in a C303S mutant⁸⁹.

I also demonstrated that inclusion of Ssa1-2CD prevented functional firefly luciferase refolding by Ssa1. These data are cohesive with prior reports that NEM-Ssa1 similarly prevented Ssa1-dependent folding but not the propensity to prevent aggregation of misfolded protein. Indeed, oxidation, alkylation, or substitution with a bulky side chain residue of C63 in Kar2 significantly promotes the “holdase” function

of that Hsp70¹⁶⁶. These data are all consistent with a model wherein oxidation disrupts functional allosteric signaling between the NBD and SBD but does not affect, and might even promote, polypeptide binding by the SBD, resulting in competition for binding to Hsp70 and preventing functionally positive folding reactions. Such a model would help explain the toxic growth phenotypes I saw upon expression of *ssa1-2CD* in yeast that still expressed the inducible SSA isoforms Ssa3 and Ssa4. Additionally, this model also substantiates a mechanism by which oxidation of only a select percent of the greatly abundant population of Ssa1 and Ssa2 could have negative effects on cell functions and growth, as it is not very likely that short term exposure to oxidants would alter the majority of present Hsp70. In contrast to the findings of Wang and colleagues, wherein oxidized Kar2 makes cells hyper-resistant to oxidative stress, I concluded with no determination of any gain of function phenotypes in the *ssa1-2CD* strain¹⁶⁶. However, it is crucial to note that our Ssa1-2CD substitution mimics the predominantly irreversible sulfinic acid thiol moiety, and reversibility has been shown to be a key determinant for oxidative regulation, as abundant oxidative stress inactivates ATP-dependent chaperones^{167,168}.

As shown by substitution with serine or alanine residues, cysteines 264 and 303 in Ssa1 are not crucial for sustaining growth at elevated temperatures, as C63 in Kar2/BiP appears to be¹⁶⁶. However, the two cysteines are crucial for promotion of stress responses and cytoprotection by cells exposed to exogenously added oxidants^{89,166}. This line of inquiry and data indicates a residue that has been evolutionarily conserved to identify and respond to an oxidative imbalance. The reversibility of cysteine modification is fundamentally important as a signal, allowing the chaperones

that have signal-responsive cysteines to transition between conformations of variable purpose, with the added participation of redox management systems, like the thioredoxin and glutathione pathways ¹⁶⁹. A fundamental example of the usefulness of Ssa1 cysteines as a sensor is the transient stimulation of the HSR upon exposure to alkylating or oxidizing agents. As yeast Hsf1 does not have cysteines, it is not able to elicit a response to such environmental situations, whereas human HSF1 contains several cysteines that are directly modified to activate the HSR and promote proteostasis ¹⁰⁷. C264/C303 of Ssa1 therefore have an directly analogous position, acting as an oxidative sensor in yeast through the recently reported repression of Hsf1 directly by the chaperone protein.

This work is now able to draw a connecting line between these two models by demonstrating that Ssa1-2CD is unable to bind either previously described site on Hsf1 *in vivo*, creating a chronically stimulated heat shock response. Of note, Ssa3/4 do not possess the cysteine contained in the outer facing lobe IIB, C303, and only contain cysteine C264, which faces the binding pocket. In agreement with the *in silico* model, this decreases the susceptibility of Ssa3/4 to oxidation, which I propose is advantageous in the face of oxidative stressors. Ssa3/4 are maintained at much lower concentrations in relation to Ssa1/2, but are induced to elevated levels in times of abundant stress exposure ⁴⁴. Interestingly, the alignment of several homologous yeast Hsp70s showed that the mitochondrial matrix-localized Ssc1 does not contain any of the three critical cysteine residues, which our data suggests may increase the resistance to cysteine-based oxidative sensing and modulation (Figure 6-1).

A.

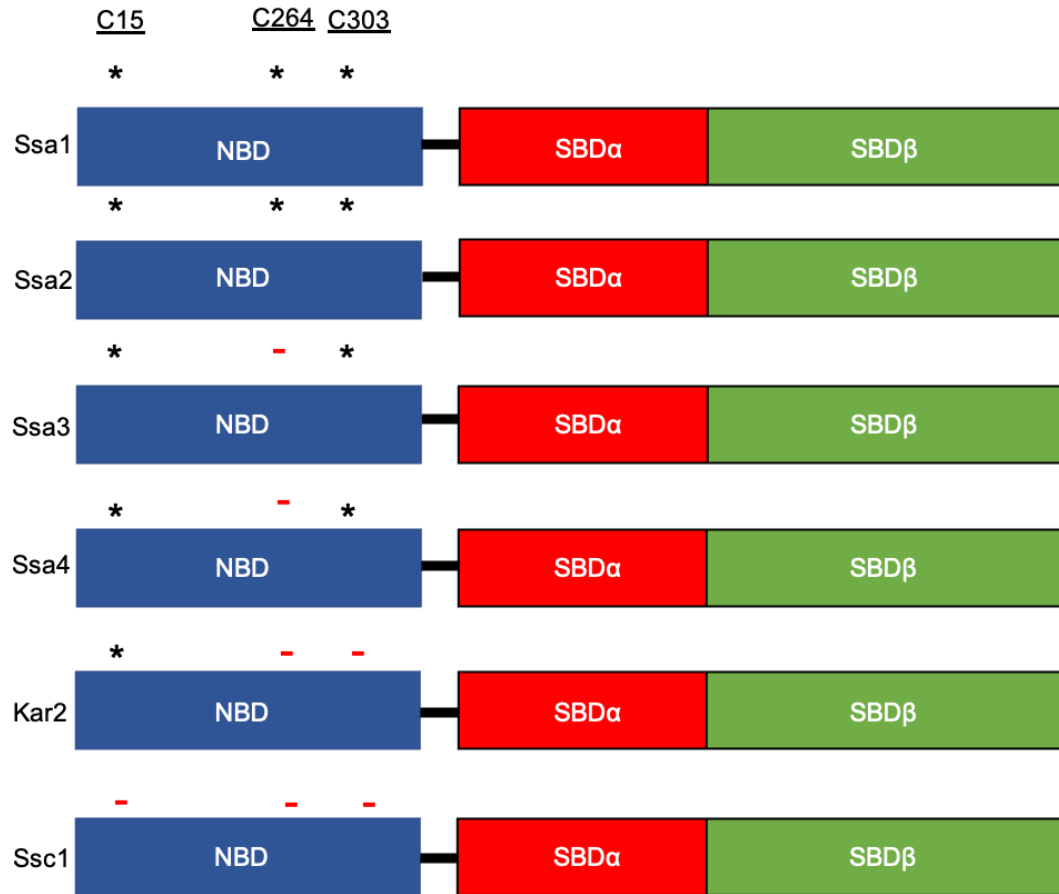


Figure 6-1: Yeast Hsp70 cysteine alignment (A) A schematic depicting the absence (-) or presence (*) of the respective cysteines C15, C264, and C303 within the indicated yeast Hsp70 proteins.

Correspondingly, the matrix NEF Mge1, which does contain cysteines, appears to instead function as a sensor of oxidative stress within the mitochondria¹⁷⁰⁻¹⁷². Re-addressing the concept of HSR regulation, I therefore imagine a situation whereby oxidative stress exposure activates Ssa1, freeing Hsf1 to activate the heat shock response, and ensuring compensatory chaperone action by the upregulation of Ssa3/4 (Figure 6-2). These two inducible Ssa chaperones can then either directly interact with the same sites on Hsf1 to attenuate the HSR, or free Ssa1 to do so, and have the additional positive characteristic of invulnerability to the present oxidative damage/signaling. This Ssa-mediated relay is highly important for oxidative sensing in yeast, as the yeast Hsf1 contains no cysteines and is thus unable to respond in the same manner. However, even in elevated stress states, the expression of Ssa3/4 (50,000 molecules per cell) is dwarfed by the presence of Ssa1 (150,000 molecules per cell). From a stoichiometric perspective, we must primarily address the potential reduction of oxidized Ssa1 as a means to manage oxidative stress. There are several means of cysteine reduction that may affect Hsp70s, including the thioredoxins Trx1 and Trx2 acting directly on oxidized cysteines or as mediators of GSSP reduction after glutathione modification¹⁷³. Additionally, chelating agents such as cadmium and lead can be removed through interaction with reduced glutathione, where they are then localized to the vacuole and eliminated^{174,175}. The balance of reduced versus oxidized glutathione is an important indicator of oxidative balance, and during times of imbalance, the pool of reduced glutathione may be depleted, leaving Hsp70 proteins more susceptible to modification by general stressors.

A.

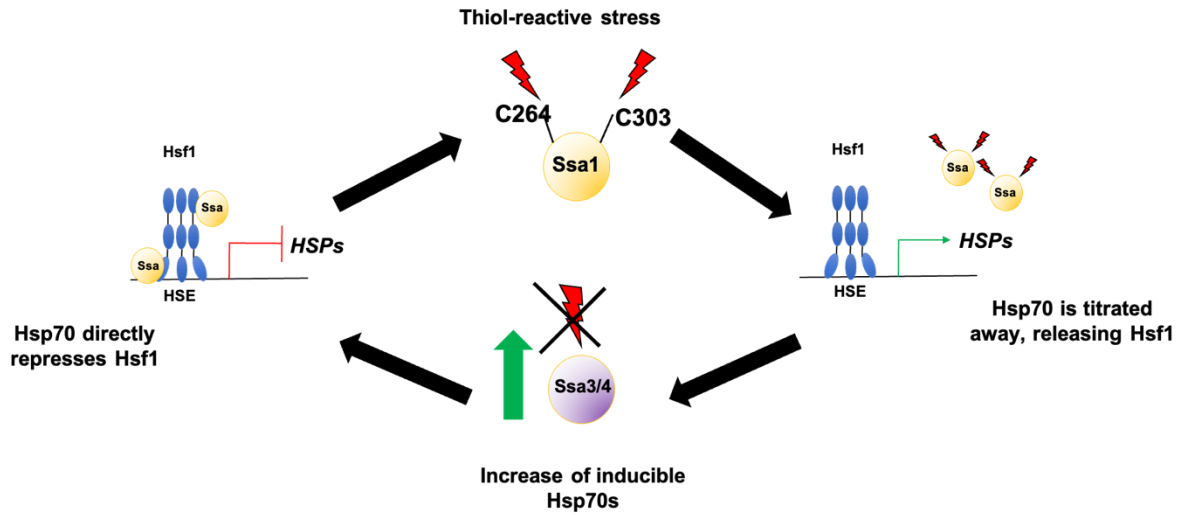


Figure 6-2: Thiol dependent regulation by Hsp70 and Hsf1 (A) A model depicting the consequences of oxidative stress and the subsequent regulation of the heat shock response by Hsf1 and Hsp70 proteins. Oxidative stress causes modification of cysteines within the Hsf1-repressor Ssa1, inducing release of Hsf1 and expression of the heat shock response. The inducible Ssa3 and Ssa4, which do not contain the relevant cysteines and are upregulated by the indicated heat shock response, alleviate the proteotoxic stress by compensating for the proteostatic duties of the nullified Ssa1. Reduction of stress eventually allows the reduction of Ssa1, which returns to Hsf1 repression and negates the heat shock response.

Experimentally, my inability to recover significant amounts of exogenously oxidized Ssa1 after treatment with DTT (Figure 3-7D) demonstrates that excessive oxidation may result in a pool of Ssa1 that is functionally irreparable, lowering the total population of Ssa1 in the cell that participates fully in active stress management. In this scenario, the stress-induced Ssa3 and Ssa4 may play an important role in replenishing the pool of active Hsp70 proteins, and that their proposed inability to respond to oxidative stress to the same extent as Ssa1 due to their lack of C264 may compensate for functions such as protection and folding assistance of polypeptides, misfolded protein refolding, and assisting in the process of degradation.

Parallels can be drawn between stress management systems when considering the KEAP/Nrf2 defense system, the Yap1-controlled oxidative stress response, and my findings of lessened Hsf1 interaction by the 2CD mutant. The KEAP protein forms part of an E3 ubiquitin ligase, interacting directly with the transcription factor Nrf2 to ensure its degradation under non-stressed conditions ¹⁰⁴. In the event of oxidative or nucleophilic stress, sensor cysteines within the KEAP protein are modified, causing conformational shift. This allows Nrf2 to escape ubiquitination by KEAP, translocate into the nucleus, and initiate activation of stress response genes ¹⁷⁶. The response is then attenuated after stress, closing the activation loop in a manner that is strikingly similar to the Ssa1-dependent model of thiol activation that I have outlined through my work. Like KEAP, Ssa1 prevents the activation of genes under control of a stress-induced transcription factor under basal conditions. If oxidative or nucleophilic stress is then sensed by cysteines in either Ssa1 or KEAP, each protein then undergoes changes which lessen the ability to

repress the action of the indicated transcription factor, subsequently allowing for activation of the stress-response genes under the control of that transcription factor. Another parallel, while operating more independently, is the activation of Yap1. Several cysteines within Yap1 sense various stressors in the cytosol, resulting in single thiol modification and disulfide bond formation within Yap1. These changes result in a rapid localization of Yap1 to the nucleus, where it promotes the activation of a host of oxidative stress response genes ¹⁰¹. The modification of the cysteines within the Ssa1 protein likely requires reduction of the affected thiols before the attenuation of Hsf1 activation by the affected Ssa1 molecules. Similarly, Yap1 requires reduction of the modified thiols before it can interact with Crm1, the protein responsible for ejecting Yap1 from the nucleus ⁷⁴. Without the nullification of the oxidative environment that results in Yap1 cysteine reduction, Yap1 remains in the nucleus and continues to promote the stress response genes it controls. The similarity between these stress responses and the thiol-dependent activation of regulatory proteins within them highlights the cells' ability to enact a multifactorial defense against stresses, which have various degrees of crossover.

I determined that several aspects of Ssa1 behavior are impaired in the *ssa1-2CD* strain. Since it would not be possible to deconstruct the pleiotropic effects of treating entire cells with exogenous oxidants, a genetic approach utilizing the oxidomimetic substitution was our primary tactic to elucidating the functional consequences of cysteine modification within the Ssa proteins. I revealed significantly reduced abilities in de novo protein folding, the extraction of incorrectly proteins from aggregates and the degradation of chronically misfolded substrates – all critical

aspects of protein homeostasis. As a whole, these phenotypes are likely to culminate in the drastically slowed growth rate of the *ssa1-2CD* mutant, its inability to promote growth as the sole SSA isoform and the abundance of gene reversion when utilizing a plasmid shuffle strategy. My results are consistent with and build upon prior results which demonstrate that an oxidomimetic allele of Hsp72 was not able to promote tau stabilization in human HeLaC3 cells ⁹⁰. Importantly, increased expression of Ssa3/4 via stimulation of the heat shock response is not able to re-enable proteostasis in the *ssa1-2CD* strain but is necessary to allow viability. Thus, there is the possibility that the *ssa1-2CD* mutant may be fully deficient in promoting the folding of proteins and the degradation of non-functional substrates within the proteome, but that a lesser yet still acceptable maintenance of proteostasis is maintained by Ssa3/4. In conclusion this work serves to elucidate the functional repercussions of irreversibly oxidized Ssa1 protein, and a broad mechanism of action for the deficiency linked to the relationship with nucleotide.

In the explorations of the OxiMouse database, I evaluated several methods of investigation regarding the oxidation of Hsp70 and Hsp110 protein cysteines. Given the similarities between Hsp70 and Hsp110 structures, there was a surprisingly wide variance in the amount of cysteine oxidation events for each tissue type. In the liver, there was a higher level of Hsp110 events (6) than Hsp70 events (5), whereas in the kidney, only a single Hsp110 event occurred, compared to five Hsp70 events. However, this research is exploring oxidation events as a consequence of aging, and each event is a comparison between the tissues of aged mice versus younger mice, defined as a minimum 1.5x-fold increase in oxidation of a particular cysteine site.

Thus, we must maintain that these cysteines may be playing an important role in both tissue samples, it is only that the extent of variation is not a consequence of age. We can also draw inverse conclusions from the same data, whereby cysteine regulation of Hsp110s may not be a primary means of managing, responding to, or sensing oxidative stress in the kidney. This is important to know, since it has been shown that oxidative stress increases and enzymatic activity decreases in both kidney and liver tissue as aging occurs ¹⁷⁷⁻¹⁷⁹. The increased oxidation in these tissues may be tied to a decrease in several oxidative management proteins, such as superoxide dismutase proteins and catalase proteins ¹⁸⁰. Given that both tissue types experience increased oxidative dysregulation but have variable levels of Hsp110 cysteine regulation, this suggests that the cysteines in question are more relevant in one tissue type than another, and it may be beneficial to future studies to determine what that variance may be.

Additional explorations concerning Hsp70 and oxidative stress

Further work is required to fully understand the consequences of oxidative stress on cell and tissue proteostasis as it relates to human health. Many industrial pollutants are oxidants or thiol-reactive molecules (e.g., heavy metals, acroleins) ¹⁸¹. Cigarette smoke contains a wide range of thiol-reactive compounds that are known to deplete cellular glutathione levels ¹⁸² Accumulation of oxidative damage is widely considered to be a key driver of aging, potentially linked to endogenous ROS generated via mitochondrial dysfunction. Indeed, oxidation of a methionine residue in

the mitochondrial Mge1 protein, a cofactor of mitochondrial matrix Hsp70, inhibits protein translocation into the organelle resulting in oxidant hypersensitivity¹⁷⁰. Recent work has systematically explored the relevancy of Hsp70s in several organisms, through several tissue types, and in many disease and lifestyle behaviors.

Copper nanoparticles are used in many widespread consumer products, such as semiconductors, sensors, antimicrobial agents, and converters. The leaching of toxic metal by-products from industrial waste sites into agricultural and watershed sites is a growing concern for technological waste management and public health¹⁸³. In *Drosophila melanogaster*, it was found that copper nanoparticles had broad impact on several consecutive generations of flies, with dose-dependent mutagenic effects that include reduced progeny, wing deformation, and increased stress indicators¹⁸⁴. The treatment of young flies with copper nanoparticles was also shown to drastically reduce the concentration of antioxidants available in offspring flies, as well as to increase the expression of Hsp70 genes and decrease the expression of superoxide dismutase *SOD2*¹⁸⁴. These results underline the impact of heavy metals as oxidative stressors and the physical impairments that can result from over-exposure.

Similarly, the heavy metal manganese has also been explored for the negative environmental and health impacts due to over-exposure. Manganese is an essential trace metal, but has the propensity to accumulate in several brain regions and negatively impact neurobehavioral function¹⁸⁵. Studies in rats found that there are several sex-dependent neurotoxic effects from manganese toxicity that directly involve oxidative stress and heat shock proteins¹⁸⁶. Post-exposure, male rats were found to have a significant loss in body weight, while female rats did not. This is

important for oxidative balance, as weight loss by inhibition of appetite and muscle mass loss has been tied to oxidative stress ¹⁸⁷. The researchers also found that while there was global upregulation of Hsp70 and Nrf2 throughout test subjects, there were distinct sex and brain region differences. In the cortex, upregulated Hsp70 and Nrf2 were only seen in females, while in the striatum, Hsp70 and Nrf2 were only upregulated in males at low doses, despite the metal accumulation being the same ¹⁸⁶. These two results together establish a wide spectrum of metals that can result in harmful organismal effects, with direct ties to oxidative stress.

Aging is heavily correlated with oxidative stress, as the concentration of reactive oxygen species steadily increases in an organism over time ⁹⁵. Similarly, as noted above, age and oxidative stress are both compounding factors for neurodegenerative disease. However, several other physical and disease states are affected by aging and oxidative stress, including vascular structural systems and diabetes. Concentrations of the 13 members of the Hsp70 family in humans have emerged as significant biomarkers for the study of biological aging, as reduced concentrations of Hsp70 have been strongly correlated with progressive aging ¹⁸⁸. Though it is only newly emerging as having a prominent role in vascular health, Hsp70 is currently being explored for its role in arterial function. Oliveira, *et. al*, recently found that the ability to produce a vascular response in mice is associated with the levels of Hsp70 ¹⁸⁹. Using phenylephrine to stimulate vascular response (localized blood pressure increase due to vascular resistance), the researchers found that middle-aged aortic tissues were less able to produce a response, and that the phenotype could be mimicked using an Hsp70-inhibitor in younger tissues, showing an age-

dependent change in tissue response that could be reproduced by Hsp70 inhibition. There was also a significantly reduced concentration of Hsp70 proteins in aged vascular tissue. Additionally, the researchers found an abundance of oxidative stress in middle-aged aortic tissues that my work suggests could be additionally altering the functionality of the already lowered levels of Hsp70 available.

Directly adjacent to the above-mentioned copper nanoparticle research, Garafolo *et. al*, explored the link between Hsp70 and superoxide dismutase in the neurodegenerative disease amyotrophic lateral sclerosis (ALS) ¹⁹⁰. Superoxide dismutases are metalloproteins that function as antioxidants, and SOD mutations often result in DNA damage and mitochondrial dysfunctions ¹⁹¹. In humans, SOD1 presence in the nucleus offers a protective advantage against the consequences of ALS. While the fly research did not extend into localization of the dismutase, Garafolo *et. al* has shown that differential gene expression patterns emerge when patients are categorized into the respective “high-SOD and low-SOD” groups. In summary, elevated levels of Hsp70 were shown to increase nuclear SOD1, and resulted in decreased DNA damage, even in elevated oxidative stress environments. Several pathways related to the heat shock response and the function of Hsp70 were also significantly altered in cells expressing high-vs-low SOD, suggesting a widely interconnecting network between antioxidant protein localization, oxidative stress imbalance, and Hsp70 presence ¹⁹⁰.

The link between oxidative stress, the heat shock response, and Hsp70 function is an increasingly well studied relationship. The hyperglycemia that is a hallmark of diabetes mellitus 2 (DM2) induces an increase in free radical

concentration ¹⁹². It has also been found that increased manganese in serum is an increased risk factor for DM2, relating research across fields to the paper mentioned above ¹⁹³. In a recent review, Hirsch, *et. al* demonstrated several interesting links between Hsp70 proteins, oxidative stress, and DM2 ¹⁹⁴. Of note, they summarized distinctions between intracellular Hsp70 (iHsp70) and extracellular Hsp70 (eHsp70). In DM2, tissue specificity plays a strong role in Hsp70 dispersion for DM2 patients. Specifically, general eHsp70 is increased, while iHsp70 is decreased, in liver, skeletal muscle tissue and adipose tissue ¹⁹⁵. Interestingly, eHsp70 resulted in an increased expression of inflammatory cytokines in DM2 patients, suggesting a negative consequence for the extracellular abundance ¹⁹⁶. Overall, this relationship between intra-vs-extracellular Hsp70 is growing in usage as an effective biomarker to calculate the progression of DM2 ¹⁹⁷. The compounding of this work serves to elaborate on the complexity of oxidative stress through several human disease, and the implications of a dysregulated stress-management system that has both positive and negative consequences.

Of a more behavior-oriented note, the link between Hsp70s and oxidative stress has also been explored through the lens of professional divers. Simulated dives cause induction of the heat shock response, as heat shock proteins have a protective effect against bubble formation during decompression. Researchers found that there is a direct relationship between the intensity of oxidative stress during the dive and the concentration of Hsp70 proteins ¹⁹⁸. Serum levels of Hsp70 were lower after dives, but interestingly, Hsp90 was elevated.

Overall, oxidation and the impact of the Hsp70 protein and heat shock network continue to be expanded and explored by researchers. There are many facets to explore, ever-widening between many niches and categories, including multiple organisms, disease states, behavioral changes, and sex-linkage. However, there seems to be an undercurrent of connection between oxidative stress and modulation of the Hsp70 protein itself.

Hsp70 modulation as a therapeutic tool

The modulation of heat shock proteins as both a target and a tool has recently garnered a substantial amount of interest from researchers. Understanding the role of chaperones in disease states provides insight into how to navigate the disease as a whole, using chaperone modulation as a lever to alter the path of treatment. Hsp70 proteins specifically have been examined for their roles as both actively expressed therapeutics and as targets of inhibitors, through a multitude of human diseases. Here, I will explore a few interesting examples that tie together oxidative stress, disease, and Hsp70 modulation as a therapeutic.

While there are several concerns about off-target action and the broadness of chaperone influence, Hsp70 is currently being investigated as a directly expressed therapeutic agent. In mice that were expressing cofilin-actin, rods were formed in neuronal dendrites and axons that were covalently linked aggregates, often leading to stroke. Transgenic expression of the inducible Hsp70 protein, while undergoing simultaneous hypothermic conditions, greatly reduced the cofilin-actin rod size in

mice, while also improving neurological outcomes and reduced stroke-related lesion size ¹⁹⁹. In NSC34 cells and ischemic rabbits, transgenically expressed, brain barrier-crossing Tat-HSP70 was shown to be a promising lead for a therapeutic agent ²⁰⁰. When undergoing neuronal stress, NSC34 cells experience simultaneous elevated oxidative stress. Transduced Tat-HSP70 in NSC34 cells significantly reduced both intracellular reactive oxygen species concentration and cell death induced by hydrogen peroxide. Additionally, the administration of Tat-HSP70 into the spinal cord of ischemic rabbits significantly reduced lipid peroxidation and increased Cu, Zn-superoxide dismutase activities, reducing oxidative stress ²⁰⁰. In rat glioblastoma cells, researchers were able to pharmacologically upregulate and downregulate Hsp70 expression using echinochrome and triptolide. When Hsp70 concentration was increased, the glioblastoma cells decreased the amount of GAPDH aggregates formed in the cell, which is a formation caused by abundant oxidative stress. When the Hsp70 concentration was decreased, GAPDH aggregations increased ²⁰¹. Similarly, down-regulated Hsp70 concentration in Burkitt's lymphoma Raji cells blocked the JAK2/STAT3 signaling pathway, inhibiting proliferation, inducing cell-cycle arrest, and promoted oxidative stress and apoptosis of the cancerous cells ²⁰². When Hsp70 expression was increased in brain tissue, insulin sensitivity and glycemic activity was restored in DM2-model mice ²⁰³. These findings serve as examples of how Hsp70 can act as a direct modulator of disease through cellular concentration increase. However, there are several concerns about off-target effects that have to be explored before we see a clinical full-Hsp70 disease treatment.

The ability to indirectly utilize Hsp70 helps to reduce the off-target effects that chaperones can induce in a cell while also benefiting from its central role in many diseases. Similar to the above-mentioned diabetes mellitus 2 link, Hsp70 is also a prospective biomarker for myocardial ischemia, with extracellular eHsp70 acting as a pro-inflammatory mediator, and intracellular iHsp70 working as an anti-inflammatory mediator. Several avenues of pre-and post-conditioning of Hsp70 proteins are promising treatment options being studied for those at risk and those that have been the subject of ischemic cardiac attack ²⁰⁴. Some very interesting methods include hot tub treatment and sauna treatment to regularly increase the load of heat shock proteins in cells ²⁰³. Several methods of inducing Hsp70 localization intent on increasing iHsp70 in sepsis patients are also being explored, as sepsis overloads the concentration of eHsp70 in sepsis patients ²⁰⁵. Adjuvant treatments are also being produced to assist the already present Hsp70 population in disease management. For example, the compound allicin, found in garlic, is shown to increase the neuroprotective effect of Hsp70s during oxidative/inflammatory injury through modulation of the counterbalance between Hsp70 and the inducible nitric oxide synthase ²⁰⁶. Hsp70s are also being considered as a component of the whole heat shock protein network, with modulators intricately affecting multiple protein players of the heat shock response ²⁰⁷. In summary, there are many exciting explorations being made into Hsp70 as it relates to disease, oxidative stress, and signal pathways. Direct or indirect modulation of Hsp70 concentration and function are sure to be beneficial to patients with a long list of ailments and several promising technologies are already becoming well-received in clinical trials.

Future Directions

To conclude, this dissertation examined and quantified the effects of thiol modification, through both exogenous and mimicked oxidation, of the cysteines C264 and C303 within the yeast Hsp70 chaperone protein Ssa1. I found that there are several functional modifications, including reduced ability to correctly fold polypeptides *de novo*, to refold misfolded proteins, and to fully degrade chronically misfolded proteins. These deficiencies appear to stem from an altered relationship with nucleotide, as deduced by a lowered ability of oxidized and oxidation-mimic Ssa1 to bind and hydrolyze ATP, a critical facet of ATPase chaperone behavior. Hopefully, my work will lay a strong foundation to continue studying the role of oxidative stress response and sensing by Hsp70 proteins.

An immediate future goal is to deduce the evolutionary benefit of reduced proteostatic capacity as a downstream consequence of oxidative stress sensing. Previous work from the Morano laboratory suggested that the inhibition of Hsp70 through oxidative stress increases the capacity of heat shock resistance⁸⁹. However, the benefit of this response has yet to be fully quantified. Determining how oxidative stress may improve cellular survival against injury through Hsp70 mediation is very important for determining the evolutionary advantage of Ssa1 to retain reactive cysteines in a very conserved protein family, especially since the Ssa1-2CS serine substitution mutant performed equally to wild type Ssa1. One clue may be to the lack of cysteines in the inducible family members, which has been touched on in the discussion for chapter 4. It is also unclear why deficiencies in degradation are

subjective, depending on substrate identity. As corroborated by the Hampton lab, Ssa1-mediated degradation does not extend to all substrates¹³². I also found that the substrate GFP^{NLS}-VHL not subjected to a variance in degradation in a *ssa1ssa2* deletion mutant. However, oxidation did affect degradation when the Hsp70-dependence was present, which suggests that oxidation may only affect substrates with particular characteristics. Determining those characteristics and extrapolating them to characteristics of disease would be very beneficial to determining which diseases Hsp70 treatment may pertain to more.

More translationally, it is of great interest to determine which of the 13 human Hsp70 proteins share characteristics of cysteine oxidation with Ssa1, whereby particular proteostatic behaviors of those proteins are significantly altered in the same manner as noted above. Hsp70s have differing profiles based on tissue type, inducibility, and intra/extracellularity. Drawing comparisons between specific human Hsp70s and the altered function caused by oxidative modification within Ssa1 could give insight as to which diseases may be more heavily impacted by oxidative stress, such that they require the same sensing ability and behavioral alterations for resident Hsp70s.

A broad range study on the interactions between Hsp70s that have undergone cysteine modification and the relevant co-chaperones would also be very beneficial. The trypsinization experiments suggest a conformational shift (which may be benefitted from additional study as well, such as through fluorescent anisotropy). The altered protein shape may also alter the relationship to co-chaperones, such as Hsp110, Hsp40, and Hsp90. More dedicated assays to refine that relationship post-

oxidation would add an understanding of the complexities for the entire system. The Robetta modeling software was used by the Gestwicki lab to determine residue shifts in the inducible human Hsp70, as discussed above ⁹⁰. In recent years, many advancements have been made in the use of software to model proteins and to modify the model protein sequences to determine how modification affects the shape of the protein structure and potential interactions with other residues and cofactors. Most notably, the use of AlphaFold 2 has vastly broadened the capability of what researchers can explore with three-dimensional predictive protein modeling. AlphaFold uses many layers of mathematical modeling to give structure to protein sequences, including the forces of attraction and repulsion that are at play in the compositional amino acids ²⁰⁸. There is also a newly updated homology modeling tool called SWISS-MODEL, which allows for imposing several sequences at once to determine structural changes ²⁰⁹. This tool can be useful for superimposing the Ssa1 protein with several types of amino acid substitutions that mimic cysteine modification and the resulting shift in the nucleotide binding domain structure that occurs following each substitution. Tryptophan, aspartic acid, and phenylalanine have all been used as substitutional mimics of modified cysteine within Hsp70s, and the SWISS-MODEL tool would be extremely effective at determining how each substitution affected the structure of the NBD ^{89,109,111}. Beyond modeling, it is also key to determine orthogonal tests measuring ATP stabilization by various mutants or treated protein isolates. One method of doing so is through the differential radial capillary action of ligand assay (DraCALA), which uses nitrocellulose spotting to determine dissociation constants, and has been employed before for quantifying the K_d of an Hsp70 NBD/ATP

interaction ¹⁰⁹. Fluorescence anisotropy, which measures the kinetics of a reaction that cause a rotational change in molecular structure, would be valuable in furthering the initial findings of my trypsinization experiment, which showed a difference in degradation profile of the 2CD mutant when incubated with ATP compared to the WT and 2CS mutants. Fluorescence anisotropy would be able to determine with higher resolution what conformational changes are occurring in the nucleotide binding domain after incubation with various nucleotides. These explorations may give valuable clues as to the potential loss of stabilization of nucleotide, loss of critical cofactors, or steric changes that weaken the ability of amino acids to interact with each other or with the phosphates of ATP.

I am also excited to see the advancements in therapeutics involving direct Hsp70 expression in cells. With the cysteine-to-serine mutants being shown to be impervious to specific oxidative injury, I am curious to see whether they may play a role in complementing chaperone function in an oxidative environment, for an array of treatments.

Bibliography

1. Hipp, Mark S., Kasturi, Prasad & Hartl, F. Ulrich. The proteostasis network and its decline in ageing. *Nature Reviews Molecular Cell Biology* vol. 20 421–435 at <https://doi.org/10.1038/s41580-019-0101-y> (2019).
2. Soto, Claudio & Pritzkow, Sandra. Protein misfolding, aggregation, and conformational strains in neurodegenerative diseases. *Nature Neuroscience* vol. 21 1332–1340 at <https://doi.org/10.1038/s41593-018-0235-9> (2018).
3. Peng, Chao, Trojanowski, John Q. & Lee, Virginia M. Y. Protein transmission in neurodegenerative disease. *Nat. Rev. Neurol.* **16**, 199–212 (2020).
4. Mayer, Matthias P. Hsp70 chaperone dynamics and molecular mechanism. *Trends in Biochemical Sciences* vol. 38 507–514 at <https://doi.org/10.1016/j.tibs.2013.08.001> (2013).
5. Gragerov, A. & Gottesman, M. E. Different peptide binding specificities of hsp70 family members. *J. Mol. Biol.* **241**, 133–135 (1994).
6. Clerico, Eugenia M., Tilitsky, Joseph M., Meng, Wenli & Gierasch, Lila M. How Hsp70 molecular machines interact with their substrates to mediate diverse physiological functions. *J. Mol. Biol.* **427**, 1575–1588 (2015).
7. Zhu, Xiaotian. Structural Analysis of Substrate Binding by the Molecular Chaperone DnaK. *Science (80-.)*. **5268**, 1606–1614 (1996).
8. Schneider, Markus, Rosam, M., Glaser, M., Patronov, A., Shah, H., Back, K.C., Daake, M.A., Buchner, J. and Antes, Iris. BiPPred: Combined

- sequence- and structure-based prediction of peptide binding to the Hsp70 chaperone BiP. *Proteins Struct. Funct. Bioinforma.* **84**, 1390–1407 (2016).
9. Andritsos, P., Tsaparas, P. , Miller, R.J. , Sevcik, KC. LIMBO: Scalable Clustering of Categorical Data. *Adv. Database Technol.* **2992**, 123–146 (2004).
 10. Peffer, Sara, Gonçalves, Davi & Morano, Kevin A. Regulation of the Hsf1-dependent transcriptome via conserved bipartite contacts with Hsp70 promotes survival in yeast. *J. Biol. Chem.* **294**, 12191–12202 (2019).
 11. van der Spuy, Jacqueline, Cheetham, Michael E. & Chappie, J. Paul. The Role of Hsp70 and Its Co-Chaperones in Protein Misfolding, Aggregation and Disease. in *Networking of Chaperones by Co-Chaperones* 122–136 (Springer New York, 2007). doi:10.1007/978-0-387-49310-7_11.
 12. Medicherla, Balasubrahmanyam & Goldberg, Alfred L. Heat shock and oxygen radicals stimulate ubiquitin-dependent degradation mainly of newly synthesized proteins. *J. Cell Biol.* **182**, 663–673 (2008).
 13. Mayer, Matthias P. & Gierasch, Lila M. Recent advances in the structural and mechanistic aspects of Hsp70 molecular chaperones. *J. Biol. Chem.* **294**, 2085–2097 (2019).
 14. Kityk, Roman, Kopp, Jürgen, Sinning, Irmgard & Mayer, Matthias P. Structure and Dynamics of the ATP-Bound Open Conformation of Hsp70 Chaperones. *Mol. Cell* **48**, 863–874 (2012).
 15. Liu, Qinglian & Hendrickson, Wayne A. Insights into Hsp70 Chaperone Activity from a Crystal Structure of the Yeast Hsp110 Sse1. *Cell* **131**, 106–

- 120 (2007).
16. Zhuravleva, Anastasia & Gierasch, Lila M. Allosteric signal transmission in the nucleotide-binding domain of 70-kDa heat shock protein (Hsp70) molecular chaperones. *Proc. Natl. Acad. Sci. U. S. A.* **108**, 6987–6992 (2011).
 17. Rosenzweig, Rina, Nillegoda, Nadinath B., Mayer, Matthias P. & Bukau, Bernd. The Hsp70 chaperone network. *Nature Reviews Molecular Cell Biology* at <https://doi.org/10.1038/s41580-019-0133-3> (2019).
 18. Hartl, F. Ulrich, Bracher, Andreas & Hayer-Hartl, Manajit. Molecular chaperones in protein folding and proteostasis. *Nature* **475**, 324–332 (2011).
 19. Young, Jason C. Mechanisms of the Hsp70 chaperone system. in *Biochemistry and Cell Biology* vol. 88 291–300 (National Research Council of Canada, 2010).
 20. Hochstrasser, Mark. Protein Degradation or Regulation: Ub the Judge. *Cell* **84**, 813–815 (1996).
 21. Varshavsky, Alexander. The ubiquitin system. *Trends Biochem. Sci.* **22**, 383–387 (1997).
 22. Hershko, Avram & Ciechanover, Aaron. The Ubiquitin system. *Annu. Rev. Biochem.* **67**, 425–479 (1998).
 23. Park SH, Bolender N, Eisele F, Kostova Z, Takeuchi J, Coffino P, Wolf DH. The Cytoplasmic Hsp70 Chaperone Machinery Subjects Misfolded and Endoplasmic Reticulum Import-incompetent Proteins to Degradation via the Ubiquitin–Proteasome System. *Mol. Biol. Cell* **18**, 153–165 (2006).
 24. Lee, Do Hee, Sherman, Michael Y. & Goldberg, Alfred L. The requirements of

- yeast Hsp70 of SSA family for the ubiquitin-dependent degradation of short-lived and abnormal proteins. *Biochem. Biophys. Res. Commun.* **475**, 100–106 (2016).
25. Gowda, Naveen Kumar Chandappa, Kandasamy, Ganapathi, Froehlich, Marcelli S., Dohmen, R. Jürgen & Andréasson, Claes. Hsp70 nucleotide exchange factor Fes1 is essential for ubiquitin-dependent degradation of misfolded cytosolic proteins. *Proc. Natl. Acad. Sci.* **110**, 5975–5980 (2013).
 26. Jones RD, Enam C, Ibarra R, Borrer HR, Mostoller KE, Fredrickson EK, Lin J, Chuang E, March Z, Shorter J, Ravid T, Kleiger G, Gardner RG. The extent of Ssa1/Ssa2 Hsp70 chaperone involvement in nuclear protein quality control degradation varies with the substrate. *Mol. Biol. Cell* **31**, 221–233 (2019).
 27. Kityk, Roman, Kopp, Jürgen & Mayer, Matthias P. Molecular Mechanism of J-Domain-Triggered ATP Hydrolysis by Hsp70 Chaperones. *Mol. Cell* **69**, 227-237.e4 (2018).
 28. Needham, Patrick G., Patel, Hardik J., Chiosis, Gabriela, Thibodeau, Patrick H. & Brodsky, Jeffrey L. Mutations in the Yeast Hsp70, Ssa1, at P417 Alter ATP Cycling, Interdomain Coupling, and Specific Chaperone Functions. *J. Mol. Biol.* **427**, 2948–2965 (2015).
 29. Lu, Zhen & Cyr, Douglas M. Protein folding activity of Hsp70 is modified differentially by the Hsp40 co-chaperones Sis1 and Ydj1. *J. Biol. Chem.* **273**, 27824–27830 (1998).
 30. Kampinga HH, Andreasson C, Barducci A, Cheetham ME, Cyr D, Emanuelsson C, Genevaux P, Gestwicki JE, Goloubinoff P, Huerta-Cepas J,

- Kirstein J, Liberek K, Mayer MP, Nagata K, Nillegoda NB, Pulido P, Ramos C, De Los Rios P, Rospert S, Rosenzweig R, Sahi C, Taipale M, Tomiczek B, Ushioda R, Young JC, Zimmermann R, Zylicz A, Zylicz M, Craig EA, Marszalek J. Function, evolution, and structure of J-domain proteins. *Cell Stress Chaperones* **24**, 7–15 (2019).
31. Schilke BA, Ciesielski SJ, Ziegelhoffer T, Kamiya E, Tonelli M, Lee W, Cornilescu G, Hines JK, Markley JL, Craig EA. Broadening the functionality of a J-protein/Hsp70 molecular chaperone system. *PLoS Genet.* **13**, 1–29 (2017).
32. Mandal, Atin K., Nillegoda, Nadinath B., Chen, Jennifer A. & Caplan, Avrom J. Ydj1 Protects Nascent Protein Kinases from Degradation and Controls the Rate of Their Maturation. *Mol. Cell. Biol.* **28**, 4434–4444 (2008).
33. Polier, Sigrun, Dragovic, Zdravko, Hartl, F. Ulrich & Bracher, Andreas. Structural basis for the cooperation of Hsp70 and Hsp110 chaperones in protein folding. *Cell* **133**, 1068–1079 (2008).
34. Shaner, Lance, Sousa, Rui & Morano, Kevin A. Characterization of Hsp70 binding and nucleotide exchange by the yeast Hsp110 chaperone Sse1. *Biochemistry* **45**, 15075–15084 (2006).
35. Dragovic, Zdravko, Broadley, Sarah A., Shomura, Yasuhito, Bracher, Andreas & Hartl, F. Ulrich. Molecular chaperones of the Hsp110 family act as nucleotide exchange factors of Hsp70s. *EMBO J.* **25**, 2519–2528 (2006).
36. Yakubu, Unekwu M. & Morano, Kevin A. Suppression of aggregate and amyloid formation by a novel intrinsically disordered region in metazoan

- Hsp110 chaperones. *J. Biol. Chem.* **296**, 100567 (2021).
37. Liu, Xiao Dong, Morano, Kevin A. & Thiele, Dennis J. The yeast Hsp110 family member, Sse1, is an Hsp90 cochaperone. *J. Biol. Chem.* **274**, 26654–26660 (1999).
 38. Raviol, Holger, Bukau, Bernd & Mayer, Matthias P. Human and yeast Hsp110 chaperones exhibit functional differences. *FEBS Lett.* **580**, 168–174 (2006).
 39. Trott A, West JD, Klaić L, Westerheide SD, Silverman RB, Morimoto RI, Morano KA. Activation of heat shock and antioxidant responses by the natural product celastrol: Transcriptional signatures of a thiol-targeted molecule. *Mol. Biol. Cell* **19**, 1104–1112 (2008).
 40. Wu, B., Hunt, C. & Morimoto, R. Structure and expression of the human gene encoding major heat shock protein HSP70. *Mol. Cell. Biol.* **5**, 330–341 (1985).
 41. Craig, Elizabeth A. & Jacobsen, Kurt. Mutations of the heat inducible 70 kilodalton genes of yeast confer temperature sensitive growth. *Cell* **38**, 841–849 (1984).
 42. Daugaard, Mads, Rohde, Mikkel & Jäättelä, Marja. The heat shock protein 70 family: Highly homologous proteins with overlapping and distinct functions. *FEBS Lett.* **581**, 3702–3710 (2007).
 43. Sousa, Rui & Lafer, Eileen M. The role of molecular chaperones in clathrin mediated vesicular trafficking. *Front. Mol. Biosci.* **2**, (2015).
 44. Lotz, Sarah K., Knighton, Laura E., Nitika, Jones, Gary W. & Truman, Andrew W. Not quite the SSAmé: unique roles for the yeast cytosolic Hsp70s. *Current Genetics* vol. 1 3 at <https://doi.org/10.1007/s00294-019-00978-8> (2019).

45. Werner-Washburne, M., Stone, D. E. & Craig, E. A. Complex interactions among members of an essential subfamily of hsp70 genes in *Saccharomyces cerevisiae*. *Mol. Cell. Biol.* **7**, 2568–2577 (1987).
46. Magdalena, Rakwalska & Sabine, Rospert. The Ribosome-Bound Chaperones RAC and Ssb1/2p Are Required for Accurate Translation in *Saccharomyces cerevisiae*. *Mol. Cell. Biol.* **24**, 9186–9197 (2004).
47. Slater, M. R. & Craig, E. A. The SSB1 heat shock cognate gene of the yeast *Saccharomyces cerevisiae*. *Nucleic Acids Res.* **17**, 4891 (1989).
48. Lopez N, Halladay J, Walter W, Craig EA. SSB, encoding a ribosome-associated chaperone, is coordinately regulated with ribosomal protein genes. *J. Bacteriol.* **181**, 3136–3143 (1999).
49. Tavaría, M., Gabriele, T., Kola, I. & Anderson, R. L. A hitchhiker's guide to the human Hsp70 family. *Cell Stress Chaperones* **1**, 23–28 (1996).
50. Radons, Jürgen. The human HSP70 family of chaperones: where do we stand? *Cell Stress Chaperones* **21**, 379–404 (2016).
51. Joanna Krakowiak, Xu Zheng, Nikit Patel, Zoë A Feder, Jayamani Anandhakumar, Kendra Valerius, David S Gross, Ahmad S Khalil, David Pincus Hsf1 and Hsp70 constitute a two-component feedback loop that regulates the yeast heat shock response. *Elife* **7**, (2018).
52. Ghaemmaghani S, Huh WK, Bower K, Howson RW, Belle A, Dephoure N, O'Shea EK, Weissman JS. Global analysis of protein expression in yeast. *Nature* **425**, 737–741 (2003).
53. Mackenzie RJ, Lawless C, Holman SW, Lanthaler K, Beynon RJ, Grant CM,

- Hubbard SJ, Eyers CE Absolute protein quantification of the yeast chaperome under conditions of heat shock. *Proteomics* **16**, 2128–2140 (2016).
54. Christiano, Romain, Nagaraj, Nagarjuna, Fröhlich, Florian & Walther, Tobias C. Global proteome turnover analyses of the Yeasts *S. cerevisiae* and *S. pombe*. *Cell Rep.* **9**, 1959–1965 (2014).
55. Keefer, Kathryn M. & True, Heather L. A toxic imbalance of Hsp70s in *Saccharomyces cerevisiae* is caused by competition for cofactors. *Mol. Microbiol.* **105**, 860–868 (2017).
56. Doyle, Shannon M. & Wickner, Sue. Hsp104 and ClpB: protein disaggregating machines. *Trends Biochem. Sci.* **34**, 40–48 (2009).
57. Lee, Sukyeong, Sowa, Mathew E., Choi, Jae-Mun & Tsai, Francis T. F. The ClpB/Hsp104 molecular chaperone—a protein disaggregating machine. *J. Struct. Biol.* **146**, 99–105 (2004).
58. Glover, John R. & Lindquist, Susan. Hsp104, Hsp70, and Hsp40: A Novel Chaperone System that Rescues Previously Aggregated Proteins. *Cell* **94**, 73–82 (1998).
59. Heuck A, Schitter-Sollner S, Suskiewicz MJ, Kurzbauer R, Kley J, Schleiffer A, Rombaut P, Herzog F, Clausen T. Structural basis for the disaggregase activity and regulation of Hsp104. *Elife* **5**, e21516 (2016).
60. Zaarur N, Xu X, Lestienne P, Meriin AB, McComb M, Costello CE, Newnam GP, Ganti R, Romanova NV, Shanmugasundaram M, Silva ST, Bandejas TM, Matias PM, Lobachev KS, Lednev IK, Chernoff YO, Sherman MY. RuvbL1 and RuvbL2 enhance aggresome formation and disaggregate

- amyloid fibrils. *EMBO J.* **34**, 2363–2382 (2015).
61. Richter, Klaus, Haslbeck, Martin & Buchner, Johannes. The Heat Shock Response: Life on the Verge of Death. *Mol. Cell* **40**, 253–266 (2010).
 62. Mogk, Axel, Bukau, Bernd & Kampinga, Harm H. Cellular Handling of Protein Aggregates by Disaggregation Machines. *Mol. Cell* **69**, 214–226 (2018).
 63. Ho, Chi ting, Grousl, Tomas, Shatz, Oren, Jawed, Areeb, Ruher-Herreros, Carmen, Semmelink, Marije, Zahn, Regina, Richter, Karsten, Mogk, Axel. Cellular sequestrases maintain basal Hsp70 capacity ensuring balanced proteostasis. *Nat. Commun.* **10**, 1–15 (2019).
 64. Basha, Eman, Friedrich, Kenneth L. & Vierling, Elizabeth. The N-terminal arm of small heat shock proteins is important for both chaperone activity and substrate specificity. *J. Biol. Chem.* (2006) doi:10.1074/jbc.M607677200.
 65. Basha, Eman, O'Neill, Heather & Vierling, Elizabeth. Small heat shock proteins and α -crystallins: Dynamic proteins with flexible functions. *Trends in Biochemical Sciences* at <https://doi.org/10.1016/j.tibs.2011.11.005> (2012).
 66. Kriehuber T, Rattei T, Weinmaier T, Bepperling A, Haslbeck M, Buchner J. Independent evolution of the core domain and its flanking sequences in small heat shock proteins. *FASEB J.* **24**, 3633–3642 (2010).
 67. Bakthisaran, Raman, Tangirala, Ramakrishna & Rao, Ch Mohan. Small heat shock proteins: Role in cellular functions and pathology. *Biochim. Biophys. Acta - Proteins Proteomics* **1854**, 291–319 (2015).
 68. Grousl T, Ungelenk S, Miller S, Ho CT, Khokhrina M, Mayer MP, Bukau B, Mogk A. A prion-like domain in Hsp42 drives chaperonefacilitated

- aggregation of misfolded proteins. *J. Cell Biol.* **217**, 1269–1285 (2018).
69. Mogk, Axel & Bukau, Bernd. Role of sHsps in organizing cytosolic protein aggregation and disaggregation. *Cell Stress Chaperones* **22**, 493–502 (2017).
70. Ungelenk S, Moayed F, Ho CT, Grousl T, Scharf A, Mashaghi A, Tans S, Mayer MP, Mogk A, Bukau B. Small heat shock proteins sequester misfolding proteins in near-native conformation for cellular protection and efficient refolding. *Nat. Commun.* **7**, 1–14 (2016).
71. Hochberg GKA, Shepherd DA, Marklund EG, Santhanagoplan I, Degiacomi MT, Laganowsky A, Allison TM, Basha E, Marty MT, Galpin MR, Struwe WB, Baldwin AJ, Vierling E, Benesch JLP. Structural principles that enable oligomeric small heat-shock protein paralogs to evolve distinct functions. *Science (80-.).* **359**, 930–935 (2018).
72. Mühlhofer M, Berchtold E, Stratil CG, Csaba G, Kunold E, Bach NC, Sieber SA, Haslbeck M, Zimmer R, Buchner J. The Heat Shock Response in Yeast Maintains Protein Homeostasis by Chaperoning and Replenishing Proteins. *Cell Rep.* **29**, 4593-4607.e8 (2019).
73. Hahn, Ji-Sook, Hu, Zhanzhi, Thiele, Dennis J. & Iyer, Vishwanath R. Genome-Wide Analysis of the Biology of Stress Responses through Heat Shock Transcription Factor. *Mol. Cell. Biol.* **24**, 5249–5256 (2004).
74. Morano, Kevin A., Grant, Chris M. & Moye-Rowley, W. Scott. The response to heat shock and oxidative stress in *saccharomyces cerevisiae*. *Genetics* **190**, 1157–1195 (2012).
75. Pincus D, Anandhakumar J, Thiru P, Guertin MJ, Erkin AM, Gross

- DS. Genetic and epigenetic determinants establish a continuum of Hsf1 occupancy and activity across the yeast genome. *Mol. Biol. Cell* **29**, 3168–3182 (2018).
76. Hentze, Nikolai, Le Breton, Laura, Wiesner, Jan, Kempf, Georg & Mayer, Matthias P. Molecular mechanism of thermosensory function of human heat shock transcription factor Hsf1. *Elife* **5**, (2016).
77. Kmiecik, Szymon W., Le Breton, Laura & Mayer, Matthias P. Feedback regulation of heat shock factor 1 (Hsf1) activity by Hsp70-mediated trimer unzipping and dissociation from DNA. *EMBO J.* **39**, (2020).
78. Zheng X, Krakowiak J, Patel N, Beyzavi A, Ezike J, Khalil AS, Pincus D. Dynamic control of Hsf1 during heat shock by a chaperone switch and phosphorylation. *Elife* **5**, (2016).
79. Zheng X, Beyzavi A, Krakowiak J, Patel N, Khalil AS, Pincus D. Hsf1 Phosphorylation Generates Cell-to-Cell Variation in Hsp90 Levels and Promotes Phenotypic Plasticity. *Cell Rep.* **22**, 3099–3106 (2018).
80. Liebelt F, Sebastian RM, Moore CL, Mulder MPC, Ovaa H, Shoulders MD, Vertegaal ACO. SUMOylation and the HSF1-Regulated Chaperone Network Converge to Promote Proteostasis in Response to Heat Shock. *Cell Rep.* **26**, 236-249.e4 (2019).
81. Purwana, Indri, Liu, Jun J., Portha, Bernard & Buteau, Jean. HSF1 acetylation decreases its transcriptional activity and enhances glucolipototoxicity-induced apoptosis in rat and human beta cells. *Diabetologia* **60**, 1432–1441 (2017).
82. Lindquist, S. & Craig, E. A. The Heat-Shock Proteins. *Annu. Rev. Genet.* **22**,

- 631–677 (1988).
83. Solís EJ, Pandey JP, Zheng X, Jin DX, Gupta PB, Airoidi EM, Pincus D, Denic V. Defining the Essential Function of Yeast Hsf1 Reveals a Compact Transcriptional Program for Maintaining Eukaryotic Proteostasis. *Mol. Cell* **63**, 60–71 (2016).
 84. Masser AE, Kang W, Roy J, Mohanakrishnan Kaimal J, Quintana-Cordero J, Friedländer MR, Andréasson C. Cytoplasmic protein misfolding titrates Hsp70 to activate nuclear Hsf1. *Elife* **8**, (2019).
 85. Truttmann MC, Zheng X, Hanke L, Damon JR, Grootveld M, Krakowiak J, Pincus D, Ploegh HL. Unrestrained AMPylation targets cytosolic chaperones and activates the heat shock response. *Proc. Natl. Acad. Sci. U. S. A.* **114**, E152–E160 (2017).
 86. Truttmann, Matthias C., Pincus, David & Ploegh, Hidde L. Chaperone AMPylation modulates aggregation and toxicity of neurodegenerative disease-associated polypeptides. *Proc. Natl. Acad. Sci. U. S. A.* **115**, E5008–E5017 (2018).
 87. Xu L, Nitika, Hasin N, Cuskelly DD, Wolfgeher D, Doyle S, Moynagh P, Perrett S, Jones GW, Truman AW. Rapid deacetylation of yeast Hsp70 mediates the cellular response to heat stress. *Sci. Rep.* **9**, (2019).
 88. Yang J, Zhang H, Gong W, Liu Z, Wu H, Hu W, Chen X, Wang L, Wu S, Chen C, Perrett S. S -Glutathionylation of human inducible Hsp70 reveals a regulatory mechanism involving the C-terminal α -helical lid . *J. Biol. Chem.* jbc.RA119.012372 (2020) doi:10.1074/jbc.ra119.012372.

89. Wang, Y., Gibney, P. A., West, J. D. & Morano, K. A. The yeast Hsp70 Ssa1 is a sensor for activation of the heat shock response by thiol-reactive compounds. *Mol. Biol. Cell* **23**, 3290–3298 (2012).
90. Miyata Y, Rauch JN, Jinwal UK, Thompson AD, Srinivasan S, Dickey CA, Gestwicki JE. Cysteine reactivity distinguishes redox sensing by the heat-inducible and constitutive forms of heat shock protein 70. *Chem. Biol.* **19**, 1391–1399 (2012).
91. Torrent, Marc, Chalancon, Guilhem, De Groot, Natalia S., Wuster, Arthur & Madan Babu, M. Cells alter their tRNA abundance to selectively regulate protein synthesis during stress conditions. *Sci. Signal.* **11**, (2018).
92. Damon, Jady R., Pincus, David & Ploegh, Hidde L. tRNA thiolation links translation to stress responses in *Saccharomyces cerevisiae*. *Mol. Biol. Cell* **26**, 270–282 (2015).
93. Chowdhary, Surabhi, Kainth, Amoldeep S. & Gross, David S. Heat Shock Protein Genes Undergo Dynamic Alteration in Their Three-Dimensional Structure and Genome Organization in Response to Thermal Stress. *Mol. Cell. Biol.* **37**, (2017).
94. Chowdhary, Surabhi, Kainth, Amoldeep S., Pincus, David & Gross, David S. Heat Shock Factor 1 Drives Intergenic Association of Its Target Gene Loci upon Heat Shock. *Cell Rep.* **26**, 18-28.e5 (2019).
95. Liguori I, Russo G, Curcio F, Bulli G, Aran L, Della-Morte D, Gargiulo G, Testa G, Cacciatore F, Bonaduce D, Abete P. Oxidative stress, aging, and diseases. *Clin. Interv. Aging* **13**, 757–772 (2018).

96. Murphy, Michael P. How mitochondria produce reactive oxygen species. *Biochem. J.* **417**, 1–13 (2009).
97. Blevins WR, Tavella T, Moro SG, Blasco-Moreno B, Closa-Mosquera A, Díez J, Carey LB, Albà MM. Extensive post-transcriptional buffering of gene expression in the response to severe oxidative stress in baker's yeast. *Sci. Rep.* **9**, (2019).
98. Hanzén S, Vielfort K, Yang J, Roger F, Andersson V, Zamarbide-Forés S, Andersson R, Malm L, Palais G, Biteau B, Liu B, Toledano MB, Molin M, Nyström T. Lifespan Control by Redox-Dependent Recruitment of Chaperones to Misfolded Proteins. *Cell* **166**, 140–151 (2016).
99. Rhee SG, Kang SW, Jeong W, Chang TS, Yang KS, Woo HA Intracellular messenger function of hydrogen peroxide and its regulation by peroxiredoxins. *Curr. Opin. Cell Biol.* **17**, 183–189 (2005).
100. Delaunay, Agnès, Pflieger, Delphine, Barrault, Marie Bénédicte, Vinh, Joelle & Toledano, Michel B. A thiol peroxidase is an H₂O₂ receptor and redox-transducer in gene activation. *Cell* **111**, 471–481 (2002).
101. Coleman, Sean T., Epping, Eric A., Steggerda, Susanne M. & Moye-Rowley, W. Scott. Yap1p Activates Gene Transcription in an Oxidant-Specific Fashion. *Mol. Cell. Biol.* (1999) doi:10.1128/mcb.19.12.8302.
102. Sykiotis, Gerasimos P. & Bohmann, Dirk. Stress-activated cap'n'collar transcription factors in aging and human disease. *Science Signaling* vol. 3 re3–re3 at <https://doi.org/10.1126/scisignal.3112re3> (2010).
103. Taguchi, Keiko, Motohashi, Hozumi & Yamamoto, Masayuki. Molecular

- mechanisms of the Keap1-Nrf2 pathway in stress response and cancer evolution. *Genes to Cells* vol. 16 123–140 at <https://doi.org/10.1111/j.1365-2443.2010.01473.x> (2011).
104. Suzuki, Takafumi & Yamamoto, Masayuki. Stress-sensing mechanisms and the physiological roles of the Keap1–Nrf2 system during cellular stress. *Journal of Biological Chemistry* vol. 292 16817–16824 at <https://doi.org/10.1074/jbc.R117.800169> (2017).
105. Boissard S, Lagniel G, Garmendia-Torres C, Molin M, Boy-Marcotte E, Jacquet M, Toledano MB, Labarre J, Chédin S. H₂O₂ activates the nuclear localization of Msn2 and Maf1 through thioredoxins in *Saccharomyces cerevisiae*. *Eukaryot. Cell* **8**, 1429–1438 (2009).
106. Collet, Jean Francois, D'Souza, Jonathan Conrad, Jakob, Ursula & Bardwell, James C. A. Thioredoxin 2, an Oxidative Stress-induced Protein, Contains a High Affinity Zinc Binding Site. *J. Biol. Chem.* **278**, 45325–45332 (2003).
107. Ahn, Sang Gun & Thiele, Dennis J. Redox regulation of mammalian heat shock factor 1 is essential for Hsp gene activation and protection from stress. *Genes Dev.* (2003) doi:10.1101/gad.1044503.
108. Zhang H, Yang J, Wu S, Gong W, Chen C, Perrett S. Glutathionylation of the bacterial Hsp70 chaperone dnaK provides a link between oxidative stress and the heat shock response. *J. Biol. Chem.* **291**, 6967–6981 (2016).
109. O'Donnell JP, Marsh HM, Sondermann H, Sevier CS. Disrupted Hydrogen-Bond Network and Impaired ATPase Activity in an Hsc70 Cysteine Mutant. *Biochemistry* **57**, 1073–1086 (2018).

110. Winter, Jeannette, Linke, Katrin, Jatzek, Anna & Jakob, Ursula. Severe oxidative stress causes inactivation of DnaK and activation of the redox-regulated chaperone Hsp33. *Mol. Cell* **17**, 381–392 (2005).
111. Wang, Jie & Sevier, Carolyn S. Formation and reversibility of BiP protein cysteine oxidation facilitate cell survival during and post oxidative stress. *J. Biol. Chem.* **291**, 7541–7557 (2016).
112. Nicklow, Erin E. & Sevier, Carolyn S. Activity of the yeast cytoplasmic Hsp70 nucleotide-exchange factor Fes1 is regulated by reversible methionine oxidation. *J. Biol. Chem.* **295**, 552–569 (2020).
113. Chalova, Anna S., Sudnitsyna, Maria V., Semenyuk, Pavel I., Orlov, Victor N. & Gusev, Nikolai B. Effect of disulfide crosslinking on thermal transitions and chaperone-like activity of human small heat shock protein HspB1. *Cell Stress Chaperones* **19**, 963–972 (2014).
114. Alderson TR, Roche J, Gastall HY, Dias DM, Pritišanac I, Ying J, Bax A, Benesch JLP, Baldwin AJ. Local unfolding of the HSP27 monomer regulates chaperone activity. *Nat. Commun.* **10**, 1–16 (2019).
115. Wemmie, J. A., Szczypka, M. S., Thiele, D. J. & Moye-Rowley, W. S. Cadmium tolerance mediated by the yeast AP-1 protein requires the presence of an ATP-binding cassette transporter-encoding gene, YCF1. *J. Biol. Chem.* **269**, 32592–32597 (1994).
116. Jacobson T, Priya S, Sharma SK, Andersson S, Jakobsson S, Tanghe R, Ashouri A, Rauch S, Goloubinoff P, Christen P, Tamás MJ. Cadmium Causes Misfolding and Aggregation of Cytosolic Proteins in Yeast. *Mol. Cell.*

- Biol.* **37**, 1–15 (2017).
117. Sharma, Sandeep K., Goloubinoff, Pierre & Christen, Philipp. Heavy metal ions are potent inhibitors of protein folding. *Biochem. Biophys. Res. Commun.* **372**, 341–345 (2008).
 118. Ford, Amy E., Denicourt, Catherine & Morano, Kevin A. Thiol stress-dependent aggregation of the glycolytic enzyme triose phosphate isomerase in yeast and human cells. *Mol. Biol. Cell* **30**, 554–565 (2019).
 119. Le, Quynh Giang, Ishiwata-Kimata, Yuki, Kohno, Kenji & Kimata, Yukio. Cadmium impairs protein folding in the endoplasmic reticulum and induces the unfolded protein response. *FEMS Yeast Res.* **16**, 49 (2016).
 120. Guerra-Moreno A, Prado MA, Ang J, Schnell HM, Micoogullari Y, Paulo JA, Finley D, Gygi SP, Hanna J. Thiol-based direct threat sensing by the stress-activated protein kinase Hog1. *Sci. Signal.* **12**, (2019).
 121. Radzinski M, Fassler R, Yogev O, Breuer W, Shai N, Gutin J, Ilyas S, Geffen Y, Tsytkin-Kirschenschweig S, Nahmias Y, Ravid T, Friedman N, Schuldiner M, Reichmann D. Temporal profiling of redox-dependent heterogeneity in single cells. *Elife* **7**, 1–33 (2018).
 122. Xu, Mengni, Marsh, Heather M. & Sevier, Carolyn S. A Conserved Cysteine within the ATPase Domain of the Endoplasmic Reticulum Chaperone BiP is Necessary for a Complete Complement of BiP Activities. *J. Mol. Biol.* **428**, 4168–4184 (2016).
 123. Hermawan, Aynih & Chirico, William J. N-ethylmaleimide-modified Hsp70 inhibits protein folding. *Arch. Biochem. Biophys.* **369**, 157–162 (1999).

124. Liu, Qinglian, Levy, Ellen J. & Chirico, William J. N-ethylmaleimide inactivates a nucleotide-free Hsp70 molecular chaperone. *J. Biol. Chem.* **271**, 29937–29944 (1996).
125. Liu, Xiao Dong, Liu, Phillip C. C., Santoro, Nicholas & Thiele, Dennis J. Conservation of a stress response: Human heat shock transcription factors functionally substitute for yeast HSF. *EMBO J.* **16**, 6466–6477 (1997).
126. Morano, Kevin A. & Thiele, Dennis J. The Sch9 protein kinase regulates Hsp90 chaperone complex signal transduction activity in vivo. *EMBO J.* **18**, 5953–5962 (1999).
127. Abrams, Jennifer L., Verghese, Jacob, Gibney, Patrick A. & Morano, Kevin A. Hierarchical functional specificity of cytosolic heat shock protein 70 (Hsp70) nucleotide exchange factors in yeast. *J. Biol. Chem.* **289**, 13155–13167 (2014).
128. Nillegoda NB, Kirstein J, Szlachcic A, Berynsky M, Stank A, Stengel F, Arnsburg K, Gao X, Scior A, Aebersold R, Guilbride DL, Wade RC, Morimoto RI, Mayer MP, Bukau B. Crucial HSP70 co-chaperone complex unlocks metazoan protein disaggregation. *Nature* **524**, 247–251 (2015).
129. Andréasson, Claes, Fiaux, Jocelyne, Rampelt, Heike, Mayer, Matthias P. & Bukau, Bernd. Hsp110 is a nucleotide-activated exchange factor for Hsp70. *J. Biol. Chem.* **283**, 8877–8884 (2008).
130. Fung, Katie L., Hilgenberg, Lutz, Wang, Nancy M. & Chirico, William J. Conformations of the nucleotide and polypeptide binding domains of a cytosolic Hsp70 molecular chaperone are coupled. *J. Biol. Chem.* **271**,

- 21559–21565 (1996).
131. Verghese, Jacob & Morano, Kevin A. A lysine-rich region within fungal BAG domain-containing proteins mediates a novel association with ribosomes. *Eukaryot. Cell* **11**, 1003–1011 (2012).
 132. Singh A, Vashistha N, Heck J, Tang X, Wipf P, Brodsky JL, Hampton RY. Direct involvement of Hsp70 ATP hydrolysis in Ubr1-dependent quality control. *Mol. Biol. Cell* **31**, mbc.E20-08-0541 (2020).
 133. Lopez-Buesa, Pascual, Pfund, Christine & Craig, Elizabeth A. The biochemical properties of the ATPase activity of a 70-kDa heat shock protein (Hsp70) are governed by the C-terminal domains. *Proc. Natl. Acad. Sci.* **95**, 15253–15258 (1998).
 134. Yoo, Haneul, Bard, Jared A. M., Pilipenko, Evgeny V. & Drummond, D. Allan. Chaperones directly and efficiently disperse stress-triggered biomolecular condensates. *Mol. Cell* **82**, 741-755.e11 (2022).
 135. Lum, Ronnie, Tkach, Johnny M., Vierling, Elizabeth & Glover, John R. Evidence for an unfolding/threading mechanism for protein disaggregation by *Saccharomyces cerevisiae* Hsp104. *J. Biol. Chem.* **279**, 29139–29146 (2004).
 136. Tkach, Johnny M. & Glover, John R. Amino acid substitutions in the C-terminal AAA+ module of Hsp104 prevent substrate recognition by disrupting oligomerization and cause high temperature inactivation. *J. Biol. Chem.* **279**, 35692–35701 (2004).
 137. Garcia, Veronica M., Nillegoda, Nadinath B., Bukau, Bernd & Morano, Kevin A. Substrate binding by the yeast Hsp110 nucleotide exchange factor and

- molecular chaperone Sse1 is not obligate for its biological activities. *Mol. Biol. Cell* **28**, 2066–2075 (2017).
138. Jeong, Woojin, Sung, Jun Park, Chang, Tong Shin, Lee, Duck Yeon & Sue, Goo Rhee. Molecular mechanism of the reduction of cysteine sulfinic acid of peroxiredoxin to cysteine by mammalian sulfiredoxin. *J. Biol. Chem.* **281**, 14400–14407 (2006).
139. Ramazi, Shahin & Zahiri, Javad. Post-translational modifications in proteins: resources, tools and prediction methods. *Database* **2021**, baab012 (2021).
140. Abrams, Jennifer L. & Morano, Kevin A. Coupled assays for monitoring protein refolding in *Saccharomyces cerevisiae*. *J. Vis. Exp.* 1–6 (2013) doi:10.3791/50432.
141. Tatsumi, Hiroki, Masuda, Tsutomu & Nakano, Eiichi. Synthesis of Enzymatically Active Firefly Luciferase in Yeast. *Agric. Biol. Chem.* **52**, 1123–1127 (1988).
142. Szabo A, Langer T, Schröder H, Flanagan J, Bukau B, Hartl FU. The ATP hydrolysis-dependent reaction cycle of the *Escherichia coli* Hsp70 system - DnaK, DnaJ, and GrpE. *Proc. Natl. Acad. Sci. U. S. A.* **91**, 10345–10349 (1994).
143. Tkach, Johnny M. & Glover, John R. Nucleocytoplasmic Trafficking of the Molecular Chaperone Hsp104 in Unstressed and Heat-Shocked Cells. *Traffic* **9**, 39–56 (2008).
144. Mohanakrishnan, Kaimal Jayasankar, Ganapathi, Kandasamy, Fabian, Gasser & Claes, Andréasson. Coordinated Hsp110 and Hsp104 Activities

- Power Protein Disaggregation in *Saccharomyces cerevisiae*. *Mol. Cell. Biol.* **37**, e00027-17 (2017).
145. Goloubinoff, Pierre & Rios, Paolo De Los. The mechanism of Hsp70 chaperones: (entropic) pulling the models together. *Trends Biochem. Sci.* **32**, 372–380 (2007).
146. Truman AW, Kristjansdottir K, Wolfgeher D, Hasin N, Polier S, Zhang H, Perrett S, Prodromou C, Jones GW, Kron SJ. CDK-Dependent Hsp70 phosphorylation controls G1 cyclin abundance and cell-cycle progression. *Cell* **151**, 1308–1318 (2012).
147. Mumberg, Dominik, Müller, Rolf & Funk, Martin. Yeast vectors for the controlled expression of heterologous proteins in different genetic backgrounds. *Gene* **156**, 119–122 (1995).
148. Garcia, Veronica M., Rowlett, Veronica W., Margolin, William & Morano, Kevin A. Semi-automated microplate monitoring of protein polymerization and aggregation. *Anal. Biochem.* **508**, 9–11 (2016).
149. Greene, Lois, Park, Yang-Nim, Masison, Daniel & Eisenberg, Evan. Application of GFP-Labeling to Study Prions in Yeast. *Protein Pept. Lett.* **16**, 635–641 (2009).
150. Cohen, Aviv, Ross, Liron, Nachman, Iftach & Bar-Nun, Shoshana. Aggregation of PolyQ Proteins Is Increased upon Yeast Aging and Affected by Sir2 and Hsf1: Novel Quantitative Biochemical and Microscopic Assays. *PLoS One* **7**, 1–10 (2012).
151. Miller SB, Ho CT, Winkler J, Khokhrina M, Neuner A, Mohamed MY, Guilbride

- DL, Richter K, Lisby M, Schiebel E, Mogk A, Bukau B. Compartment-specific aggregates direct distinct nuclear and cytoplasmic aggregate deposition. *EMBO J.* **34**, 778–797 (2015).
152. Fernandez-Funez P, Sanchez-Garcia J, de Mena L, Zhang Y, Levites Y, Khare S, Golde TE, Rincon-Limas DE. Holdase activity of secreted Hsp70 masks amyloid- β 42 neurotoxicity in *Drosophila*. *Proc. Natl. Acad. Sci. U. S. A.* **113**, E5212–E5221 (2016).
153. Cugusi S, Mitter R, Kelly GP, Walker J, Han Z, Pisano P, Wierer M, Stewart A, Svejstrup JQ. Heat shock induces premature transcript termination and reconfigures the human transcriptome. *Mol. Cell* **82**, 1573-1588.e10 (2022).
154. Xiong, Sinan, Chng, Wee-Joo & Zhou, Jianbiao. Crosstalk between endoplasmic reticulum stress and oxidative stress: a dynamic duo in multiple myeloma. *Cell. Mol. Life Sci.* **78**, 3883–3906 (2021).
155. Fribley, Andrew, Zhang, Kezhong & Kaufman, Randal J. Regulation of apoptosis by the unfolded protein response. *Methods Mol. Biol.* **559**, 191–204 (2009).
156. Feleciano, Diogo R. & Kirstein, Janine. Collapse of redox homeostasis during aging and stress. *Mol. Cell. Oncol.* **3**, 1–2 (2016).
157. Salmon, Adam. Update on the oxidative stress theory of aging: Does oxidative stress play a role in aging or healthy aging? *Mol. Cell. Biochem.* **23**, 1–7 (2012).
158. Harman, D. Aging: a theory based on free radical and radiation chemistry. *J. Gerontol.* **11**, 298–300 (1956).

159. Xiao H, Jedrychowski MP, Schweppe DK, Huttlin EL, Yu Q, Heppner DE, Li J, Long J, Mills EL, Szpyt J, He Z, Du G, Garrity R, Reddy A, Vaites LP, Paulo JA, Zhang T, Gray NS, Gygi SP, Chouchani ET. A Quantitative Tissue-Specific Landscape of Protein Redox Regulation during Aging. *Cell* **180**, 968-983.e24 (2020).
160. Le Moan, Natacha, Clement, Gilles, Le Maout, Sophie, Tacnet, Frédérique & Toledano, Michel B. The *Saccharomyces cerevisiae* proteome of oxidized protein thiols: Contrasted functions for the thioredoxin and glutathione pathways. *J. Biol. Chem.* **281**, 10420–10430 (2006).
161. Brandes, Nicolas, Reichmann, Dana, Tienson, Heather, Leichert, Lars I. & Jakob, Ursula. Using quantitative redox proteomics to dissect the yeast redoxome. *J. Biol. Chem.* **286**, 41893–41903 (2011).
162. Brandes N, Tienson H, Lindemann A, Vitvitsky V, Reichmann D, Banerjee R, Jakob U. Time line of redox events in aging postmitotic cells. *Elife* **2013**, 1–18 (2013).
163. Yang, Jing, Carroll, Kate S. & Liebler, Daniel C. The expanding landscape of the thiol redox proteome. *Mol. Cell. Proteomics* **15**, 1–11 (2016).
164. Wang Z, Ying Z, Bosy-Westphal A, Zhang J, Schautz B, Later W, Heymsfield SB, Müller MJ. Specific metabolic rates of major organs and tissues across adulthood: Evaluation by mechanistic model of resting energy expenditure. *Am. J. Clin. Nutr.* **92**, 1369–1377 (2010).
165. Lee-Yoon, Dongsin, Easton, Douglas, Murawski, Melanie, Burd, Randy & Subject, John R. Identification of a Major Subfamily of Large hsp70-like

- Proteins through the Cloning of the Mammalian 110-kDa Heat Shock Protein
*. *J. Biol. Chem.* **270**, 15725–15733 (1995).
166. Wang, Jie, Pareja, Kristeen A., Kaiser, Chris A. & Sevier, Carolyn S. Redox signaling via the molecular chaperone BiP protects cells against endoplasmic reticulum-derived oxidative stress. *Elife* **3**, e03496 (2014).
167. Ulrich, Kathrin, Schwappach, Blanche & Jakob, Ursula. Thiol-based switching mechanisms of stress-sensing chaperones. *Biol. Chem.* **402**, 239–252 (2021).
168. Reichmann, Dana, Voth, Wilhelm & Jakob, Ursula. Maintaining a Healthy Proteome during Oxidative Stress. *Mol. Cell* **69**, 203–213 (2018).
169. Picazo, Cecilia & Molin, Mikael. Impact of hydrogen peroxide on protein synthesis in yeast. *Antioxidants* **10**, (2021).
170. Marada A, Allu PK, Murari A, PullaReddy B, Tammineni P, Thiriveedi VR, Danduprolu J, Sepuri NB. Mge1, a nucleotide exchange factor of Hsp70, acts as an oxidative sensor to regulate mitochondrial Hsp70 function. *Mol. Biol. Cell* **24**, 692–703 (2013).
171. Allu PK, Marada A, Boggula Y, Karri S, Krishnamoorthy T, Sepuri NB. Methionine sulfoxide reductase 2 reversibly regulates Mge1, a cochaperone of mitochondrial Hsp70, during oxidative stress. *Mol. Biol. Cell* **26**, 406–419 (2015).
172. Karri S, Singh S, Paripati AK, Marada A, Krishnamoorthy T, Guruprasad L, Balasubramanian D, Sepuri NBV. Adaptation of Mge1 to oxidative stress by local unfolding and altered Interaction with mitochondrial Hsp70 and Mxr2. *Mitochondrion* **46**, 140–148 (2019).

173. Greetham D, Vickerstaff J, Shenton D, Perrone GG, Dawes IW, Grant CM. Thioredoxins function as deglutathionylase enzymes in the yeast *Saccharomyces cerevisiae*. *BMC Biochem.* **11**, 3 (2010).
174. Ortiz DF, Kreppel L, Speiser DM, Scheel G, McDonald G, Ow DW. Heavy metal tolerance in the fission yeast requires an ATP-binding cassette-type vacuolar membrane transporter. *EMBO J.* **11**, 3491–3499 (1992).
175. Stephen, Duncan W. S. & Jamieson, Derek J. Glutathione is an important antioxidant molecule in the yeast *Saccharomyces cerevisiae*. *FEMS Microbiol. Lett.* **141**, 207–212 (1996).
176. Liam, Baird & Masayuki, Yamamoto. The Molecular Mechanisms Regulating the KEAP1-NRF2 Pathway. *Mol. Cell. Biol.* **40**, e00099-20 (2020).
177. Lozada-Delgado, Janice G., Torres-Ramos, Carlos A. & Ayala-Peña, Sylvette. Aging, oxidative stress, mitochondrial dysfunction, and the liver. in *Aging* (eds. Preedy, Victor R. & Patel, Vinood B. B. T. *Aging* (Second Edition)) 37–46 (Academic Press, 2020). doi:<https://doi.org/10.1016/B978-0-12-818698-5.00004-3>.
178. Navarro, Ana & Boveris, Alberto. Rat brain and liver mitochondria develop oxidative stress and lose enzymatic activities on aging. *Am. J. Physiol. Integr. Comp. Physiol.* **287**, R1244–R1249 (2004).
179. Csiszar, A., Toth, J., Peti-Peterdi, J. & Ungvari, Z. The aging kidney: role of endothelial oxidative stress and inflammation. *Acta Physiol. Hung.* **94**, 107–115 (2007).
180. Zhang, Hongqiao, Davies, Kelvin J. A. & Forman, Henry Jay. Oxidative stress

- response and Nrf2 signaling in aging. *Free Radic. Biol. Med.* **88**, 314–336 (2015).
181. Rahman, Irfan. Pharmacological antioxidant strategies as therapeutic interventions for COPD. *Biochim. Biophys. Acta - Mol. Basis Dis.* **1822**, 714–728 (2012).
182. Täger M, Piecyk A, Köhnlein T, Thiel U, Ansorge S, Welte T. Evidence of a defective thiol status of alveolar macrophages from COPD patients and smokers. Chronic obstructive pulmonary disease. *Free Radic. Biol. Med.* **29**, 1160–1165 (2000).
183. Ameh, Thelma & Sayes, Christie M. The potential exposure and hazards of copper nanoparticles: A review. *Environ. Toxicol. Pharmacol.* **71**, 103220 (2019).
184. Saudi, M. A. & Said, O. A. M. Exposure to copper nanoparticles induces oxidative stress and alters Hsp70 and Sod2 gene expression in *Drosophila melanogaster*. *Egypt. J. Pure Appl. Sci.* **60**, 36–50 (2022).
185. Akingbade, Grace T., Ijomone, Omamuyovwi M., Imam, Aminu, Aschner, Michael & Ajao, Moyosore S. D-Ribose-L-Cysteine Improves Glutathione Levels, Neuronal and Mitochondrial Ultrastructural Damage, Caspase-3 and GFAP Expressions Following Manganese-Induced Neurotoxicity. *Neurotox. Res.* **39**, 1846–1858 (2021).
186. Ijomone OM, Iroegbu JD, Morcillo P, Ayodele AJ, Ijomone OK, Bornhorst J, Schwerdtle T, Aschner M. Sex-dependent metal accumulation and immunoexpression of Hsp70 and Nrf2 in rats' brain following manganese

- exposure. *Environ. Toxicol.* 2167–2177 (2022) doi:10.1002/tox.23583.
187. Miah MR, Ijomone OM, Okoh COA, Ijomone OK, Akingbade GT, Ke T, Krum B, da Cunha Martins A Jr, Akinyemi A, Aranoff N, Antunes Soares FA, Bowman AB, Aschner M. The effects of manganese overexposure on brain health. *Neurochem. Int.* **135**, 104688 (2020).
188. Martínez de Toda, I. & De la Fuente, M. The role of Hsp70 in oxi-inflammaging and its use as a potential biomarker of lifespan. *Biogerontology* **16**, 709–721 (2015).
189. Oliveira, Amanda A. De, Mendoza, Valentina O., Priviero, Fernanda, Webb, R. Clinton & Nunes, Kenia P. Age-Related Decline in Vascular Responses to Phenylephrine Is Associated with Reduced Levels of HSP70. *Biomolecules* **12**, 1–11 (2022).
190. Garofalo M, Pandini C, Bordoni M, Jacchetti E, Diamanti L, Carelli S, Raimondi MT, Sproviero D, Crippa V, Carra S, Poletti A, Pansarasa O, Gagliardi S, Cereda C. RNA Molecular Signature Profiling in PBMCs of Sporadic ALS Patients: HSP70 Overexpression Is Associated with Nuclear SOD1. *Cells* **11**, 1–18 (2022).
191. Bordoni M, Pansarasa O, Dell'Orco M, Crippa V, Gagliardi S, Sproviero D, Bernuzzi S, Diamanti L, Ceroni M, Tedeschi G, Poletti A, Cereda C. Nuclear Phospho-SOD1 Protects DNA from Oxidative Stress Damage in Amyotrophic Lateral Sclerosis. *J. Clin. Med.* **8**, (2019).
192. Kowluru, Vibhuti & Kowluru, Renu A. Increased oxidative stress in diabetes regulates activation of a small molecular weight G-protein, H-Ras, in the

- retina. *Mol. Vis.* **13**, 602–610 (2007).
193. Shan Z, Chen S, Sun T, Luo C, Guo Y, Yu X, Yang W, Hu FB, Liu L. U-Shaped Association between Plasma Manganese Levels and Type 2 Diabetes. *Environ. Health Perspect.* **124**, 1876–1881 (2016).
194. Hirsch, Gabriela Elisa & Heck, Thiago Gomes. Inflammation, oxidative stress and altered heat shock response in type 2 diabetes: the basis for new pharmacological and non-pharmacological interventions. *Arch. Physiol. Biochem.* **128**, 411–425 (2022).
195. Akerfelt, Malin, Morimoto, Richard I. & Sistonen, Lea. Heat shock factors: integrators of cell stress, development and lifespan. *Nat. Rev. Mol. Cell Biol.* **11**, 545–555 (2010).
196. Mahmoud, Fadia F., Haines, David, Dashti, Ali A., El-Shazly, Sherief & Al-Najjar, Fawzia. Correlation between heat shock proteins, adiponectin, and T lymphocyte cytokine expression in type 2 diabetics. *Cell Stress Chaperones* **23**, 955–965 (2018).
197. Goettems-Fiorin PB, Costa-Beber LC, Dos Santos JB, Friske PT, Sulzbacher LM, Frizzo MN, Ludwig MS, Rhoden CR, Heck TG. Ovariectomy predisposes female rats to fine particulate matter exposure's effects by altering metabolic, oxidative, pro-inflammatory, and heat-shock protein levels. *Environ. Sci. Pollut. Res. Int.* **26**, 20581–20594 (2019).
198. Szyller, Jakub, Kozakiewicz, Mariusz, Siermontowski, Piotr & Kaczerska, Dorota. Oxidative Stress, HSP70/HSP90 and eNOS/iNOS Serum Levels in Professional Divers during Hyperbaric Exposition. *Antioxidants* **11**, 1008

- (2022).
199. Kurisu, Kota & , Jesung You, , Zhen Zheng , Seok Joon Won, Raymond A Swanson, Yenari, Midori A. Cofilin-actin rod formation in experimental stroke is attenuated by therapeutic hypothermia and overexpression of the inducible 70 kD inducible heat shock protein (Hsp70). *Brain Circ.* **5**, 225–233 (2019).
 200. Kim W, Kwon HJ, Jung HY, Yoo DY, Moon SM, Kim DW, Hwang IK. Tat-HSP70 protects neurons from oxidative damage in the NSC34 cells and ischemic damage in the ventral horn of rabbit spinal cord. *Neurochem. Int.* **129**, 104477 (2019).
 201. Lazarev VF, Nikotina AD, Mikhaylova ER, Nudler E, Polonik SG, Guzhova IV, Margulis BA. Hsp70 chaperone rescues C6 rat glioblastoma cells from oxidative stress by sequestration of aggregating GAPDH. *Biochem. Biophys. Res. Commun.* **470**, 766–771 (2016).
 202. Xu NW, Chen Y, Liu W, Chen YJ, Fan ZM, Liu M, Li LJ. Inhibition of JAK2/STAT3 signaling pathway suppresses proliferation of Burkitt's lymphoma raji cells via cell cycle progression, apoptosis, and oxidative stress by modulating HSP70. *Med. Sci. Monit.* **24**, 6255–6263 (2018).
 203. Mulyani WRW, Sanjiwani MID, Sandra, Prabawa IPY, Lestari AAW, Wihandani DM, Suastika K, Saraswati MR, Bhargah A, Manuaba IBAP. Chaperone-based therapeutic target innovation: Heat shock protein 70 (HSP70) for type 2 diabetes mellitus. *Diabetes, Metab. Syndr. Obes. Targets Ther.* **13**, 559–568 (2020).
 204. Song, Yan Jun, Zhong, Chong Bin & Wang, Xian Bao. Heat shock protein 70:

- A promising therapeutic target for myocardial ischemia–reperfusion injury. *J. Cell. Physiol.* **234**, 1190–1207 (2019).
205. Sulzbacher, Maicon Mac Hado, Ludwig, Mirna Stela & Heck, Thiago Gomes. Oxidative stress and decreased tissue HSP70 are involved in the genesis of sepsis: HSP70 as a therapeutic target. *Rev. Bras. Ter. Intensiva* **32**, 585–591 (2020).
206. Mazzei, Luciana, Belen Ruiz-Roso, Maria, De Las Heras, Natalia, Ballesteros, Sandra, Torrespalazzolo, Carolina, Ferder, Leon, Beatriz Carmago, Alejandra, Manucha, Walter. Allicin neuroprotective effect during oxidative/inflammatory injury involves AT1-Hsp70-iNOS counterbalance axis. *Biocell* **44**, 671–681 (2020).
207. Chaudhury, Subhabrata, Keegan, Bradley M. & Blagg, Brian S. J. The role and therapeutic potential of Hsp90, Hsp70, and smaller heat shock proteins in peripheral and central neuropathies. *Med. Res. Rev.* **41**, 202–222 (2021).
208. Jumper J, Evans R, Pritzel A, Green T, Figurnov M, Ronneberger O, Tunyasuvunakool K, Bates R, Žídek A, Potapenko A, Bridgland A, Meyer C, Kohl SAA, Ballard AJ, Cowie A, Romera-Paredes B, Nikolov S, Jain R, Adler J, Back T, Petersen S, Reiman D, Clancy E, Zielinski M, Steinegger M, Pacholska M, Berghammer T, Bodenstein S, Silver D, Vinyals O, Senior AW, Kavukcuoglu K, Kohli P, Hassabis D. Highly accurate protein structure prediction with AlphaFold. *Nature* **596**, 583–589 (2021).
209. Waterhouse A, Bertoni M, Bienert S, Studer G, Tauriello G, Gumienny R, Heer FT, de Beer TAP, Rempfer C, Bordoli L, Lepore R, Schwede T. SWISS-

MODEL: homology modelling of protein structures and complexes. *Nucleic Acids Res.* **46**, W296–W303 (2018).

Vita

Alec Morgan Santiago was born on October 15, 1992, in Albuquerque, NM, to Jessica Santiago. Mr. Santiago attended Del Norte High School, before enrolling at Auburn University, where he graduated in 2017 with a Bachelor of Science degree in Microbiology. In June, 2017, he enrolled in the MD Anderson Cancer Center UTHealth Graduate School of Biomedical Sciences. In June 2018, he joined the lab of Kevin A. Morano, PhD, where he completed his research. In his tenure as a graduate student, Alec held several positions, including chair of several science conference committees, Executive Director of Enventure, host of Incorporating Science, and co-founder of Van Heron Labs. In his free time, Alec enjoys frequent exercise, reading, building new entrepreneurial projects, and learning about biotechnology.